AN ELECTROCHEMICAL IMMUNOBIOSENSOR FOR DENGUE VIRUS NS1 PROTEIN DETECTION

NADIYA TAHA DARWISH

DISSERTATION SUBMITTED IN PARTIAL FULFILLMENT OF THE REQUIREMENTS FOR THE DEGREE OF DOCTOR OF PHILOSOPHY

DEPARTMENT OF CHEMISTRY
FACULTY OF SCIENCE
UNIVERSITY OF MALAYA
KUALA LUMPUR

2016

UNIVERSITI MALAYA
ORIGINAL LITERARY WORK DECLARATION

Name of Candidate: Nadiya Taha Darwish
Registration/Matric No: SHC 12 0033
Name of Degree: Doctor of Philosophy
Title of Project Paper/Research Report/Dissertation/Thesis ("this Work"):

An electrochemical immunobiosensor for dengue virus NS1 protein detection

Field of Study: Chemistry

I do solemnly and sincerely declare that:

(1) I am the sole author/writer of this Work;
(2) This Work is original;
(3) Any use of any work in which copyright exists was done by way of fair dealing and for permitted purposes and any excerpt or extract from, or reference to or reproduction of any copyright work has been disclosed expressly and sufficiently and the title of the Work and its authorship have been acknowledged in this Work;
(4) I do not have any actual knowledge nor ought I reasonably to know that the making of this work constitutes an infringement of any copyright work;
(5) I hereby assign all and every rights in the copyright to this Work to the University of Malaya ("UM"), who henceforth shall be owner of the copyright in this Work and that any reproduction or use in any form or by any means whatsoever is prohibited without the written consent of UM having been first had and obtained;
(6) I am fully aware that if in the course of making this Work I have infringed any copyright whether intentionally or otherwise, I may be subject to legal action or any other action as may be determined by UM.

Candidate's Signature Date

Subscribed and solemnly declared before,

Witness's Signature Date

Name:
Designation:

ABSTRACT

The dengue virus (DENV) is one of the most common viral diseases in South East Asia with 50-100 million cases being reported every year. Rapid and accurate diagnosis of dengue virus is important to avoid critical stage of the infection. A label-free electrochemical immunosensor was developed for direct detection of the dengue virus unstructured protein (NS1). The biosensing interface consists of antifouling moieties (zwitterionic molecules) and linker molecules where the linker molecule is used to immobilize the biorecognition molecules (monoclonal anti-NS1 IgG antibody). The combination of monoclonal antibodies and antifouling molecules is an innovative design that improves the ability of biosensor in detecting the target analyte in a complicated sample. The ratios of antifouling molecules 4-sulfophenyl (SP) and 4-trimethylammoniophenyl (TMAP) to linker molecules 1,4-phenylenediamine (PPD) or 4-aminobenzoic acid (PABA) that provided the greatest resistance to non-specific protein adsorptions of bovine serum albumin labelled with fluorescein isothiocyanate (BSA-FITC) and cytochrome c labelled with rhodamine B isothiocyanate (Cyt c-RBITC) were determined by confocal laser scanning microscopy (CLSM). As a standard control, 2-[2-(2-methoxyethoxy) ethoxy] acetic acid (OEG) was used due to its known antifouling properties. The combination of (SP:TMAP:PPD) with a ratio of 0.5:1.5:0.37 showed the best antifouling capability and the deposition of these molecules was confirmed by using X-ray photoelectron spectroscopy (XPS) and field emission scanning electron microscopy (FESEM). The immunosensor was prepared by modification of indium tin oxide (ITO) electrodes with SP: TMAP: PPD. Then, the gold nanoparticles (AuNPs) (20 nm) were attached. Thereafter, 1, 4-phenylenediamine (3 mM) was used to derivatize the AuNPs to help in attachment of the monoclonal anti-NS1 antibody. Differential Pulse Voltammetry (DPV) and Electrochemical Impedance Spectroscopy (EIS) were used to study the stepwise fabrication of the immunosensor and to obtain the calibration curve for the NS1 antigen. The NS1 detection was

performed in Fe $(CN)_6^{3-}/Fe(CN)_6^{4-}$. The coefficient of determination (R^2) and correlation coefficient (R) for the calibration curve obtained through DPV method were 0.85 and -0.74, respectively. With the EIS technique, the R^2 obtained was 0.94 and the R obtained was 0.95. A good detection limit of 5 ng mL^{-1} was reached. The immunosensor showed good stability for 21 days with a relative standard deviation (RSD) of 0.1% and good reproducibility with RSD of 0.02%. The selectivity study showed that the immunosensor was specific to the NS1 antigen and also the change in charge transfer (R_{ct}), before and after incubation of the biosensor in human serum albumin (HSA) and human IgG antibody solutions was only 1.9% and 10.2% respectively, as compared to the change in charge transfer when the immunosensor was incubated in 50 ng mL^{-1} NS1. The immunosensor had low cross reactivity with human sera infected with malaria parasites and that the change in R_{ct} was only 5.2% as compared to the change in charge transfer when the immunosensor was incubated in 1 μg mL^{-1} NS1 solution. Therefore, this immunosensor is believed to have an excellent potential in the clinical application for diagnosis of the deadly DENV during the early phase of illness.

ABSTRAK

Virus denggi merupakan virus yang sering menular di Asia Tenggara dengan purata 50-100 juta kes direkodkan setiap tahun. Diagnosis yang tepat dan pantas adalah penting untuk mengelakkan jangkitan kritikal virus wabak ini. *Immunosensor* elektrokimia bebas label dengan sensitiviti dan selektiviti yang tinggi telah dibangunkan untuk mengesan protein virus denggi yang tidak berstruktur, (NS1). Antara muka biopenderia terdiri daripada moieti *antifouling* (molekul zwitterion) dan molekul penghubung dimana molekul penghubung ini digunakan untuk pegun molekul bio-pengecam (antibodi monoklonal anti-NS1 IgG). Gabungan molekul antibodi monoklonal dan *antifouling* merupakan reka bentuk inovatif yang meningkatkan keupayaan biopenderia dalam mengesan sasaran analit dalam sampel yang rumit . Nisbah molekul *antifouling*, 4- sulfofenil (SP) dan 4-trimetilammoniofenil (TMAP) bersama molekul penghubung fenilindiamina (PPD) atau asid 4-aminobenzoik (PABA) yang menyediakan rintangan paling tinggi terhadap penyerapan protein tak-spesifik serum albumin lemb) yang dilabel dengan fluoresin isosianat (FITC-BSA) dan sitokrom c dilabel dengan rodamina B isosianat (Cyt c-RBITC) ditentukan dengan mikroskop laser imbasan sefokus. Kombinasi tersebut ditentukan oleh laser imbasan mikroskop konfokal (CLSM). Sebagai kawalan, asetik 2-[2(2-metoksietoksi]etoksi] (OEG) telah digunakan kerana sifat *antifouling* sudah diketahui. Gabungan (SP:TMAP:PPD) dengan nisbah 0.5:1.5:0.37 menunjukkan keupayaan *antifouling* terbaik dan pemendapan molekul ini yang disahkan dengan menggunakan spektroskopi fotoelektron sinar-X dan mikroskop medan pancaran imbasan elektron (FESEM). *Immunosensor* telah disediakan dengan pengubahsuaian elektrod timah indium oksida (ITO) dengan SP: TMAP: PPD Seterusnya, nanopartikel emas (AuNPs) (20 nm) digabungkan. Kemudian, 1,4-fenilindiamina (3 mM) digunakan untuk bahan terbitan AuNPs bagi membantu

gabungan antibodi (monoklonal anti-NS1 Teknik voltammetri denyutan berbeza (DPV) dan spektroskopi impedansi elektrokimia (EIS) telah digunakan untuk mengkaji setiap langkah fabrikasi *immunosensor* dan untuk mendapatkan lengkungan penentuukuran bagi antigen NS1. Pengesanan NS1 elah dilaksanakan dalam $Fe(CN)_6^{3-}/Fe(CN)_6^{4.}$ Penentuan pekali (R^2) dan pekali kolerasi (R) untuk lengkungan penentuukuran didapati melalui kaedah DPV adalah masing-masing 0.84 dan -0.74. Dengan teknik EIS, R^2 yang diperoleh adalah 0.94 dan R adalah 0.95. Had pengesanan yang baik 5 ng mL^{-1} telah dicapai. *Immunosensor* NS1 menunjukkan kestabilan yang baik untuk 21 hari dengan relatif sisihan piawai (RSD) sebanyak 0.1% dan kebolehulangan yang baik dengan RSD 0.02%. Kajian selektiviti i menunjukkan *immunosensor* adalah khusus untuk antigen NS1 dan juga perubahan dalam pindahan cas (R_{ct}), sebelum dan selepas pengeraman biopenderia dalam serum albumin manusia (HSA) dan larutan antibodi IgG (manusia) hanya masing-masing 1.9% dan 10.2%, apabila dibandingkan dengan perubahan dalam pemindahan cas apabila *immunosensor* diperam dalam 50 ng mL^{-1} NS1. *Immunosensor* ada ketindakbalasan silang rendah dengan serum manusia yang dijangkiti parasit malaria dan perubahan dalam R_{ct} yang diperolehi adalah 5.2% berbanding dengan perubahan pemindahan cas apabila *immunosensor* diperam dalam larutan 1 g mL^{-1}-NS1. Oleh itu, *immunosensor* ini dipercayai mempunyai potensi yang tinggi untuk aplikasi klinikal bagi mendiagnos wabak DENV semasa fasa awal penyakit.

Acknowledgements/ Dedication

In the name of Allah, the Most Gracious and the Most Merciful. Alhamdulillah, all praises to Allah for the strengths and His blessing in achieving this thesis. I would like to express my sincere gratitude to my supervisor Dr. Khor Sook Mei for the continuous support of my Ph.D study and research, for her motivation, enthusiasm. Her guidance helped me in all the time of research and writing of this thesis. I would like to give my deepest thanks and special appreciation to my supervisor, Prof Dr Yatimah Binti Alias, for her supervision and constant support. Special mention goes to Ms Marhaini with my sincere thanks for her support and effort in handling the purchasing process for chemicals and equipment used in this research. My thanks go to my lab mates… for the stimulating discussions and constructive comments.

I would like to dedicate this work to my parents whose prayers have enabled me to reach this significant target of my life and to my loving husband and children for their unconditional love, endless encouragement and support.

TABLE OF CONTENTS

LIST OF FIGURES

LIST OF TABLES

LIST OF SYMBOLS AND ABBREVIATIONS

PABA	4-aminobenzoic acid
BSA-FITC	Bovine serum albumin labelled with fluorescein isothiocyanate
°C	Celsius (Centigrade)
CNS	Central nervous system
R_{CT}	Charge transfer resistance
CFE	Chitosan- carbon fiber electrode
CLSM	Confocal laser scanning microscopy
CV	Cyclic Voltammetry
Cyt c- RBITC	Cytochrome c labelled with rhodamine B isothiocyanate
DF	Dengue fever
DENV	Dengue virus
DHF	Dengue haemorrhagic fever
DSS	Dengue shock syndrome
DNA	Deoxyribonucleic acid
DPV	Differential pulse voltammetric
DCC	*N,N'*-Dicyclohexylcarbodiimide
DMSO	Dimethyl sulfoxide
miniEC	Electrochemical microfluidic
EIS	Electrochemical impedance spectroscopy
eV	electron volt
ER	Endoplasmic reticulum
EDX	Energy-dispersive X-ray
E. protein	Envelope protein
ELISA	Enzyme-linked immunosorbent assay
EDC	1-ethyl-3-(3-dimethylaminopropyl)carbodiimide

FE-SEM	Field-emission scanning electron microscopy
GCE	Glassy carbon electrode
GAGs	Glycosaminoglycans
GPI	Glycosylphosphatidyl inositol
AuNP	Gold nanoparticles
HAI	Hemagglutination-inhibition
Hz	Hertz
HAS	Human serum albumin
NHS	N-hydroxysulfosuccinimide
Immunoglobulin	Ig
ITO	Indium tin oxide
kDa	Kilo Dalton
LFIA	lateral-flow immunochromatographic assay
OEG	2-[2-(2-methoxyethoxy) ethoxy]acetic acid
µg	Microgram
µm	Micrometer
mg	Milligram
mL	Milliliter
mm	Millimeters
mM	Millimolar
$mV \cdot s^{-1}$	Millivolt per second
ng	Nanogram
NASBA	Nucleic acid sequence-based amplification
NS1	Non-structural proteins
nm	Nanometer
OFIS	Optical fiberimmunosensor

Ω	Ohm
Q	Phase constant element
PPD	1,4-Phenylenediamine
PBS	Phosphate buffer saline
pM	Picomolar
Px	Pixel
PVB	Polyvinyl butyral
PEG	Poly(ethylene glycol)
PCR	Polymerase chain reaction
pfu	Plaque-forming unit
QCM	Quartz crystal microbalance
RT-PCR	Real time - polymerase chain reaction
RSD	Relative standard deviation
R_S	Resistance of the electrolyte solution
rpm	Revolutions per minute
SAM	Self-assembled monolayer
SPR	Surface plasmon resonance
SP	4-sulfophenyl
TMAP	4-Trimethylammoniophenyl
V	Volt
W	Warburg impedance
XPS	X-ray photoelectron spectroscopy

LIST OF APPENDICES

CHAPTER 1: INTRODUCTION

Dengue infection is recognized as one of the dangerous and deadly diseases that affects the human's life in subtropical and tropical regions of the world (Decker, 2012). The number of travellers in the world is expected to be 1.6 billion in 2020, mainly in common tourist destinations (Ashley, 2011). Due to the absence of an efficient treatment or vaccine, a proper diagnostic technique is required to diagnose the disease reliably and promptly. There are several types of diagnostic tests for the detection of the dengue virus (DENV). The traditional diagnostic techniques for dengue virus include virus isolation in cell culture (Yamada *et al.*, 2002), serological testing (Barkham *et al.*, 2006), and polymerase chain reaction (PCR) (Dash *et al.*, 2008; Raengsakulrach *et al.*, 2002). Although, in some researches virus isolation is considered as the best detection test for dengue virus in these studies, virus was detected using dengue type-specific monoclonal antibodies for immuno-fluorescent staining, and this means that virus isolation was only part of the entire diagnosis process.

Furthermore, virus isolation has some other limitations. The isolation is only possible if the sera samples are taken before fever onset. (Suwandono *et al.*, 2006; Yamada *et al.*, 2002). The sensitivity of the isolation technique was found to be only 63%, and such low value of sensitivity was due to low levels of viable virus number. Moreover, the improper preparation of blood samples such as inadequate or inappropriate specimen collection, storage, and transport usually yield false-negative results. Furthermore, the binding between the dengue virus and its antibody complexes prevents the isolation of dengue virus. (Dash *et al.*, 2008; Kumaria & Chakravarti, 2005; Raengsakulrach *et al.*, 2002). Using real time polymerase chain reaction (RT-PCR) techniques to detect dengue virus also has some problems, such as giving false-negative results because of the variation of DENV serotypes and the absence of a standard protocol (Guzman &

Kouri, 2004; Houng *et al.*, 2001; Raengsakulrach *et al.*, 2002). In some of the RT-PCR protocols, PCR inhibitors are used, such as antibiotics and haemoglobin, and this might reveal the reason of the loss of sensitivity due to their direct conjugation with DNA or DNA polymerases (Barkham *et al.*, 2006; Prado *et al.*, 2005). Serological tests, which have been used for dengue virus detection, are not very specific because the IgM and IgG immunoglobulins of dengue virus are very cross-reactive with the flavivirus antibodies that are co-circulating as a result of vaccination or a prior infection (i.e., Japanese encephalitis virus, Powassan/Deer tick virus). Moreover, serological tests require to use two sera specimens taken in the acute and convalescence phases (Watthanaworawit *et al.*, 2011). Because of these limitations, the use of more than one test (e.g., NS1 antigen ELISA, IgM antibody ELISA and/or real time reverse transcription-polymerase chain reaction (rRT-PCR)) has been suggested to confirm the disease in a patient's serum sample (Teles, 2011; Watthanaworawit *et al.*, 2011).

Biosensors, and especially electrochemical immunosensors, compared with the conventional tests for the detection of dengue virus, have received increased importance due to their sensitivity, simplicity, and specificity (Kryscio & Peppas, 2012). Before recent improvement in nanotechnology field, electrochemical biosensors have been restricted by inadequate sensitivity results; therefore, the labelling technique was utilized. Nevertheless, labelling process may cause structural changes to the host macromolecules, and this technique is also costly and requires longer time for clinical sample preparation. These difficulties have been overcome by using a label-free design with a nanoparticle-customized electrochemical technique. The use of nanoparticles helps enlarge the electrode surface area and boosts the electrode interface with more bio-recognition molecules because it has a higher surface-to-volume ratio. As a result of that, the sensitivity of biosensor increased (Shinde *et al.*, 2011). Furthermore, gold nanoparticles have been used to fabricate the interfaces of the biosensors because of

their redox properties and their ability to sense the analyte in the pM range (Shinde *et al.*, 2011), (Gole *et al.*, 2001; Oliveira *et al.*, 2009b). Therefore, label-free immunosensor based on gold nanoparticle was used in this study. The genomic biosensors for DENV diagnosis target viral nucleic acids; however, the dengue viral nucleic acids are kept inside the infected cell, a lysis step is required prior to performing the other steps in the test procedure. Additionally, the quantity of viral nucleic acid outside the viral cell is very small and it exists in an unstable form (Su *et al.*, 2003). Considering the limitations of the existing DENV detection techniques, immunosensors have potential for diseases detection, not only because of the specific interaction between the antigen and antibody protein but also because of their ability to detect very low concentrations of analytes from different infected blood specimens (Eissa *et al.*, 2012b). In current researches, consideration has been given to the diagnosis of the biomarker NS1 antigen. NS1 has several important characteristics. The NS1 antigen is secreted extracellularly from the host infected cell during the early stage of DENV infection, with its concentration up to 50 µg mL^{-1} (Libraty *et al.*, 2002; Young *et al.*, 2000), even when viral RNA detection is negative (Alcon *et al.*, 2002). Furthermore, the NS1 antigen exists in a dengue patient's sera starting from day 1 up to day 9 or even to day 18 after the onset of fever, and the lasting of NS1 antigen for such relatively long time has been confirmed by *in vivo* studies on the NS1 secretion *via* an ELISA assay (Alcon *et al.*, 2002; Xu *et al.*, 2006). This shows that NS1 is significant for early diagnosis and can be detectable in patient's sera before dengue antibodies (IgM and IgG) are produced (Lapphra *et al.*, 2008; Young *et al.*, 2000).

The proteomic structure of NS1 is conserved in all four dengue serotypes. Subsequently, cross reactivity between all Dengue virus serotypes is expected and this is another advantage for using NS1 as it can react with the four Dengue serotypes and consequently can detect all DENV1, DENV2, DENV3 and DENV4 in acute patient

plasmas (Liu *et al.*, 2006; Puttikhunt *et al.*, 2003). Another advantage of the biomarker NS1 is highly conserved antigen which is a promising alternative for the serum glycoprotein (Alcon *et al.*, 2002) and also it is specific for DENV infection because NS1 is non-reactive with other viruses such as West Nile virus and yellow fever virus (Liu *et al.*, 2006) (Kumarasamy *et al.*, 2007) and Japanese encephalitis (Singh *et al.*, 2010). Furthermore, unlike viral genetic materials and nucleic acids, NS1 is stable because of the N-linked glycans at the two glycosylation sites Asn-130 and Asn-207 (Rozen-Gagnon *et al.*, 2012). Moreover, NS1 antigen is detectable in both primary and secondary infections of Dengue fever (Schilling *et al.*, 2004). NS1 can also be detected in Dengue haemorrhagic fever (DHF), and the existence of NS1 in Dengue haemorrhagic fever has been confirmed by other studies including the Platelia™ NS1 Antigen test (Lapphra *et al.*, 2008), the Antigen ELISA for NS1 and the lateral-flow immunochromatographic assay (rapid LFIA test) (Najioullah *et al.*, 2011). Nevertheless, it is found that lower level of NS1 antigens is detected in patient's sera with secondary infections and this may be due to the antigen NS1–antibody (Ag-Ab) immune complexes which inhibit NS1 detection and therefore further boosting in detecting NS1 antigen is required (Lapphra *et al.*, 2008) and for this demand, using signal amplifiers in biosensor design might be an effective approach. Therefore, gold nanoparticles have been involved in this research to fabricate the biosensors interfaces.

In this research, an indium tin oxide (ITO) electrode was used because of its stability in both physical and electrochemical characteristics, its capability to be modified with macromolecules on its surface because it allows the adhesion of these molecules (Choi *et al.*, 2007; M. Chockalingam *et al.*, 2011). ITO also has large electrochemical working window and excellent electrical conductivity (Choi *et al.*, 2007; M. Chockalingam *et al.*, 2011) (Lin *et al.*, 2007a; Lin *et al.*, 2007b). Biofouling means the accretion of cells, proteins and other biological materials onto a bare electrode surface. For a fast clinical

diagnosis, immunosensors are used to detect disease analytes such as proteins, nucleic acids or other disease biomarkers at very low level of concentrations from complicated clinical sample media (Atias *et al.*, 2009; Cavalcanti *et al.*, 2012 b; Chen *et al.*, 2013; Dias *et al.*, 2013; Shiddiky, Kithva, Kozak, *et al.*, 2012a). Such an accumulation of biofouling materials subsequently leads to reduced analyte diffusion and perfusion to the biosensor interface, which eventually causes a decline in biosensor response and sensitivity. Poly (ethylene glycol) (PEG) and self-assembled monolayers with oligo (ethylene glycol) chains (OEG-SAMs) have been utilized to obstruct the adsorption of biofouling substances (Yu *et al.*, 2011).

However, these polymers are not stable and undergo auto-oxidation in biological sample (Brahim *et al.*, 2002; Zhang *et al.*, 2000) and its efficiency depends on the concentrations and chain lengths of PEG and OEG and the sample temperature. (Akkahat *et al.*, 2012; Gui *et al.*, 2013 b; Yeh *et al.*, 2007). Zwitterionic polymers such as phosphorylcholine, sulfobetaine, and carboxy betaine have been applied as antifouling coating as they contain both anionic and cationic groups. However, using of the long chains of zwitterionic polymers passivates the electrode surface and causes loss to electrode sensitivities. Zwitterionic polymers of short-chain molecules show low stability (Gittens *et al.*, 2013; Gui *et al.*, 2013 b; Shi *et al.*, 2011). Therefore, zwitterionic phenyl layers have been suggested in this study because they are stable and do not passivate the electrode surface as it has a shorter electron transfer pathway to the transducer surface (Gui *et al.*, 2013 b) , and due to the mentioned characteristics of zwitterionic phenyl, it can be considered as a good alternative for other antifouling coating in biosensing applications.

The aim of this research is to develop a simple, specific and sensitive electrochemical impedance immunosensor for detection of the NS1 antigen biomarker. First, the

electrochemical behaviour of individual molecules were studied. The individual deposited compounds were 4-sulfophenyl (SP) and 4-trimethylammoniophenyl (TMAP) as antifouling molecules. 1, 4-phenylenediamine (PPD) and 4-aminobenzoic acid (PABA) as linker molecules. Then, it followed by testing the antifouling capability of ITO electrodes modified with a combination of SP: TMAP: PPD [combination 1: 4-sulfophenyl (SP), 4-trimethylammoniophenyl (TMAP), and 1, 4-phenylenediamine (PPD and for the ITO electrodes modified with a combination of SP: TMAP: PABA combination 2: 4-sulfophenyl (SP), 4-trimethylammoniophenyl (TMAP), and 4-aminobenzoic acid (PABA)]. For the control experiment, 2-[2-(2-methoxyethoxy) ethoxy] acetic acid (OEG), was used as the antifouling molecule on the ITO slides. The deposited molecules were characterized by using electrochemical measurement, XPS, FESEM and EDX techniques.

The immunosensor were fabricated by using the surface interface which showed the best antifouling properties and the deposited 1, 4-phenylenediamine molecule was linked to gold nanoparticles (AuNPs). The AuNPs were further modified with 1, 4-phenylenediamine. Monoclonal anti-NS1 IgG antibodies were used to functionalize the distal amine group of 1, 4-phenylenediamine. The fabrication of immunosensor steps and NS1 antigen detection were examined using EIS and DPV techniques. This sensing interface was used for the detection of the NS1 antigen. Reproducibility, selectivity, cross reactivity and stability were carried out for the prepared immunosensor.

OBJECTIVES OF STUDY

1. To study the electrochemical behaviour of deposited compounds: 4-sulfophenyl (SP), 4-trimethylammoniophenyl (TMAP), 1,4-phenylenediamine PPD and 4-aminobenzoic acid (PABA) by finding the reductive adsorption peaks , and by testing the passivation of the working electrode toward the penetration of negatively charged redox-active species $[Fe(CN)_6]^{4-/3-}$ and positively charged redox-active species $[Ru(NH_3)_6]^{3+}$.

2. To fabricate a biosensing interfaces on indium tin oxide electrode via electrodeposition of linker molecules (COOH or NH_2) and charged, antifouling moieties ($(-SO^{3-}$ and $^{+}(Me)_3$).

3. To investigate the antifouling capability of the two mixtures at different ratios against (BSA-FITC) and Cyt c- RBITC by using Confocal Laser Fluorescent Microscope.

4. To fabricate the immunosensor, using the mixture of anti-fouling molecules (which showed the best antifouling capability) and monoclonal antibody to detect the NS1 antigen.

5. To find out the calibration plot corresponding to the change of NS1 antigen concentration, by using electrochemical impedance spectroscopy and differential pulse voltammetry techniques.

6. To test the reproducibility, stability, selectivity and cross reactivity of the fabricated immunosensor.

7. To test the fabricated immunosensor in clinical samples from patients infected with dengue virus.

CHAPTER 2: LITERATURE REVIEW

2.1 Dengue virus

Dengue viruses belong to Flavivirus genus, which also has yellow fever virus, the West Nile virus, and encephalitis virus. Dengue virus is an enveloped virus, with a diameter of about 50 nm. The particle of dengue virus is spherical in shape and contains a single, positive-sense RNA genome of about 11,000 nucleotides with only one open-reading frame (ORF). This ORF encodes a single polyprotein precursor arranged in the order of NH2-C-prM-E-NS1-NS2A-NS2B-NS3-NS4A-NS4B-NS5-COOH. Co- and post-translational proteolytic processing produce three structural proteins which form the virion: the C protein encapsulates the viral genomic RNA to form the nucleocapsid, and the nucleocapsid is covered by a lipid bilayer, which contains both viral membrane (prM protein) and envelope protein (E proteins) (Bessaud *et al.*, 2006; Lim *et al.*, 2013).

Non-structural proteins of dengue virus (NS1–NS5), which are expressed in infected cells, are important for virus replication, virion assembly, and in evading the host immune response. Primarily, the non-structural proteins are found in the cytoplasm to form reproduction complexes, which at the end involve in viral RNA fabrication. DENV NS1, is a hydrophilic membrane-associated homodimer, produced in rough endoplasmic reticulum. The C-terminal residues of NS1 are suggested to be involved in the NS1-associated pathogenesis as the mutation in NS1 protein disrupts the RNA fabrication. Therefore, it is important to explore the crystal structure for NS1 protein as well as that of viral NS1-NS2A catalytic domain, which is essential in establishing the estimated 3-D conformation of NS1 subunit and to study its role and implication in viral pathogenesis. NS2B acts as chaperone, which participates in the folding of NS3 subunit in its active conformation, and therefore playing an important role in regulating substrate enzyme interaction and in membrane association. DENV NS3 and NS5 are the

best-characterized non-structural proteins, which are multifunctional proteins containing several enzymatic activities. Non-structural protein NS4 consists of two subunits, NS4A and NS4B. NS4A involves in intracellular membrane modulation and its C-terminal end helps in the translocation of NS4B subunit. The biological function of NS4b subunit has not been investigated, though latest researches showed that it may possibly work as an interferon antagonist (Bhakat *et al.*, 2014; Lim *et al.*, 2013).

Dengue viruses is a flavivirus with an RNA nucleic acid and is categorized into 4 serotypes based on the number of antigens that the viruses have in common and is numbered as DENV1, DENV2, DENV3 and DENV4. Dengue disease stages were earlier classified via the World Health Organisation into dengue fever (DF), dengue haemorrhagic fever (DHF) and dengue shock syndrome (DSS). Patient infected with any serologic type does not acquire immunity to dengue's other serotypes. The first or primary infection of dengue fever may develop to serious sickness in second infection with other serotypes and this is because of the immunity after infection is type-specific and immunity for four serotypes continues for short time (Ashley, 2011).

Though, the dengue virus is cross-reactive, there is no cross-protective immunity and patient could be infected with DF up to 4 times, giving the chance for different serotypes of the sickness, ranging from DF to DHF and DSS (Dale Carroll *et al.*, 2007; Decker, 2012). DF transmits from person to another person by bites from the *Aedes* mosquito, which receives the virus from an infected person. The virus replicates in the mosquito body and is transmitted into another person's body that the mosquito bites. The presence of *Aedes* mosquito in urban areas is due to the fact that *Aedes aegypti* mosquito lays its eggs in water tanks rather than ponds or ditches. In the outbreak occurred in United States in 2001, it has been revealed that, the *Ae. albopictus*, *Ae. polynesiensis*, and *Ae. Scutellar* Mosquitoe also capable of transmitting DF, while only

Ae. albopictus is discovered during the Hawaiian epidemic (Bakshi, 2007; Decker, 2012; Guzman & Kouri, 2003).

2.2 History of dengue fever

The first report for the disease similar to DF was in the late 18th century, and it was a temporary outbreak. It was suggested that DF originally is transmitted by travel and commercial shipments between Asia and South America. The DF pandemic that took place following the World War II was due to the environmental damage, displaced people, and discarded military equipment that became hosts for insects' reproduction. In the 20th century, DHF/DSS was recognised as a diagnostic symptoms for dengue disease. After that, the cases have globally increased and dengue disease has spread to other regions of the world (Guzman & Kouri, 2003).

Deadly dengue infection was first reported in an outbreak in the capital Manila, Philippines in 1953-1954. During a period of 10-15 years, it had developed to endemic throughout Southeast Asia. In Singapore, the first epidemic was in 1960 and in that outbreak, both older children and adults infected with a low mortality. However, a harsh epidemic of Dengue/DHF happened in Delhi in 1996 and about 10,252 cases were reported and there were 423 deaths (Bakshi, 2007). An international mutual work was in 1949 to minimize the mosquito reproduction, which subsequently decreased the number of DF cases. However, the reduction in use of the anti-insects dichlorodiphenyltrichloroethane (more commonly known as DDT) led to the rising in DF cases in 1970 and it was one of the most pandemic diseases (Decker, 2012).

Although the WHO data between 1992 and 1998 show that South East Asia has had a stable number of DF cases, the rate of infected cases in the Western Pacific has raised 4

fold. The infected patients' number in the Americas has increased 8fold during the same period. WHO in 1980 announced that 1,033,417 is the number of DF cases in the American region. By 2002, the number had increased to 8,491,416. Currently, about 100 countries have endemic DF, with an expected 100 million infected cases yearly (Decker, 2012).

2.3 Geographic distribution of the disease

The regions with the highest rate of DF infections are in the Asia–Pacific region, both central and south America and southeast of the Gulf of Mexico. In Africa, dengue is found to be less frequent and this may be due to the dry environment in this region which is unsuitable for mosquito's reproduction. In 2009, dengue re-emerged in Florida after a 75-year absence. In 2010, epidemics have been declared in the Philippines, the Caribbean, Central America and Sri Lanka. It is predicted that in year 2020 the transmission via travellers would rise, while the rate of international arrivals are to hit approximately 1.6 billion, particularly in the common tourist destinations (Ashley, 2011). DF can be found in subtropical and tropical regions because climate can help the reproduction of *Aedes* mosquito which incubates the dengue virus in its body. Congested urban areas with unsuitable hygiene can affect outbreaks of DF (Decker, 2012). Global warming and climate changes could support the spread, prevalence, and geographic range expanding of DF. Warming global temperatures increase the risk of DF infections by increasing the rate of rainfall and habitat for vectors (Decker, 2012).

2.4 Dengue fever symptoms

Dengue fever disease presents with diverse symptoms, from mostly no symptom to

severe disease. Secondary infection with another serotype of the dengue virus can lead to an endothelial leak and bleeding, which are symptoms of dengue haemorrhagic fever (DHF). Unfortunately, a small number of patients with DHF can develop circulatory failure and refractory shock, which is known as dengue shock syndrome (DSS) and can lead to death. Nevertheless, DHF and DSS based on the disease serotype possibly happen with a first dengue infection (Bakshi, 2007). The mortality rate for (DSS) dengue is reported as being about 1-5% (Ashley, 2011). The incubation period of dengue fever after the mosquito bite is commonly 4 to 7 days, and the range for incubation period is 3-14 days. Normally, the DF appears with a high fever that could reach 39ºC or even higher (Bakshi, 2007).

Typically, spots can be observed on the skin of infected patient. The symptoms of nausea, vomiting, harsh muscular pain and headache could also occur (Ashley, 2011; Dale Carroll *et al.*, 2007). DHF is known mainly through the haemoglobin concentration, hemorrhagic symptoms and vascular leakage, and could subsequently cause death for patient. Inadequate information is received about the disease development to dengue hemorrhagic fever (DHF). Nevertheless DHF could develop because of the viral virulence antigen, host hereditary and acquired factors, multiple infections and immune pathological reactions (Chen *et al.*, 2007).

2.5 Dengue fever diagnosis methods

Several types of diagnostic tests are used for detecting the dengue virus. The traditional diagnostic technique for dengue virus is isolation in cell culture, serological testing, PCR methods and, more recently, immunochromatographic test (ICT) for the rapid detection of NS1 antigen. Moreover, biosensors have gained a

growing attention in recent years in medicine and nanotechnology (Figure 2.1).

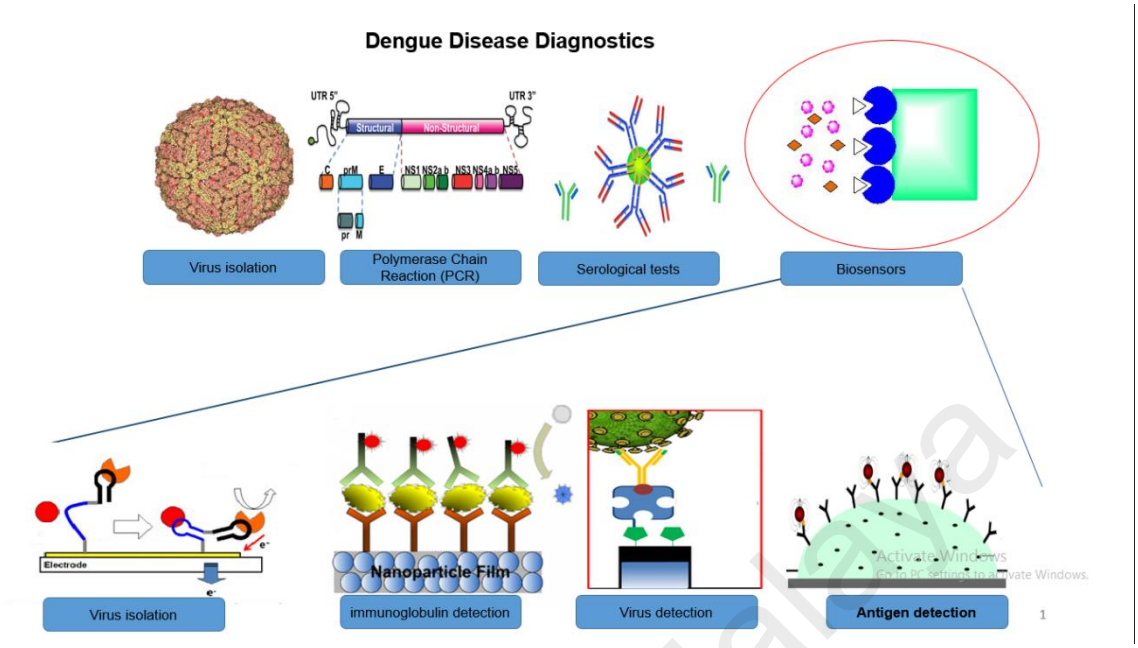

Figure 2-1: Dengue disease diagnostic method

2.5.1 Dengue virus isolation method

The commonly known test to identify the dengue virus is virus isolation in a cell culture or live mosquitoes, and this test has been known as the ideal test during the last century (Wright & Pritt, 2012; Yamada *et al.*, 2002). Isolated viruses can be used for genomic analyses, which could also help to give molecular epidemiological data by further examining isolated viruses. Therefore, virus isolation can provide extra information about the patients. Although virus isolation is recommended as the most reliable diagnostic test in some of the scientific research, it is boosted by using dengue type-specific monoclonal antibodies for immuno-fluorescent staining, and the results showed that virus isolation can be applied as a part of the detection process (Henchal *et al.*, 1983). The viral isolation has been proven to be more effective than the PCR technique; however, this point of efficiency and sensitivity can be approached only if the patient's sera samples are collected before the fever

onset (Suwandono *et al.*, 2006; Yamada *et al.*, 2002). Even though the specificity is 100% for both virus isolation and RT-PCR, the viral culture sensitivity technique was shown to be only 63% (Kumaria & Chakravarti, 2005). Moreover, virus isolation needs expensive laboratory equipment and chemicals to preserve the cell line and requires time from days to weeks; a successful isolation depends on several reasons, such as low numbers of viable virus, unsuitable preparation of samples, and construction of virus-antibody complexes (Raengsakulrach *et al.*, 2002). Therefore, the diagnosis by virus isolation varies from 20% to 80%, because only active virus can be reproduced in the cell culture, and this feature is highly dependent on the specimen collection (Dash *et al.*, 2008; Kumaria & Chakravarti, 2005).

2.5.2 Dengue virus detection by polymerase chain reaction (PCR)

The technique of polymerase chain reaction (PCR) is an amplification of DNA to produce cDNA from a target RNA through a reverse transcription reaction; PCR has been applied worldwide for robust and sensitive detection of dengue viruses and other infectious diseases. Numerous (RT-PCR) protocols have been presented to diagnose and identify dengue serotypes in clinical samples (Deubel *et al.*, 1990), (Morita *et al.*, 1991), (Lanciotti *et al.*, 1992), (Chang *et al.*, 1994), (Seah *et al.*, 1995), (Yenchitsomanus *et al.*, 1996), (Meiyu *et al.*, 1997), (Sudiro *et al.*, 1998), (Harris *et al.*, 1998), (Laue *et al.*, 1999).

The clinical samples used in the past studies were taken from different sources, such as sera (De Paula *et al.*, 2004), plasma (Hue *et al.*, 2011), tissue from fatal cases (Rosen *et al.*, 1989), mosquitos (Muller *et al.*, 2010), infected cell cultures (Liew & Chow, 2006), CNS (central nervous system) (Tahir *et al.*, 2006), saliva and urine (Mizuno *et al.*, 2007), and from blood dropped onto filter paper (Prado *et al.*, 2005).

Those protocols are different in the RNA purification step, primer sites, methods to detect the RT-PCR products, and methods of virus typing. The most significant factor for the success of the PCR protocol is to use the most conserved coding region, but it is difficult to identify the right conserved coding region because of the viral genome variability. Different regions in the dengue genome have been suggested for the PCR technique, such as the capsid region (C), envelope protein (E), prM region and non-structural proteins NS1, -NS2A, -NS2B -NS, -NS5 (Guzman & Kouri, 2004; Raengsakulrach *et al.*, 2002).

The dengue virus 3′-noncoding region (3′-NR), which has nearly 400 bp, is presented as the most conserved sequence for serotypes and serotype-specific detection sequences (Houng *et al.*, 2001). Other factors that also have a strong effect on the PCR sensitivity are the quantity of nucleic acid used for amplification step (De Paula *et al.*, 2004), the PCR parameters such as time and temperature used in protocol and the efficiency of the enzymes (Raengsakulrach *et al.*, 2002). Gamma irradiation could also have a significant effect on the sensitivity of the polymerase chain reaction (PCR) protocol. The diagnostic protocol used to detect long amplification products, is less sensitive as compare to procedures used to detect short amplicons. The influence of gamma irradiation was noticed when a 2050 bp RNA sequence in a Nested RT-PCR was employed as no remarkable damage was observed to the specimen of < 600 bp prepared and treated by a gamma irradiation and tested by real time PCR (Lemmer *et al.*, 2004). Furthermore, some of the RT-PCR protocols have PCR inhibitors such as antibiotics and haemoglobin, which might clarify the loss of sensitivity due to their direct binding with DNA or DNA polymerases (Barkham *et al.*, 2006; Prado *et al.*, 2005). The thermal cycler type used in PCR procedure can also effect the amplification step (Raggi *et al.*, 2003). Even though false positive results and cross reactivity can be avoided by excluding

sequences that are found in the dengue virus nucleic acid, such as the DNA/RNA of the human, mosquito and contaminants during the primer designs (Anez *et al.*, 2008). Many of the RT-PCR protocols have two problems: a false negative result because of the genomic difference in the DENV serotypes and the nonexistence of a standard protocol. Furthermore, PCR can only detect DF infection during the early stage of the infection, and it is not efficient anymore after 5-7 days. Moreover, using RT-PCR for dengue detection is not appropriate in an endemic region because it needs expensive reagents, apparatuses, and laboratory technicians with high level of skill.

2.5.3 Dengue virus detection by serological tests

The word "serology" typically is used to describe the diagnostic identification of antibodies or antigen in the serum and other body fluids. IgM, IgG and more recently NS1 are mostly used in serological diagnostic tests. In the primary dengue infection, the body immune response is usually characterized by a slow and low-titer of produced immunoglobulins. The increment of the IgM antibody starts by days 3-5, and the IgG is quantifiable only after 5-7 days of the sickness. The IgM titers in subsequent infection rise much more slowly than IgG titers level and could cause in false negative result. However, IgG levels increase rapidly in the second infection and might be detected during the acute phase of the illness. Immunoglobulin G levels could persist for several years and show high cross reactivity with other flaviviruses (Guzman & Kouri, 2004).

The Hemagglutination-inhibition (HAI) test has been usually used to distinguish between primary and secondary dengue infection (Rivetz *et al.*, 2009). However, HAI test is not able to detect the serotyping of the dengue viral infection and is not

available as a commercial test kit (Wright & Pritt, 2012). MAC-ELISA-IgM is used to detect dengue-specific IgM antibodies in the infected patient's sera by immobilization of IgM, where the anti-human IgM antibody is first immobilize on the ELISA wells (Vazquez *et al.*, 2003). False-positive results in this test have mainly been attributed to cross-reactivity with co-circulating antibodies and in the serum of patients with malaria parasites or leptospirosis and in patient's sera from other flaviviruses, such as Japanese encephalitis (Guzman & Kouri, 2004) (A-Nuegoonpipat *et al.*, 2008).

One of the serological tests to detect the anti-dengue IgG is the MAC-ELISA anti-dengue IgG detection test and it is also carried out by immobilizing IgG via anti-human IgG antibody that earlier was fixed on the ELISA plate wells. Nevertheless, dengue-specific IgG tests are less specific than IgM because they are cross-reactive and have no conserve epitopes among the 4 dengue serotypes, unlike IgM, which binds only with epitopes of the current infecting serotype (Guzman *et al.*, 2010). The efficiency and specificity of conventional serological techniques for dengue diagnosis highly depend on several factors, such as the quality of the used antigens that are applied with the ELISA method, the collected specimen type (*e.g.*, serum, whole blood, and saliva), the dengue virus serotype (Wright & Pritt, 2012) and the IgM and IgG level (De Paula *et al.*, 2004). Immunochromatography test (ICT) e.g. dengue NS1 Ag STRIP Kit is also used for rapid detection of NS1 antigen. The strip in ICT has two detection lines: a control line (C) which contains biotin e gold colloidal particles coated with streptavidin' complex and a test line (T) which contains (monoclonal anti-NS1antibodies (mAb) NS1 Ag gold colloidal particles coated with anti-NS1 mAb' complex). The presence of both T and C lines after incubation with serum sample suggests a positive result. Even though this test is simple to be carried out in any laboratory and it offers good specificity, its

sensitivity may vary depending on serotype of the dengue virus and type of infection (primary and secondary infection) (Huang *et al.*, 2013; Shenoy *et al.*, 2014) and immunochromatography test can be less sensitive or less precise compared to PCR test (Huang *et al.*, 2013).

In conclusion, serological tests using IgM and IgG are potentially cross reacting with other co-circulating flavivirus antibodies due to either prior infection or vaccination (*e.g.,* Japanese encephalitis virus, Powassan/Deer tick virus). Additionally, these tests need two sera specimens (taken in the acute and convalescence stages of infection) (Watthanaworawit *et al.*, 2011). Due to these restrictions, more than one test is needed to be done beside the serological test to confirm the infection in the patient's serum (*e.g.*, NS1 antigen ELISA, IgM antibody ELISA and/or rRT-PCR) (Teles, 2011; Watthanaworawit *et al.*, 2011). NS1 antigen detection test should be also used as complement test, because the sensitivity of DF detection can be increased when it is done along with IgM capture ELISA test (Shenoy *et al.*, 2014; Zhang *et al.*, 2014).

2.5.4 Dengue virus detection by biosensors

For dengue fever diagnosis by using biosensor, diverse analytes were used such as RNA, cDNA, IgM, IgG, glycoprotein-E, NS1 protein and viral particles, where different types of biosensors have been utilized to detect these biomarkers initially including the piezoelectric biosensor. The principal of piezoelectric biosensor depends on using an oscillating voltage at the resonance frequency of the piezoelectric crystal and detecting the frequency alterations according to the required analyte bins with biomolecules on the crystal face. The piezoelectric sensors are usually classified into three types: quartz crystal microbalance (QCM),

surface acoustic wave (SAW) and bulk acoustic wave (BAW). The second type of biosensors is optical biosensor which works based on converting a natural reaction by an optical signal, such as the absorbance, fluorescence, chemiluminescence, of surface plasmon resonance, to measure the reflective change in the light (Kryscio & Peppas, 2012). Third, electrochemical biosensors are based on the detection of the analyte by labelling or tagging an essential element in the electrochemical reaction (Table 2.1). Commonly used labels might be enzymes (*e.g.*, peroxidase, glucose oxidase, alkaline phosphatase or catalase) or ferrocene or In^{2+} salts, and redox mediators (e.g., $K_3Fe\ [(CN)]_6^{3-/4-}$; methylene blue). Electrochemical sensors can be categorized into diverse types according to their mode of measurement, such as potentiometric (voltage), amperometric (current), impedimetric (impedance), conductometric (conductance) and field effect transistors (voltage) (Kryscio & Peppas, 2012). The advantages, disadvantages, limitation and challenges for these types of biosensor have been presented in Table 2.1.

The electrochemical biosensor has been selected for this study due to its high sensitivity suggesting that electrochemical biosensor can detect the analytes at very low levels of concentration. Electrochemical biosensors also are low in cost and easy to fabricate especially when label-free technique was utilized (Table 2.1). The electrochemical impedance spectroscopy (EIS) was used in this work because this technique is sensitive in data analysis and analyte quantification. Electrochemical Impedance Spectroscopy (EIS) has many advantages in comparison with other electrochemical techniques. EIS is a non-destructive method for the evaluation of a wide range of materials because a small amplitude ac signal is applied to system being studied such as coatings, anodized films and corrosion inhibitors.

Moreover, it can also provide detailed information of the systems under examination; parameters such as, electrochemical mechanisms and reaction kinetics and detection of localized corrosion (El ouadi *et al.*, 2014).

Table 2.1: Classification of biosensors for dengue virus detection

Biosensor type	Advantages	Disadvantages	Limitations	Challenges	Reference
Piezoelectric	Sensitive due to the high elastic modulus, cost effective for imprinted polymers as no monoclonal antibodies are used.	Inadequate recognition properties in imprinted polymers.	High detection limit of analyte.	Increase the oscillation level.	(Su *et al.*, 2003),(Wu *et al.*, 2005),(Tai *et al.*, 2006),(Chen *et al.*, 2009).
Optical	Potential in low detection limits and useful for screening a large number of samples concurrently.	Need costly microscope equipped with fluorescence filters, other electronics and a computer to calculate and quantify the fluorescent signal.	Long time required for labelling the analyte.	Label free detection.	(Atias *et al.*, 2009; Baeumner *et al.*, 2002; Fletcher *et al.*, 2010; Kumbhat *et al.*, 2010; Lee *et al.*, 2009; Melendez *et al.*, 1997; Zaytseva *et al.*, 2005).
Electrochemical	High Sensitivity, Simplicity and low cost.	Labelling target analyte requires more time.	Limited size of the electroactive area.	Boosting the interface of biorecognition element with the electrode surface.	(Andrade *et al.*, 2011; Dias *et al.*, 2013; Gole *et al.*, 2001; Oliveira *et al.*, 2009a, 2009b; Oliveira *et al.*, 2011; Wang *et al.*, 2007).

2.5.5 Biosensor types for dengue virus detection

2.5.5.1 Biosensors based on genomic detection

Biomarkers of dengue virus was classified and included in Table 2.2. In the studies carried out by Baeumner *et al.* (Baeumner *et al.*, 2001; Wu *et al.*, 2001), the nucleic acid sequence-based amplification (NASBA) technique has been further improved (Baeumner *et al.*, 2002) by utilizing electrochemiluminescence and liposome amplification. The reporter (DNA probe) is linked to the exterior of dye-covered liposomes. The capture probes (dengue serotype-specific probes) are immobilized on a strip of polyethersulfone membrane. An amplified target sequence is added to the liposomes and is then introduced to the membrane. After the migration of the mixture, the liposome-target sequence couples are captured in the capture zone by hybridization of the target sequence with a capture probe. The quantity of the target sequence is indirectly estimated by the liposome amount, which can be measured with a reflectometer device. Serotypes 1, 2 and 4 were detected; nevertheless, serotype 3 showed slight cross reactivity with biosensors that were prepared for the detection of serotypes 1 and 4. However, detecting nucleic acid by using NASBA assay needs high and professional technical skills (McBride, 2009), Moreover, it was shown in a comparative study between NASBA and RT-PCR for virus diagnosis that the NASBA assay produced less reliable signals for target biomarker (Houde *et al.*,2006)

Table 2.2: Classification of dengue virus analytes

Detection Mode	Advantages	Disadvantages	Challenges	Limitation	References
Genomic	Able to discriminate between dengue virus serotypes.	Required high technical skill for nucleic acid isolation.	Instability of viral nucleic acid.	Detection within viremia phase only.	(Baeumner *et al.*, 2002; Chen *et al.*, 2009; Fletcher *et al.*, 2010; Iqbal *et al.*, 2000; Kwakye *et al.*, 2006; Martins De Souza *et al.*, 2009; Nascimento *et al.*, 2011; Rivet *et al.*, 2011; Teles *et al.*, 2007; Zaytseva *et al.*, 2005).
Immunoglobulin	Easy sample preparation from patient sera.	Required pair of specimens (from viremia and convalescence phases). Cross-reactivity with co-circulating flavivirus antibodies.	Prolonged time for primary and secondary antibodies' incubation and blocking steps.	Primary dengue infection is characterized by a slow and low titer of IgG antibody response. IgG antibodies rise rapidly in second infection.	(Atias *et al.*, 2009; Kumbhat *et al.*, 2010; Lee *et al.*, 2009).
Virus particle	Only specific for dengue virus detection.	Detection for only specific dengue serotype.	Virus sensing by specific binding of dengue viral particles to its serotype 2-specific immunoglobulin G antibody within the thin alumina layer.	Detectable within viremia phase only.	(Cheng *et al.*, 2012; Nguyen *et al.*, 2012).
Antigen	Easy sample preparation from patient sera.	Cross-reactivity with both co-circulating flavivirus antibodies IgM and IgG.	To immobilize the antigen on the electrode surface with high intensity and high activity.	Specific to one analyte such as virus glycoprotein, envelope protein (E-protein) and NS1.The electrode modification's compound has to react with different glycoprotein pattern in investigated sera.	(Andrade *et al.*, 2011; Cavalcanti *et al.*, 2012 b; Dias *et al.*, 2013; Oliveira *et al.*, 2009a, 2009b; Oliveira *et al.*, 2011; Su *et al.*, 2003; Wu *et al.*, 2005).

A microfluidic biosensor design based on using RNA hybridization and fluorescence detection was proposed for dengue RNA diagnosis. In this biosensor, magnetic beads were utilized to immobilize the capture probe, and the reporter probes were linked to liposomes (Figure 2.2). When a dengue nucleic acid is existing, then a homology is happening between the capture probe and the specific nucleic acid on one side and the reporter probe and the same RNA molecule were on the other side. Then, when the specific sandwich is assembled, the detection will be done by the binding of liposomes with encapsulated fluorescent dye *via* fluorescence microscopy through the addition of the detergent solution (*n*-octyl B -D-glucopyranoside, OG). The RNA detection sensitivity was 0.125 nM and 50 pM for intact and lysed liposomes, and this proposed biosensor could discriminate between the four dengue virus serotypes (Zaytseva *et al.*, 2005).

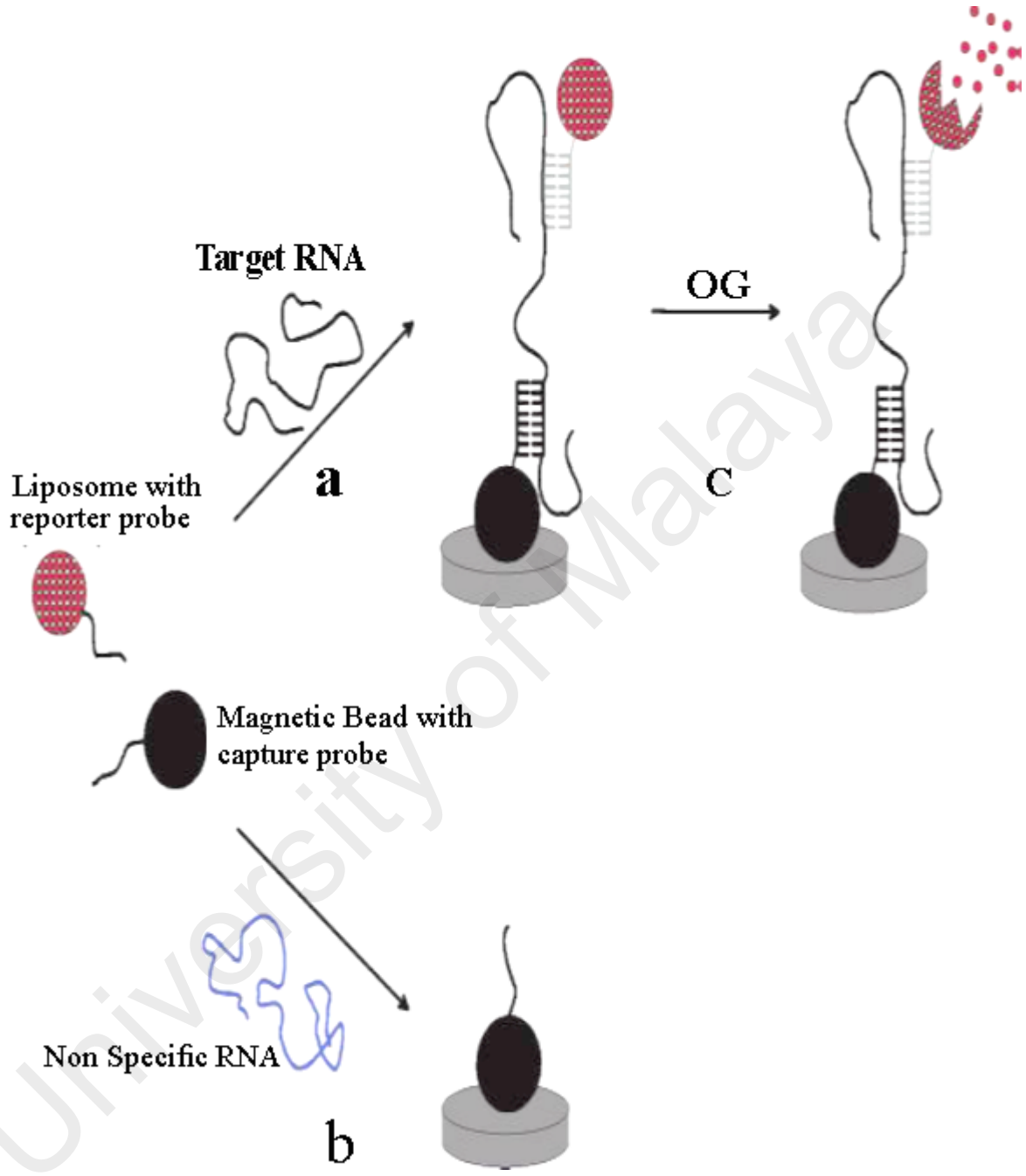

Figure 2-2: Recognition principle and detection schemes used in the biosensor.
When a specific dengue RNA is present (a), a sandwich is formed between the reporter probe, the RNA molecule, and the capture probe. The specific complexes are detected by intact liposomes with encapsulated fluorescent dye by means of fluorescence microscopy. Upon addition of the detergent solution (n-octyl β-d-glucopyranoside, OG), the liposomes release the fluorescence molecules (c) and the fluorescence signal is detected at the time when lysed liposomes pass the detection zone. No signal is detected in the presence of nonspecific RNA (b). Retrieved from ref. (Zaytseva *et al.*, 2005). Copyright 2005. American Chemical Society.

Electrochemical biosensors to detect dengue virus nucleic acid have also been proposed. An electrochemical microfluidic biosensor (miniEC) has been used to replace fluorescence detection with an electrochemical detection design. Liposome signal amplification for hybridized RNA in an integrated minipotentiostat device has also been prepared by utilizing short sequence DNA probes that have homology with the nucleic acid RNA or DNA. In this microfluidic biosensor (miniEC), magnetic microbeads were linked to a capture probe, while the reporter probe is linked to redox label-entrapping liposomes. When the nucleic acid is detected, the lyposomes produce the redox marker and then cause signal amplification. The miniEC biosensor reached a diagnosis limit that is 10× lower than that of the lab-bench method (Kwakye *et al.*, 2006). Employing the microfluidics is useful due to the fact that they require a small quantity of sample, which will subsequently decrease the quantity of the reagents required to do the detection test. Additionally, biosensor based on a microfluidic system could improve the efficiency and decrease the cross contamination by assembling it with sensing parts (Rivet *et al.*, 2011). Nevertheless, microfluidic biosensors were believed to be more competent if microfluidic protein/enzyme based pathogen sensing or microfluidic cell-based pathogen sensing was used instead of using nucleic acid analytes because of the long process of nucleic acid isolation and analysis (Mairhofer *et al.*, 2009).

A circulating-flow quartz crystal microbalance (QCM) is also proposed to detect the dengue nucleic acid in clinical sera sample that contains the dengue virus (Chen *et al.*, 2009). Two types of gold nanoparticles were attached to QCM by the target sequences to amplify the signal upon DNA capturing. The amplified sequences work as a link for the layer-by-layer AuNPs probes' hybridization in this device. The result of DNA-QCM biosensor showed that it is able to diagnose the virus in sera that contains only 2 PFU mL^{-1} with high sensitivity and specificity. However, DNA-

QCM biosensor needs high technical skills in cultivation of the virus and nucleic acid extraction (McBride, 2009).

Electrochemical genosensor to detect the dengue virus RNA was presented by Teles *et al.* (Teles *et al.*, 2007). In this model, ferrocene as an electroactive indicator was used based on its special adhesive to single DNA strands. Complimentary DNA was placed on the chitosan glassy carbon electrode (GCE) surface. Voltammetric detection is based on ferrocene adhesion and the hybridization between the two strands. In another model of genosensors, Martins *et al.* (Martins De Souza *et al.*, 2009) prepared pencil lead graphite as an inexpensive and renewable electrode. A DNA probe with a complimentary sequence was electrostatically immobilized on the pencil lead graphite electrode surface that was synthesized with poly-L-lysine solution. Electrochemical sensing of hybridization between the probe and target was conducted by applying differential pulse voltammetric (DPV) and sweeping the electrode potential technique between -6 and 0 Volt, using methylene blue as a hybridization label. To test the specificity, the prepared biosensor was tested with poly-L-lysine and the result showed no current peaks, suggesting that the polymer material did not interfere with the result. At the same time, the electrode tested with modified oligonucleotides showed current peaks in the potential range that is the characteristic of an oxi-reduction process between DNA guanines and methylene blue (Martins De Souza *et al.*, 2009). The polymer material had no effect on the result because only the working electrode, which has been tested with oligonucleotides, showed current peaks and no signal was obtained when testing the biosensor with a poly-l-lysine. Nevertheless, to avoid false negative results, a high level of optimization is required to find the optimum condition and to produce the detection signal by hybridization between the probe and the complementary DNA strand (Iqbal *et al.*, 2000).

To discriminate between different dengue serotypes in patients' sera at picomolar levels, a complex of gold nanoparticles-polyaniline hybrid and SH-terminal groups were bonded to three dengue serotype-specific primers 3 AuNpPANI-ST (1–3). These primers with complexes were able to identify the dengue nucleic acid in the sample of infected sera at picomolar levels. The results of CV and EIS techniques showed a homology between the primers and their complimentary DNA (Nascimento *et al.*, 2011). The Pan region, the shared sequence in the four serotypes in addition to the particular sequence for each serotype, was revealed by a modular fluorescent biosensor. This genomic biosensor has linkers (target complements and triggers). When link happens between the linker and the targeted DNA, the trigger links to the aptamer and releases nuclease. Afterwards, the signaling molecule is produced (Fletcher *et al.*, 2010). A silicon nanowire (SiNW) was used to prepare a label-free biosensor. In this model, the sensor interface was covalently attached to a specific peptide nucleic acid (PNA) that is complementary to the DEN-2 (69 bp) sequence. The electrical measurement is calculated by finding the change in the resistance before and after the hybridization. The ability of this label-free biosensor to detect DEN-2 even in the un-purified RT-PCR was claimed. Even though this module is specific for only one serotype, a label-free biosensor is beneficial in avoiding the gradual leakage of the label, and also it can be used in care applications, and additionally, this design is cost effective (Zhang *et al.*, 2010). However, the limitation for all of these genomic biosensors is the stability of the viral nucleic acids and also the limitations in detecting DF only within the viremia stage (Su *et al.*, 2003).

2.5.5.2 Biosensors based on immunoglobulin detection

In many studies, optical biosensors have been suggested for detecting immunoglobulins in the dengue patient's sera. Optical biosensors and fluorescence-based transducers are relatively pricy, but they have advantages of low detection limits and optical biosensors which make them suitable for screening a large number of samples alongside (Kwakye *et al.*, 2006). Chemiluminescent optical fiberimmunosensor (OFIS) has been prepared to detect anti-dengue (IgM) in human serum specimens (Atias *et al.*, 2009). In this proposed biosensor, a colorimetric IgM detection *via* (MAC-ELISA) is used (Figure 2.3). The detection procedure in OFIS requires several steps (the addition of goat anti human IgM, mouse anti Den, goat anti mouse IgG-HRP conjugate and dengue antigen) to detect the analytes. However, OFIS is a commendable design as the result showed that it is sensitive and comparable to chemiluminescent MAC-ELISA and the colorimetric MAC-ELISA by 10 and 100 times, respectively, and the chemiluminescent with OFIS might be more efficient, if used in the early phase of DF infection to detect viral envelop protein, membrane or non-structural protein such as NS1 antigen.

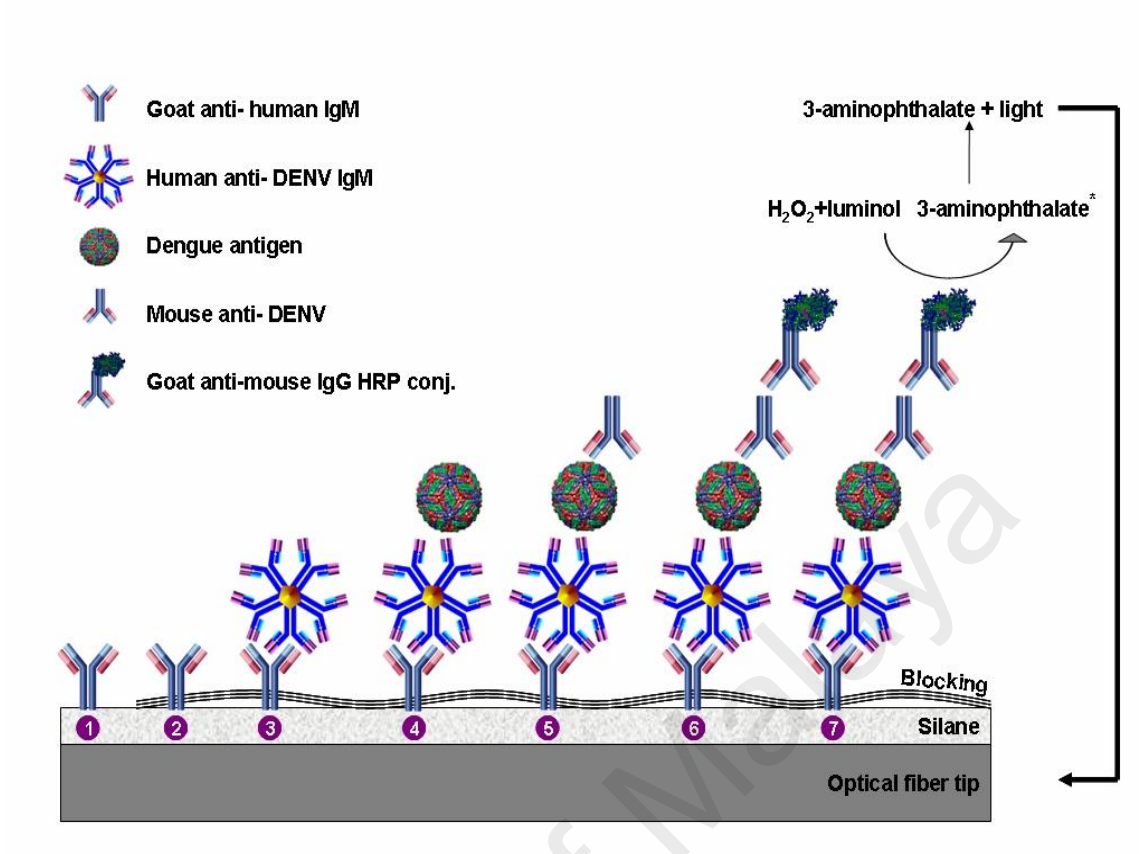

Figure 2-3: Biosensor assembly on the modified optical fiber immunosensor (OFIS). (1) Ester moiety of the cross-linker allows covalent linking of the capture antibody through the amino group. (2) Adding blocking reagent to minimize non-specific binding. (3) Serum sample is tested for anti-DENV- IgM. (4) Detecting specific anti-DENV IgM via DENV-2 antigen. (5) Introducing mouse anti-DENV antibodies. (6) Chemiluminescent detection of goat anti-mouse IgG. (7) Luminous signal is developed and reflected into the optical fiber. Retrieved with permission from ref. (Atias *et al.*, 2009). Copyright 2009 Elsevier B.V.

An innovative biosensor was presented by using integrated fluorescent immunoassay (FIA) and a microfluidic system. In this biosensor, a magnetic bead-virus complex was utilized for rapid identification of the immune-globulins IgM and IgG during a dengue infection. This novel microfluidic device consists of one-way micro-pumps, a four-membrane-type micro-mixer, two-way micro-pumps and an on-chip micro-coil array, to simultaneously achieve fast serological analysis of both (IgG) and (IgM) antibodies. The detection is made by calculation of the concentration of secondary antibodies with labelled fluorescence *via* using an optical detection module. The detection time was about 30 min, and the detection limit was 21 pg

(Lee *et al.*, 2009). FIA is a valuable biosensor because of its ability to detect two analytes at same time, and it can be more useful if the two analytes represent the two phases of dengue infection: the viremia phase (by detecting RNA or one of the dengue antigens) and the fever phase, which begins with the fever symptom (by detecting IgG or IgM).

Label-free and real-time assay SPR phenomenon is used in another proposed device to detect the dengue virus IgM optoelectronically: the dengue virus antigen (the name not mentioned in this research paper) was used as the sensing element by using a golden sensor chip to capture the viral antigen *via* a self-assembled monolayer (SAM) of 11-mercaptoundecanoic acid and amide coupling (Kumbhat *et al.*, 2010). In the SPR phenomenon, when a biomolecule is bonded to a metal surface, changes happen to the refractive index and to the angle of incidence, which afterward causes SPR excitation (Melendez *et al.*, 1997). There is a resonance angle in a direct immunoassay that shows the existence of IgM antibodies in infected sera (Kumbhat *et al.*, 2010).

2.5.5.3 Biosensors based on dengue virus particles detection

Detection of dengue virus type 2 virus (DENV-2) cells was claimed by using a nanoporous alumina-modified platinum electrode (Cheng *et al.*, 2012). This model of detection is based on detecting the electrode's Faradaic current response to the redox probe, ferrocenemethanol. The electrochemical signal is responsive to the immune complexes reaction between the tested dengue virus and its monoclonal antibody immobilized, inside the alumina nanochannels (Figure 2.4) (Cheng *et al.*, 2012). This electrochemical immunobiosensor was sensitive to detecting DENV-2 in 1 pfu mL^{-1}, but it was not able to respond to the other serotypes even when pfu was

10^3 mL^{-1}, however, this nanobiosensor can be used for mosquito surveillance in the field. In another suggested biosensor, a nanoporous alumina biosensor was utilized to measure the response toward the specific binding of dengue serotype 2 (Denv2) viral particles to its serotype 2-specific immunoglobulin G antibody inside a thin alumina layer by using the Faradaic electrochemical impedance technique. The detection sensitivity in nanoporous alumina biosensor was similar to nanoporous alumina-modified platinum electrode with 1 pfu mL^{-1} detection limit (Nguyen *et al.*, 2012). Although the impedimentary-based biosensor needs a long time to monitor a whole spectrum in a wide frequency region, it could still be potential and find a market because it is portable and can be used in field of infection. Moreover, it has a low cost and acceptable sensitivity (Teles, 2011).

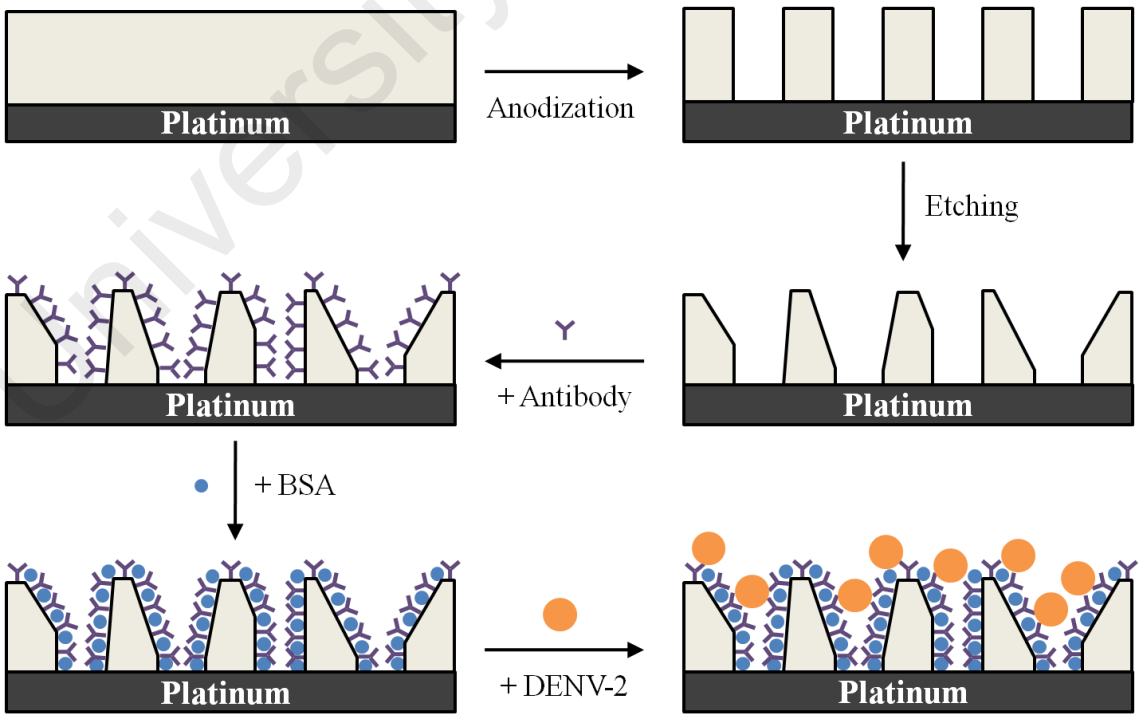

Figure 2-4: Design of membrane-based electrochemical nanobiosensor
Retrieved with permission from ref. (Cheng *et al.*, 2012).Copyright 2012 Elsevier B.V.

Lately, an immunocapture-based biosensor was presented by Chen and his colleagues (Chen *et al.*, 2013) for detecting DV1 by coating magnetic beads with monoclonal antibody against DV1 E protein and with the complex of magnetic beads- monoclonal antibody attached to matrix, which were prepared by a seed layer method to be suitable for protein detection by matrix-assisted laser desorption/ionization time-of-flight mass spectrometry (MALDI-TOF MS). The DV1 detection limit was 105 pfu mL^{-1}, which is about 100- to 1000-fold less than the number of particles in DF and DHF patients' sera three days after onset of the dengue disease. However, serotype-specific diagnosis of dengue virus is beneficial in epidemiological studies but not in clinical diagnosis when there might be more than one serotype existing in the infected region.

These studies confirmed that the electrochemical impedance spectroscopy (EIS) is a powerful, sensitive, cost-effective, and easy tools, especially if label-free analyte is detected as the sample requires no treatment prior to analyte detection. Moreover, EIS technique is a helpful technique to study electrical and electrochemical properties by using electrochemical signal transduction and by using EIS and it is easy to monitor electrode surface modifications by investigating the impedance curves. (Lopez Rodriguez *et al.*, 2015; Mozaffari *et al.*, 2014). Therefore, label-free impedimetric biosensor as a simple, sensitive and cost-effective biosensor is proposed in our study to monitor the changes in the concentration of NS1 antigen.

2.5.5.4 Biosensors based on antigen detection

Using gold nanoparticles (AuNPs) with polyvinyl butyral (PVB) (Oliveira *et al.*, 2009b), concanavalin A (Oliveira *et al.*, 2009a), polyaniline hybrid (Andrade *et al.*, 2011) or Fe_3O_4 nanoparticles (Oliveira *et al.*, 2011), all of these designs of

biosensors were applied to detect glycoproteins and immune response products from DF patients who have been infected by the dengue virus by the immobilization of Lectins (proteins or glycoproteins from different sources). Most of the serum proteins are glycosylated if there is any disease infection, and glycoproteins will be changed to abnormal glycoproteins (*e.g.,* liver disease, cancer or dengue fever). These structural changes could help to provide the basis for clinical and diagnostic tests (Turner, 1992). Nevertheless, the presence of these glycoproteins in sera of infected patient might be due to a dengue virus infection or other diseases.

One of the structural proteins, namely envelope protein (Eprotein) has also been used to detect a dengue infection, and a chitosan-carbon fiber electrode (CFE) fabricated biosensor was proposed for this purpose. On the interface of the biosensor, anti DENV antibodies were immobilized on the chitosan (CHIT) matrix. The measurements of this amperometric biosensor showed a sensitive detection with 0.94 ng mL^{-1} (Cavalcanti *et al.,* 2012 b). Nevertheless, E. protein existed in the structural composition of other flaviviruses. Therefore, E. Protein cross reactivity can affect the sensitivity of the assay when it is used in an endemic area where other circulating flaviviruses are existing (CDC, 2010). Piezoelectric-based sensors have been applied in many biosensor researches for dengue antigen detection, and NS1 antigen is one of these antigens. The model quartz crystal microbalance (QCM) has been suggested by Su *et al.* (Su *et al.*, 2003) to detect both NS1 and E-protein *via* a mixture of anti-NS1 monoclonal antibodies and anti-E Protein monoclonal antibodies that are attached to the QCM-immunochip. The QCM is located between two spacers to allow the liquid containing the target analytes to be in contact with only one side and, afterward, this design can help to produce oscillations (Figure 2.5). The measurements showed that the sensitivity was higher by 100-fold than the sandwich ELISA assay and the detection limit for this method was 0.05 µg mL^{-1} (Su *et al.,* 2003).

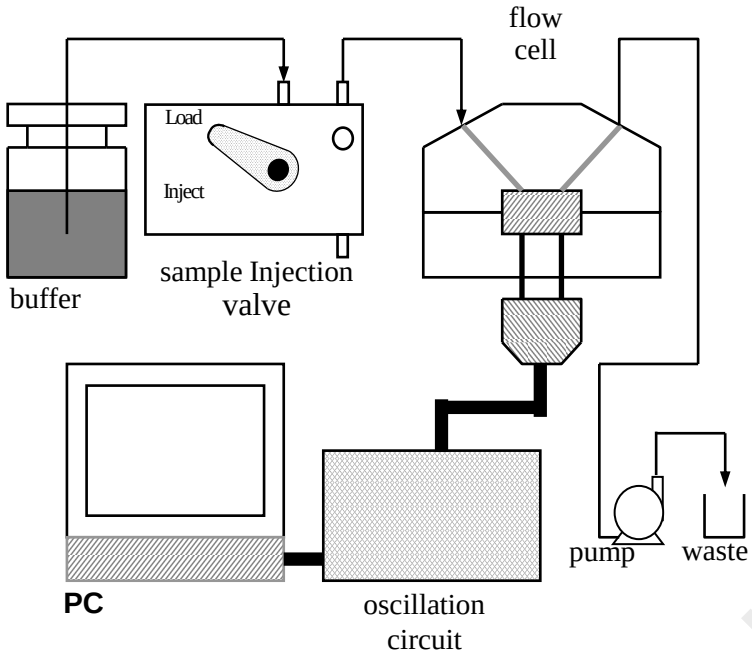

Figure 2-5: Schematic diagram of flow injection system.
Retrieved with permission from ref. (Su *et al.*, 2003). Copyright 2002 Elsevier Science B.V.

To reduce the dilution percentage and to improve the sensitivity limit, Wu and his co-workers (Wu *et al.*, 2005) used the quartz crystal microbalance (QCM) to produce an immunochip by using a couple of monoclonal antibodies((mAb 17-2 for protein E) and (mAb 8-1 for protein NS1)) onto the QCM surface covered with protein A. However, there was no enhancement in the sensitivity as the detection limit in the patients' samples was 1.727±0.291 μg $mL^{-1}$and 0.740±0.191 μg mL^{-1} to dengue E and NS-1 protein, respectively (Wu *et al.*, 2005). Recently, Ana Carolina and her colleagues (Dias *et al.*, 2013) prepared an immunosensor to detect NS1 (a non-structure protein) by immobilizing anti-NS1 antibodies to carbon nanotube-screen-printed electrodes (CNT-SPE) *via* an ethylene diamine film. The detection limit by using this biosensor and a spiked blood serum sample was 12 ng mL^{-1}, and the sensitivity was 85.59 μA mM^{-1} cm^{-2}. The detection limit and sensitivity are very

beneficial for the dengue virus detection if the same detection limit can be reached by using real patient sera. The advantages, disadvantages, limitations and challenges of analyte detection types (genomic, immunoglobulin, antigen and virus particles) have been presented in this study in Table 2.2.

2.6 Non-structural (NS1) protein

Non-structural 1 is detectable in dengue patients sera because it is produced as secreted form in addition to a membrane-linked protein, whereas, other non-structural proteins are produced as intracellular forms (Das *et al.*, 2009). NS1 is about 50 kDa protein with a great conserved sequence (70%) in the flavivirus family and in all dengue serotypes. Glycoprotein of NS1 contains six intra molecular disulfide bonds, twelve invariant cysteine residues and a pair of conserved *N*-linked glycans maturation process (Somnuke *et al.*, 2011).

Non-structural protein1 is initially converted into a hydrophilic monomer which binds to the endoplasmic reticulum (ER). Soluble NS1 is also able to link back to plasmic membrane *via* an association with certain sulphated glycosaminoglycans (GAGs). Eventually, infected cells will present NS1 on their surface, possibly by glycosylphosphatidyl inositol (GPI) linkage, lipid raft interaction or *via* an unknown mechanism (Somnuke *et al.*, 2011) There are numerous researches which confirm that diverse types of NS1 are necessary in the life cycle of dengue virus (Lemes *et al.*, 2005; Somnuke *et al.*, 2011). On the other hand, some researchers revealed that anti-NS1 might provide protection for dengue virus. Undeniably, both (IgG and IgM) anti NS1 antibodies have been found circulating in serum in primary and secondary stages of infection and in different levels (Ramirez *et al.*, 2009; Schilling *et al.*, 2004) (Figure 2.6). In mammalian cells, the NS1 is typically produced in

dimeric form. Even though crystal structure of flavivirus NS1 is not confirmed, some researches stated that secreted type of NS1 is a hexameric barrel with lipids molecules and 12 cysteine residues which make six disulfide bonds (Rozen-Gagnon *et al.*, 2012).

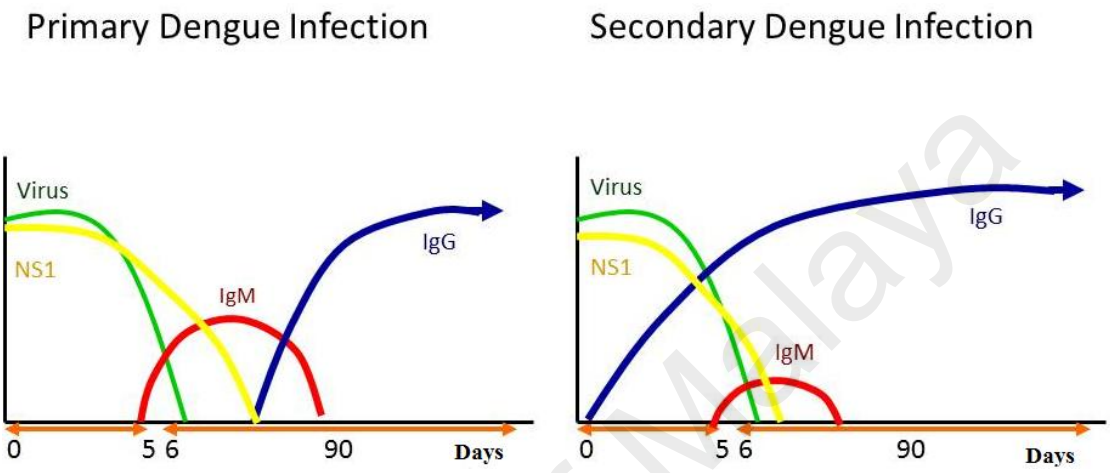

Figure 2-6: Immunological response to dengue infection.
Retrieved from ref. (CDC, 2010). Centers for disease control and prevention.

In most of researches related to studying the structure of flavivirus NS1, bacterial expression system has been used. The bacterial expression is suitable to be used in synthesizing non-glycosylated recombinant proteins because the bacteria are easy to handle. Nevertheless, expression level of numerous eukaryotic genes is low in the *E. coli* because of the toxicity of foreign protein; the difference in codon preference and the mRNA difference and these factors cause low expression level afterward. In bacterial system such as *E. Coli* host, the NS1 is not easy to be found in a soluble form and the post-translationally modifications are not completed during protein expression (Amorim *et al.*, 2010).

To enhance the expressed protein quantity, codon optimization for NS1 gene can be done before cloning into host expression vector (Das *et al.*, 2009) in addition to

optimize the expression by inducer, temperature and time (Volonte *et al.*, 2008). The produced protein can be refolded by applying the best protocols in the three methods: size-exclusion chromatography or by dilution and solvent exchange by dialysis and filtration (Li *et al.*, 2004). To overcome the solubility problem, SUMO star (small ubiquitin-like modifier; S∗) fusion tag can be incorporated in expression system as it has been previously confirmed that this tag can enhance the expressed protein solubility (Rozen-Gagnon *et al.*, 2012).

2.7 Anti- fouling coating in biosensing application

For clinical diagnosis, immunosensors and other types of biosensor are designed to detect disease biomarkers such as nucleic acids, proteins or other disease analytes at very low level of concentrations from complicated clinical sample (Atias *et al.*, 2009; Cavalcanti *et al.*, 2012 b; Chen *et al.*, 2013; Dias *et al.*, 2013; Shiddiky *et al.*, 2012 a). Biofouling is the accumulation of proteins, cells and other biological materials onto a bare electrode surface and such an accretion of undesired substances leads to reduced biomarker detection by reducing the diffusion and perfusion of the biomarker to the sensor interface, which ultimately causes a reduction in sensor response and sensitivity. Polymers such as polyurethane, polyvinyl chloride, poly (dimethylsiloxane) and poly (methacrylate) have been used as antifouling coatings for biosensing surfaces, where they ensure selective transport of a targeted analyte to the biosensing interface while inhibiting biofouling substances from approaching the electrode surface (Akkahat *et al.*, 2012; Chae *et al.*, 2007; Gabriel *et al.*, 2012; Salomon *et al.*, 2012; Wang *et al.*, 2013). Even though these polymers are very efficient in experimental stage, their functional stability is greatly affected by the biocompatibility of the biosensor materials in contact with the biological sample (Brahim *et al.*, 2002; Zhang *et al.*, 2000). Poly (ethylene glycol) (PEG) and self-assembled monolayers with oligo (ethylene glycol) chains

(OEG-SAMs) have been used to inhibit the adsorption of biofouling and non-desired proteins (Yu *et al.*, 2011).

The efficiency of anti-biofouling polymers in complex samples, *e.g.*, human sera, is influenced by several factors, such as the concentrations and chain lengths of PEG and OEG as well as temperature. The modified surface by using these antifouling molecules can attract additional non-specific proteins at 37°C. Furthermore, surfaces grafted with PEG and OEG undergo auto-oxidation in most biochemically relevant solutions for *in vivo* research (Akkahat *et al.*, 2012; Gui *et al.*, 2013 b; Yeh *et al.*, 2007). As other type of antifouling coating, zwitterionic polymers such as phosphorylcholine, sulfobetaine, and carboxy betaine, have been applied as non-fouling substances. Zwitterionic polymers in phosphorylcholine, sulfobetaine and carboxy betaine, contain both anionic and cationic groups. Using zwitterions in anti-biofouling coatings was first done by Hayward and Chapman based on using polymerizable phosphatidylcholines. Phosphorylcholine polymers have been utilized in different applications which need resistance to protein adsorption, mostly implants (Hayward & Chapman, 1984). The incorporation of zwitterionic moieties into alkanethiol SAMs has been carried out by Whitesides and co-workers (Kevin & Whitesides, 1993). Holmlin (Holmlin *et al.*, 2001) has found zwitterionic SAMs containing mixture of two long-chain alkanethiols, respectively. Bearing $-SO^{3-}$ and $-N^{+}(Me)_3$ terminal groups were very effective in resisting protein adsorptions (comparable with OEG SAMs). However, using the long-chains of zwitterionic polymers can lead to producing high-impedance layers and afterward cause losses of electrode sensitivities. On the other hand, short-chain molecules show low stability (Gittens *et al.*, 2013; Gui *et al.*, 2013 b; Shi *et al.*, 2011). Aryl diazonium salt derived layers have been increasingly investigated as antifouling coating to reduce nonspecific protein adsorption because they are stable layers and have good sensing capability. Gooding and co-workers examined zwitterionic phenyl

derivative layers containing charged moieties, such as $–SO^{3-}$ and $–N^{+}(Me)_3$, grafted onto glassy carbon surfaces as a substitute to OEG phenyl layers and found that the deposited zwitterionic phenyl derivative layers provide better chemical stability and a shorter electron transfer pathway to the transducer surface (Gui *et al.*, 2013 b). Therefore, zwitterionic phenyl layers have been suggested in this research as efficient alternatives to conventional antifouling molecules due to their antifouling characteristics. Moreover, zwitterionic phenyl layers do not totally passivate the electrode surface and consequently, they allow faradaic electrochemistry. Henceforth, they can be used in biosensor fabrication. In biomaterials field, indium tin oxide (ITO) as a biosensing substrate has an increasing significance because of its combined properties of transparency, conductivity and biocompatibility (Shah *et al.*, 2009). Very limited number of studies has inspected the use of antifouling molecules on ITO for bioassay application. To date, only hydrophilic polyacrylic acid brushes (Shiddiky, Kithva, Sakandar, *et al.*, 2012 b) and zwitterionic polymer brushes (Li *et al.*, 2012) have been explored as antifouling agents. Nevertheless, in these studies, only negatively charged protein BSA-FITC was utilized to assess the antifouling capability of grafted layer. Therefore, the testing of only a single protein may not represent the complex clinical samples, such as blood plasma and serum that include different types of proteins. In another group of researches, the zwitterionic polymers were grafted onto the ITO surface by using surface-initiated atom transfer radical polymerization (SI-ATRP). Even though the deposited organic coatings showed stability in aqueous solution, the SI-ATRP technique was time consuming and had moderate output (Liu & Su, 2006).

In conclusion, the literature contains no account of research studied the capability of these antifouling moieties after they have been modified along with linker molecules, such as 1,4-phenylenediamine (PPD) or 4-aminobenzoic acid (BAPA). A linker molecule is required for the attachment of biorecognition molecules (*e.g.*, antibodies,

enzymes, DNA, or aptamers) close to the transducer surface. The incorporation of zwitterionic phenyl layers with a linker molecule is useful for improving the selectivity of the biosensing interface, which is resistant to the nonspecific adsorption of proteins, and for providing a shorter response time for specific analyte detection (i.e., low impedance due to a shorter electron pathway).

Electrochemical immunosensor has been used in this study because it is sensitive, simple and low in cost especially when label-free analyte is utilized. Label-free biosensor is useful in order to overcome the gradual leakage of the label, and also it can be used in care applications. Using monoclonal antibodies in this study is expected to help in providing specific detection for analyte because this type of antibody has monovalent affinity and can react to the same epitope as its own antigen. These studies have been stated in literature review confirming that the electrochemical impedance spectroscopy (EIS) is a powerful, sensitive, cost-effective and easy-to-apply technique, especially if label free analyte is detected, as no prior treatment is required for the used sample. Moreover, EIS technique is a helpful technique to study electrical and electrochemical properties by using electrochemical signal transduction. Furthermore, by using EIS, it is easy to monitor electrode surface modifications by observing the impedance curves. Therefore, label-free impedimetric biosensor is proposed in our study to monitor the changes in the concentration of NS1 antigen. The use of nanoparticles in this study was to increase the electrode surface area and boosts the interface with more bio-recognition molecules because it has a high surface-to-volume ratio. Moreover, gold nanoparticles have been introduced to modify the interfaces of the biosensors due to their redox properties and their capability to increase the sensor sensitivity.

NS1 antigen biomarker has been selected for this study because NS1 has many important features. The NS1 antigen is secreted extracellularly from the host cell during the early stage of DF, with concentration up to 50 μg mL^{-1} starting from day 1 until two weeks of infection. This point suggests that NS1 is efficient for early diagnosis and can be detectable before dengue antibodies (IgM and IgG) are produced in patient sera. Moreover, NS1 is stable, conserved in all dengue serotypes. NS1 can be detected in both primary and secondary infections and in both dengue fever (DF) and dengue hemorrhagic fever (DHF).

CHAPTER 3: EXPERIMENTAL PROCEDURES

3.1 Reagents and materials

ITO coated glass slides size 0.7 mm (T) x 355 mm (W) x 406 mm (L)), which had a surface resistance $\leq 7\ \Omega$, was purchased from Sanyo (Japan). Dichloromethane, methanol, potassium carbonate, dimethyl sulfoxide (DMSO), 4-sulfophenyl (SP), 1,4-phenylenediamine (PPD), 4-aminobenzoic acid (BAPA), sodium nitrite ($NaNO_2$), potassium chloride (KCl), potassium dihydrogen phosphate (KH_2PO_4), potassium phosphate dibasic (K_2HPO_4), hydrochloric acid (HCl), potassium ferricyanide ($K_3Fe(CN)_6$), hexamine ruthenium (III) chloride ($Ru(NH_3)_6Cl_3$), sodium carbonate (Na_2CO_3) with 99% purity, 20 nm gold nanoparticles, sodium bicarbonate ($NaHCO_3$), rhodamine B isothiocyanate, bovine serum albumin-fluorescein isothiocyanate (BSA-FITC), cytochrome C (from bovine heart) and 2-[2-(2-methoxyethoxy)ethoxy]acetic acid (OEG), human serum albumin (HAS) and sodium chloride (NaCl) were purchased from Sigma-Aldrich (USA). 4-Trimethylammoniophenyl (TMAP) was obtained from Acros (USA). Human IgG was obtained from Thermo Fisher Scientific (USA). The NS1 antigen and monoclonal anti-NS1 IgG antibody were purchased from Genscript (USA). All solutions were prepared using Milli-Q water (18 $M\Omega \cdot cm^{-1}$) (Purelab, US). Syringe filter (non-sterile, 13 mm diameter) was purchased from Merck Millipore (Germany). Amicon Ultra-15 centrifugal filter devices (3 kDa MW cut-off) were obtained from EMD Millipore (USA). Microscope cover slides were purchased from Superior Marienfeld (Germany).

3.2 ITO cleaning

The ITO substrates were cut to 10 mm (W) x 15 mm (L) size with glass cutter. ITO substrates were washed and cleaned in an ultrasonicator, using dichloromethane solvent for 10 min and then 99% methanol solvent for another 10 min, followed by washing with 0.5 M K_2CO_3 in a 3:1 methanol: Milli-Q water mixture was under sonication for 30 min to eliminate any residual organic contaminants. The ITO substrates were then rinsed several times with copious amounts of Milli-Q water, dried and kept in a nitrogen-filled container (Chockalingam *et al.*, 2011).

3.3 Electrochemical measurements

All voltammetry measurements were done by using an AutoLabIII potentiostat (Metrohm AutoLab, Netherlands) and a conventional three-electrode system comprising an ITO working electrode, a platinum wire as the auxiliary electrode and Ag/AgCl (3.0 M NaCl) as the reference electrode. The ITO slide was placed between the cell blocks (Teflon cell base and Teflon cell body) of the Plate Material Evaluating Cell. Two screws of 20 mm were used to attach the cell blocks. An O-ring made of rubber was placed on the conducting side of ITO to avoid leakage of the electrolyte solution. The Teflon cap was used to place the platinum electrode, and the reference electrode inside the electrolyte solution. All applied potentials were measured relative to the Ag/AgCl reference electrode at room temperature. The surface passivation studies on the modified sensing interface were done in two aqueous solutions containing two redox probes either $[Fe(CN)_6]^{4-/3-}$ or $[Ru(NH_3)_6]^{3+}$ and cyclic voltammetry (CV) was used to confirm the deposition of the functionalized layers on the electrode surfaces. The

respective redox-active solution of (1 mM) concentration was composed of 0.05 M KCl, 0.05 M K_2HPO_4, and 0.05 M KH_2PO_4 and was adjusted to pH 7.0.

Differential pulse voltammetry (DPV) and electrochemical impedance spectroscopy (EIS) techniques were used to probe the integrity of the functionalized layers on the electrode surfaces and to obtain the calibration curve for NS1 antigen at different concentration. The electrodeposition of different layers onto the ITO electrode surface was performed using cyclic voltammetry at 0.2 V- to 0.6 V for 5 cycles at the scan rate 100 $mV \cdot s^{-1}$. The following parameters were applied for the DPV measurements: initial potential (-0.2 V); end potential (0.6 V); modulation amplitude, 25 mV; modulation time, 0.05 s; interval time, 0.5 s, and step potential, 5 mV. The EIS measurements were performed within the frequency range of $0.1–10^3$ Hz and 10 points per decade of frequencies with single sine wave type at room temperature. Nova software was utilized to model the complex circuit and to find the resistance of the electrolyte solution (RS), phase constant element (Q), Warburg impedance (W), and charge transfer resistance (RCT). The surface studies on the modified sensing interface were performed in an aqueous solution containing redox probes $[Fe(CN)_6]^{4-/3-}$ (1 mM) that was composed of 0.05 M KCl, 0.05 M K_2HPO_4, and 0.05 M KH_2PO_4 and adjusted to pH 7.0.

3.4 The ITO surface passivation studies

The electrodeposition of different compounds onto the ITO electrode surface was performed using cyclic voltammetry at -0.6 V to 0.2 V at scan rate of 100 $mV \cdot s^{-1}$. In the first set of experiments, the ITO surface modification was performed using only a single compound: (SP), (PPD), (BAPA), or (TMAP) to find the reductive adsorption peaks for each of the used compounds and to find the adequate concentration of compound to

passivate the working electrode toward the penetration of negatively charged redox-active species $[Fe(CN)_6]^{4-/3-}$ and/ or positively charged redox-active $[Ru(NH_3)_6]^{3+}$. The ITO was modified with 5 mM, 10mM or 30 mM of SP, BAPA, or TMAP. For PPD compound, the ITO was modified with 2mM and 5mM. In the second set of experiments, the ITO electrodes were modified with a combination of SP: TMAP: PPD at different molar ratios: 1:1:0.37 (mix 1), 1.5:0.5:0.37 (mix 2), 0.5:1.5:0.37 (mix 3). In the third set of experiments, the ITO electrodes were modified with a combination of SP: TMAP: PABA at different molar ratios: 0.8:1:0.2 (mix 1), 1:1:0.1 (mix 2) and 0.5:1:0.2 (mix 3) 0.5:1:0.5 (mix 4) 1:1:0.2 (mix 5). The ratio of combination shows the best passivation toward $[Fe(CN)_6]^{4-/3-}$ and $[Ru(NH_3)_6]^{3+}$ redox probes. In control experiment, 2-[2-(2-methoxyethoxy) ethoxy] acetic acid (OEG) was used as the antifouling molecule on the ITO slides. The OEG was deposited on the ITO by the electrodeposition of a mixed layer of 4-aminobenzoic acid (8 mM) and 1, 4-phenyldiamine (2 mM). The fabrication of ITO interface was done by using carbodiimide chemistry: the OEG was linked to the COOH moieties of PPD amine groups by incubating the modified surface in an ethanol solution containing 10 mM OEG and 40 mM DCC for 6 h at room temperature. In all of the above-mentioned experiments, modification by *in situ* methods was carried out in which aryl diazonium cations were electrochemically reduced with two times the molar amount of $NaNO_2$ in 0.5 M HCl. The prepared solution was purged with nitrogen gas for 20 min before the electrodeposition and surface modification. The electrodeposition was made by using cyclic voltammetry at -0.6 V to 0.2 V; at scan rate 100 $mV \cdot s^{-1}$ (Eissa *et al.*, 2012a; Liu *et al.*, 2009; Liu *et al.*, 2011b). The surface passivation studies in the four set of experiments were performed in two aqueous solutions containing two redox probes either $[Fe(CN)_6]^{4-/3-}$ or $[Ru(NH_3)_6]^{3+}$ and cyclic voltammetry (CV) was used to confirm the deposition of the functionalized layers on the electrode surfaces. The respective

redox-active solution of (1 mM) concentration was composed of 0.05 M KCl, 0.05 M K_2HPO_4, and 0.05 M KH_2PO_4 and was adjusted to pH 7.0.

3.5 ITO surface characterization *via* XPS analysis

Wide scan spectra and core level spectra were obtained for SP: TMAP: PPD and SP: TMAP: BAPA modified ITO surfaces using X-ray photoelectron spectroscopy (XPS) (AXIS Ultra DLD spectrometer with a hemispherical analyser, a multichannel detector and a monochromatic Al-Kα source; 1486.6 eV). Spectra were accumulated at a take-off angle of 90° with a 0.9 mm^2 spot size at a pressure of less than 1×10^{-8} mbar. Survey scans (0−1000 eV) were carried out at a 1.0 eV step size, 100 ms dwell time, and 100 eV analyser pass energy. High-resolution scans (S2p, C1s, and N1s) were performed using a 0.1 eV step size, and 20 eV pass energy. Binding energies of elements were adjusted with reference to the C1s peak of graphitic carbon (284.4 eV).

3.6 ITO surface characterization *via* FE-SEM analysis

The surfaces modified with ITO/SP: TMAP: PPD/ AuNPs, ITO/SP: TMAP: PABA, ITO/gold nanoparticles (AuNPs) and bare ITO were morphologically investigated using a Hitachi SU8000 field-emission scanning electron microscope (Tokyo, Japan). The four slides were characterized at slow scan speeds less than 2 kV and at 50,000× magnification. The testing area was 2.1 mm at an accelerating voltage of 2 kV. AuNPs were used to confirm the presence of PPD terminal amine groups. AuNPs were immobilized by immersing ITO/SP: TMAP: PPD and bare ITO in an AuNPs solution

for 3 h at room temperature (Liu *et al.*, 2011b). Energy-dispersive X-ray (EDX) was also used to characterize and find the atomic ratio for the grafted AuNPs.

3.7 Conjugation of cytochrome c to rhodamine B isothiocyanate

The rhodamine B isothiocyanate (RBITC) fluorescent dye was conjugated with Cyt c by following the procedure reported by Gui *et al.*, 2013a. Ten milligrams of Cyt c protein was dissolved in 1 mL of 0.1 M sodium carbonate-bicarbonate buffer (pH 9.05), and of 10 mg/mL of RBITC was dissolved in dimethyl sulfoxide (DMSO). 0.25 mL of RBITC solution was added to obtain a fivefold molar excess of Cyt c relative to RBITC. The tube containing the mixed solutions was enveloped with aluminum foil and incubated in the dark for 1 h under continuous magnetic stirring. Syringe filter (0.22 μm pore size) was used to filter the mixture. The clear conjugated solution was afterward transferred to an Amicon Ultra-15 centrifugal filter device (3 kDa MW cut-off). The solution was poured in filter device, which was placed inside the centrifuge tube. The capped filter device was centrifuged in the swinging bucket rotor for 10 min at 4,000 rpm. The solution in the upper reservoir of the filter device contained the labelled Cyt c- RBITC (12 kDa), which was then identified by using fluorescence spectroscopy. The fluorescence emission spectra of the rhodamine B fluorescent (RBITC) dye alone and the fluorescence emission spectra of rhodamine B fluorescent (RBITC) conjugated with Cyt c were measured using Fluorescence Spectroscopy. Both RBITC and Cyt c- RBITC solutions were diluted in PBS (pH 7.4) to concentration of 1mM. The excitation of RBITC was 530 nm and the emission was monitored between 500-1000 nm. The Cyt c-RBITC solution was kept at -20°C until use for antifouling study. The concentration of labelled Cyt c was calculated using Beer Lambert law. The absorbance value for Cyt c was found using UV-Vis spectroscopy (Shimadzu, Japan).

3.8 The antifouling study *via* CLSM imaging

The modified ITO slides were kept in clean Petri dishes, then it were submerged in an adequate amount of either 1 mg/mL BSA-FITC (an example of a negatively charged protein) or 2 mg/mL Cyt c- RBITC (an example of a positively charged protein); both of BSA-FITC and Cyt c- RBITC solutions were prepared using PBS buffer, pH 7.4. The Petri dishes containing the slides were kept in darkness for 1 h, followed by rinsing the slides and transferring it to another Petri dish that contained only solution of PBS. The ITO slides were kept and soaking for 7 min to remove weakly adsorbed proteins from the surfaces of the modified slides. Subsequently, the slides were rinsed with Milli-Q water to eliminate any remaining residues. The nitrogen gas was used to dry the fluorescent-labelled-protein-adsorbed slides surfaces. The samples were mounted with 50% aqueous glycerol solution and then the slides were put face-down onto a 22 × 60 mm^2 microscope cover slides. Finally, the ITO slides containing the fluorescent-labelled-protein were fixed on the microscope cover slides by using adhesive tape on the sides of the ITO slide only. Three replicates were tested for each type of modified surface (different molar ratios). Five images were captured under 10× magnification for survey studies. Fifteen images were captured under 63× magnification, and their mean gray values were calculated by using Image J (IJ-1.48 g. jar) software to find the fluorescence of the adsorbed proteins. The mean gray values were compared among different surface types.

BSA-FITC and Cyt c- RBITC proteins adsorbed onto functionalized electrode surfaces were measured using a confocal laser fluorescence microscope (Leica Microsystems Pty, Ltd., USA) equipped with an argon laser (at 29% power) and operated in the xyz scan mode (step size 0.04 µm). Images (1024 × 1024 px^2) were captured at 8-bit resolution using the Las AF software (Origin). The imaging was carried out using two

objective lenses: an HCX PL APO CS 10.0 × 0.40 Dry UV and an HCX PL APO lambda blue 63.0 × 1.40 OIL UV. The gray value represents the fluorescence intensity. Captured TIF-format images were further analysed using Image J (IJ-1.48 g. jar) software to calculate the mean gray value after background subtraction. For reference, the emission bandwidth of BSA-FITC ranges from 506 nm to 575 nm. In case of Cyt c-RBITC, the bandwidth ranges from 524 nm to 594 nm.

3.9 The fabrication of an electrochemical impedance immunosensor

The modification of bare ITO electrode was performed using a combination of 4-sulfophenyl, 4-trimethylammoniophenyl and 1, 4-phenylenediamine (SP: TMAP: PPD) at molar ratio of 0.5:1.5:0.37. This ratio was nominated because it showed the best antifouling proficiency against positively (BSA-FITC) and negatively charged proteins (Cyt c- RBITC) (Darwish *et al.*, 2014). For modification of the ITO interface, an in situ method was applied in which aryl diazonium cations were electrochemically reduced with two times the molar amount of $NaNO_2$ in 0.05 M HCl. The prepared solution was purged with nitrogen gas for 20 min before the surface modification. The electrodeposition was done using cyclic voltammetry at -0.6 V to 0.2 V; the electrodes were scanned for 5 cycles at 100 $mV \cdot s^{-1}$ to form the first layer on the ITO substrate (Eissa *et al.*, 2012a; Liu *et al.*, 2009; Liu *et al.*, 2011b). This surface is referred to as surface 1 (Fig 3.1). Then, the distal amine groups of 1,4-phenylenediamine were converted to diazonium groups by incubating surface 1 in $NaNO_2$ and 0.5 M HCl solution to produce a 4-phenyl diazonium chloride-modified interface. Subsequently, the modified surface was scanned at potential between 0.6 V and -0.8 V in solution contains gold nanoparticles (AuNPs) resulted in the electrochemical reduction of the diazonium moieties to radicals that bind to the AuNPs to produce a covalent bond (Liu *et al.*, 2012); this is referred to as surface 2 (Scheme 1). The next step was done by

using, 1, 4-phenylenediamine (3 mM) to functionalize the AuNPs on surface 2 to help for the subsequent attachment of the monoclonal anti-NS1 IgG antibody to be immobilized on the AuNPs. The AuNPs were functionalized with 1,4-phenylenediamine by scanning using potential between 0.2 V and -0.6 V in a 0.5 M HCl solution containing 1 mM $NaNO_2$ and 3 mM 1,4-phenylenediamine for three cycles at a scan rate of 100 mV s^{-1}. This surface is referred to as surface 3 (Figure 3.1). Prior to Monoclonal anti-NS1 IgG antibodies immobilization, the monoclonal anti-NS1 antibodies were incubated with 1-ethyl-3-(3-dimethylaminopropyl) carbodiimide (EDC) (200 mM) and *N*-hydroxysulfosuccinimide (NHS) (50 mM) crossing reagent for 30 min to activate the carboxyl group of the monoclonal antibodies (Sharma *et al.*, 2010). After that, 50 µL of this solution was pipetted on the surface 3 and incubated for 45 min at room temperature to link the monoclonal antibody to the amine group of 1,4-phenylenediamine. Then, the modified ITO slides were washed with 50 mM NaCl to remove any extra-unbound antibodies on the ITO surface, and then they were rinsed with 10 mM phosphate buffer solution at pH 7.4. This surface is referred to as surface 4. Surface 4 is the sensing interface of the immunosensor has been utilized for the detection of the NS1 biomarker. The NS1 antigen has been spiked into diluted human sera (10% in PBS, pH 7.4.) at different concentrations. The human sera spiked with NS1 antigen (50 µL) was pipetted onto surface 4 and the ITO slides were incubated for 45 min at room temperature. Finally, the immunosensors were washed thoroughly with PBS (pH 7.4) prior to testing the slides using the differential pulse voltammetry and electrochemical impedance spectrometry measurements. Diagnostic tools currently used for dengue virus detection in hospitals are mainly immunochromatography test for dengue NS1 Ag and capture IgM and IgG ELISA. However, Enzyme-linked immunosorbent assay (ELISA) can only be useful when there is 4-fold rise in antibody titer with paired tested sera in patients presenting with signs and symptoms that are

consistent with dengue virus infection. Moreover, the Elisa test required is time consuming as several steps of primary and secondary antibody incubation and washing steps. Immunochromatography test is simple to perform in any laboratory and it offer excellent specificity but the sensitivity may depend on serotype of the dengue virus and type of infection (Huang et al., 2013; Shenoy et al., 2014). Therefore, the electrochemical impedance spectrometry selected to be used in this study because it is a sensitive technique and the sample testing and data analysis for obtained results based on EIS measurement will not exceed 50 minutes.

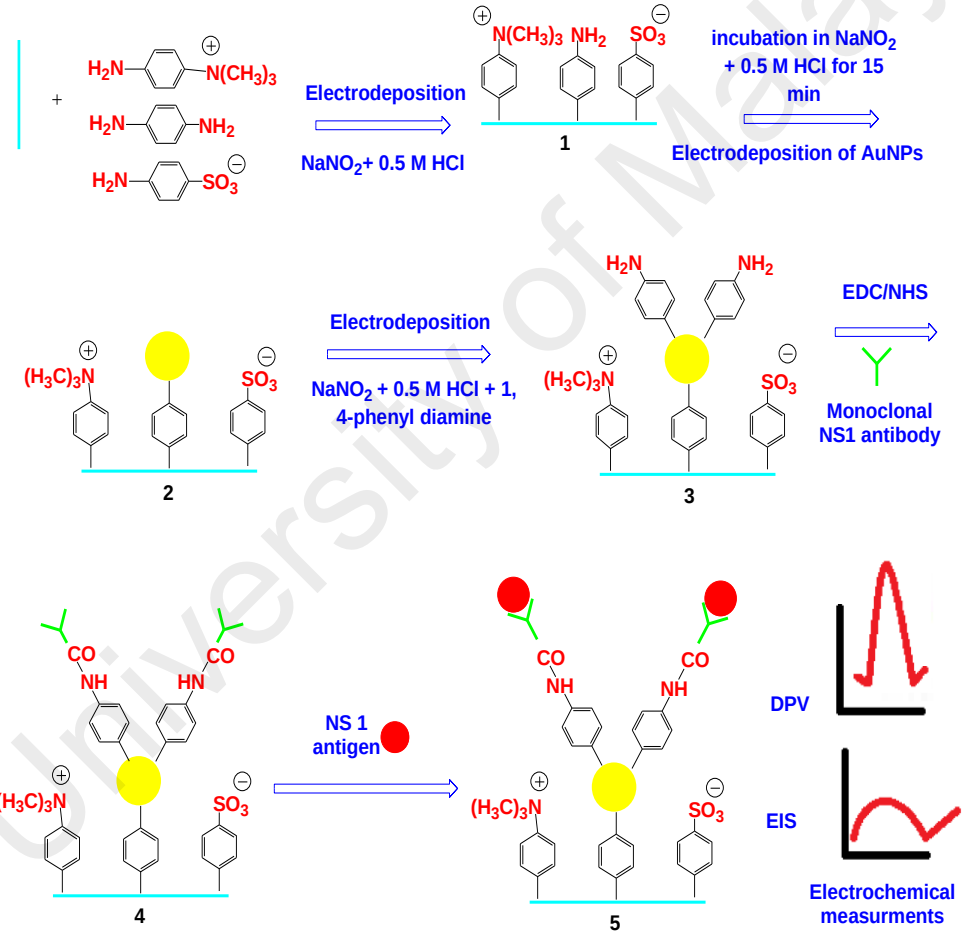

Figure 3-1: Schematic of the fabrication of an electrochemical immunosensor for NS1 antigen in early stage of dengue virus infection.

3.10 The analytical performance of the NS1 immunosensor studies

3.10.1 The reproducibility study of the NS1 immunosensor

The reproducibility of the fabricated immunosensor was tested by examining five different modified electrodes as mentioned in section 3.9. The immunosensors were incubated in a NS1 antigen solution (100 ng mL^{-1}) for 45 min. Subsequently, the slides were soaked first in PBS (pH 7.4) for 5 min, and then, they were rinsed carefully with PBS (pH 7.4) to remove any non-specifically adsorbed NS1 antigen. The peak current of DPV was found for each slide, and the relative standard deviation for the total 5 tested slides was calculated.

3.10.2 The selectivity and cross reactivity studies

Twelve slides were prepared as described in section 3.9. For the selectivity study, three of these immunosensors were incubated with 50 µL of NS1 antigen (50 ng mL^{-1}). Another three synthesized immunosensors were incubated with 50 µL of human serum albumin (HSA) (50 ng mL^{-1}) from normal human sera. The last three modified slides were incubated with 50 µL of human immunoglobulin (IgG) (50 ng mL^{-1}). After 45 min of incubation, the slides were electrochemically measured using EIS technique. Then, the R_{ct} of the slides incubated with NS1 antigen was compared to R_{ct} of the slides incubated with HSA and human IgG.

For the cross-reactivity study, six modified slides were prepared as described in section 3.9. Three of these slides were incubated with 50 µL of 10% human sera diluted with PBS (pH 7.4) and spiked with NS1 antigen (1 µg mL^{-1}). Another three of the prepared immunosensors were incubated with 50 µL of 10% human sera diluted with PBS (pH

7.4) taken from a patient who was infected with the malaria parasite. After 45 min of incubation, the slides were electrochemically measured using EIS. The R_{ct} of the slides incubated with the NS1 antigen was compared to the R_{ct} of the slides incubated with the infected sera from patient infected with malaria parasites.

3.10.3 The stability study of the NS1 immunosensor

The stability of the prepared immunosensor was also examined, 18 modified slides were prepared as described in section 3.9. The NS1 immunosensor was incubated in 50 µL of NS1 antigen (100 ng mL^{-1}) for 45 min. Three of these slides were tested on the same day. The other 15 immunosensors were stored in 10 mM PBS (pH 7.4) at 4°C. Afterward, 3 slides were tested by DPV technique each day for days of 1, 7, 14, 21, 30 and 60 to find the stability of the synthesized immunosensor over a 60-day period. Prior to each test, the NSI immunosensor was carefully rinsed with 10 mM PBS (pH 7.4). DPV technique was used to measure the peak current for each slide, and then the relative standard deviation was calculated.

3.10.4 The testing of NS1 immunosensor in clinical samples.

The potential use of the developed immunosensor in clinical diagnostics was further tested by using five actual sera samples from patients infected with DENV. Beforehand, these samples were tested in UMMC and confirmed positive for NS1 and negative for IgM and IgG by both ELISA-based serological assays and Dengue NS1 Ag + Ab Combo tests. As control samples, five normal sera samples were collected from patients with negative results for NS1, IgM, and IgG from UMMC. The positive and negative

sera samples were serially diluted to various dilution factors (1:10, 1:100, 1:500, and 1:1000) by using PBS (pH, 7.4). The modified slides were incubated with 50 μL of diluted sera at the various dilutions. After incubation for 45 min, the slides were electrochemically measured using EIS. Then, the R_{ct} values of slides incubated with positive sera samples was compared to the R_{ct} values of slides incubated with negative sera samples.

CHAPTER 4: RESULTS AND DISCUSSION

4.1 Electrochemical measurements of single aryl diazonium cations

4.1.1 Electrochemical measurements of 4-sulfophenyl

The reductive adsorption peaks of 4-sulfophenyl (SP) showed an irreversible cathodic peak located at -0.47 V (Figure 4.1, b1). The reduction in peak currents confirms the deposition of SP molecules on the ITO electrode surface. The reductive adsorption has been discussed for this figure, because the compound showed the best passivation toward $[Fe(CN)_6]^{4-/3-}$and $[Ru(NH_3)_6]^{3+}$ redox probes at concentration of 10 mM). This result is similar to the CV results previously reported for glassy carbon surfaces modified with SP compound (Vila & Belanger, 2012; Vila *et al.*, 2007). The cyclic voltammograms for bare ITO in 1 mM $[Fe(CN)_6]^{4-/3-}$ indicated a pair of well-defined redox peaks. Electrode surfaces modified with aryl diazonium cations, (SP) 5 mM (Figure 4.1, a1-3), showed good passivation toward the penetration of negatively charged redox-active species, when the modified surface was tested in $[Fe(CN)_6]^{4-/3-}$. Best passivation was obtained when the ITO was modified with 10 mM of SP compound (Figure 4.1, b1-3). However, ITO surface modified with 30 mM of SP (Figure 4.1, c1-3) compound exhibited less passivation toward the penetration $[Fe(CN)_6]^{4-/3-}$ redox probe as compared to ITO modified with (SP) 5 mM and (SP) 10 mM. The weak passivation by using 30 mM of SP can be explained by the fact that the modification solution tends to be saturated and the diazotation reaction and electrodeposition become inefficient for steric reasons. Moreover, such conditions limit the diffusion of the diazonium cations and the aryl radicals to the modified interface (Allongue *et al.*, 1997). The surfaces modified with 5 mM, 10 mM or 30 mM of SP compound showed weak passivation properties toward the penetration of positively charged redox active species, when the surfaces were tested in 1 mM $[Ru(NH_3)]_6^{3+}$. This weak passivation was likely the consequence of the negatively charged layer

formed on the ITO electrode surface, which repelled $[Fe(CN)_6]^{4-/3-}$, but at the same time, it allowed the penetration of $[Ru(NH_3)_6]^{3+}$ from the solution to ITO electrode surface.

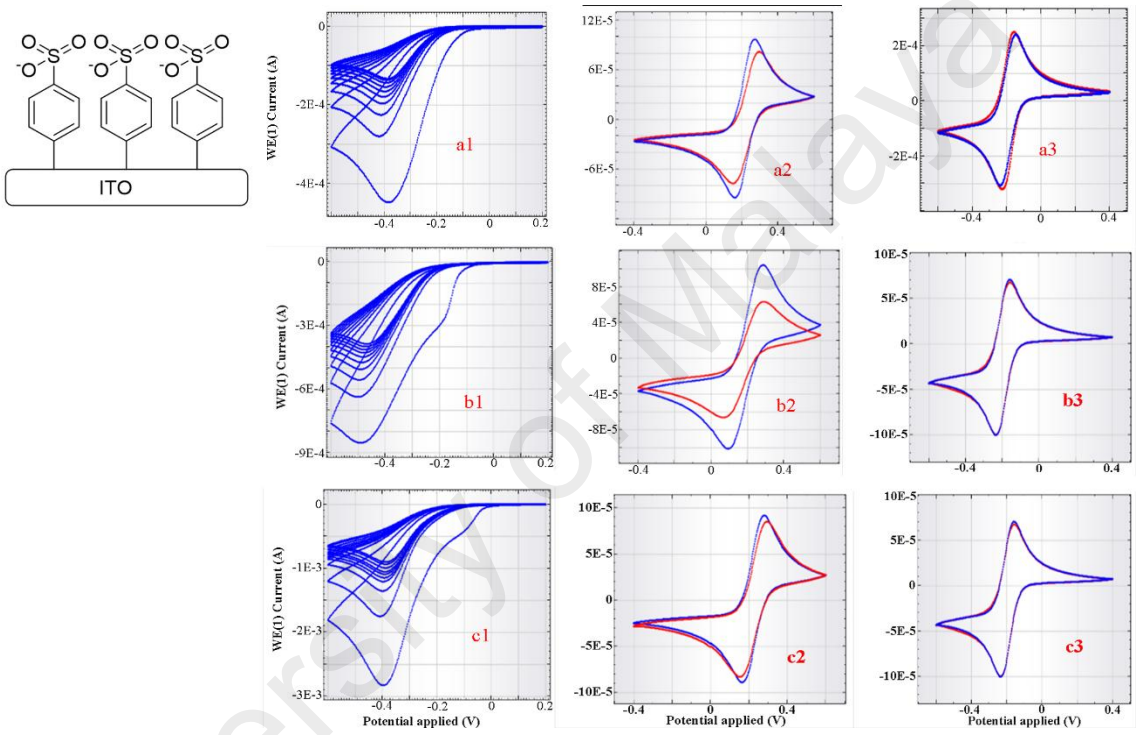

Figure 4-1: Cyclic voltammograms of reductive adsorption and surface passivation of 4-sulfophenyl (SP)
Cyclic voltammograms of (1) reductive adsorption; (2) surface passivation study tested in 1 mM $Fe(CN)_6]^{4-/3-}$ before (blue) and after (red) surface modification; (3) surface passivation study tested in 1 mM $[Ru(NH_3)_6]^{3+}$ before and after surface modification for (a) surface modified with 5 mM of 4-sulfophenyl (SP) (b) surface modified with 10 mM 4-sulfophenyl (SP)) (c) surface modified with 30 mM of 4-sulfophenyl (SP) Note: the aryl diazonium cations were electrochemically reduced with two times the molar amount of $NaNO_2$, 0.5 M HCl, 10 cycles scans of CV at 100 mV s-1).

4.1.2 Electrochemical measurements of 4-Trimethylammoniophenyl

The reductive adsorption peaks of 4-trimethylammoniophenyl (TMAP) appeared at -0.26 V (Figure 4.2, b1). The reduction in peak currents confirms the deposition of TMAP molecules on the ITO electrode surface. The surfaces modified with 5 mM , 10 mM or 30 mM (Figure 4.2) showed weak passivation properties toward the penetration of $[Fe(CN)_6]^{4-/3-}$. Electrode surfaces modified with TMAP 5 mM (Figure 4.2, a1-3) showed good passivation toward the penetration of positively charged redox-active species when the modified surface was tested in $[Ru\ (NH_3)_6]^{3+}$. This positively charged aryl diazonium cation allowed $[Fe\ (CN)_6]^{4-/3-}$ to penetrate through the layer, although it prevented $[Ru(NH_3)_6]^{3+}$ from diffusing closer to ITO electrode surface. The modification of ITO surface with TMAP aryl diazonium cation required a high concentration (10 mM) and up to 10 CV scan cycles to obtain partial blocking of ITO electrode surface (Figure 4.2, b1-3). The difficulty in forming a close-packed layer of this compound may be the consequence of the steric hindrance caused by three methyl groups of TMAP, which hinders the forming of a densely packed structure between the TMAP molecules (Combellas *et al.,* 2008). Best passivation was obtained when ITO was modified with 10 mM of TMAP compound. However, ITO surface modified with 30 mM of TMAP compound showed less passivation toward the penetration $[Ru\ (NH_3)]_6^{3+}$ redox probe as compared to ITO modified with TMAP 5 mM and TMAP 10 mM.

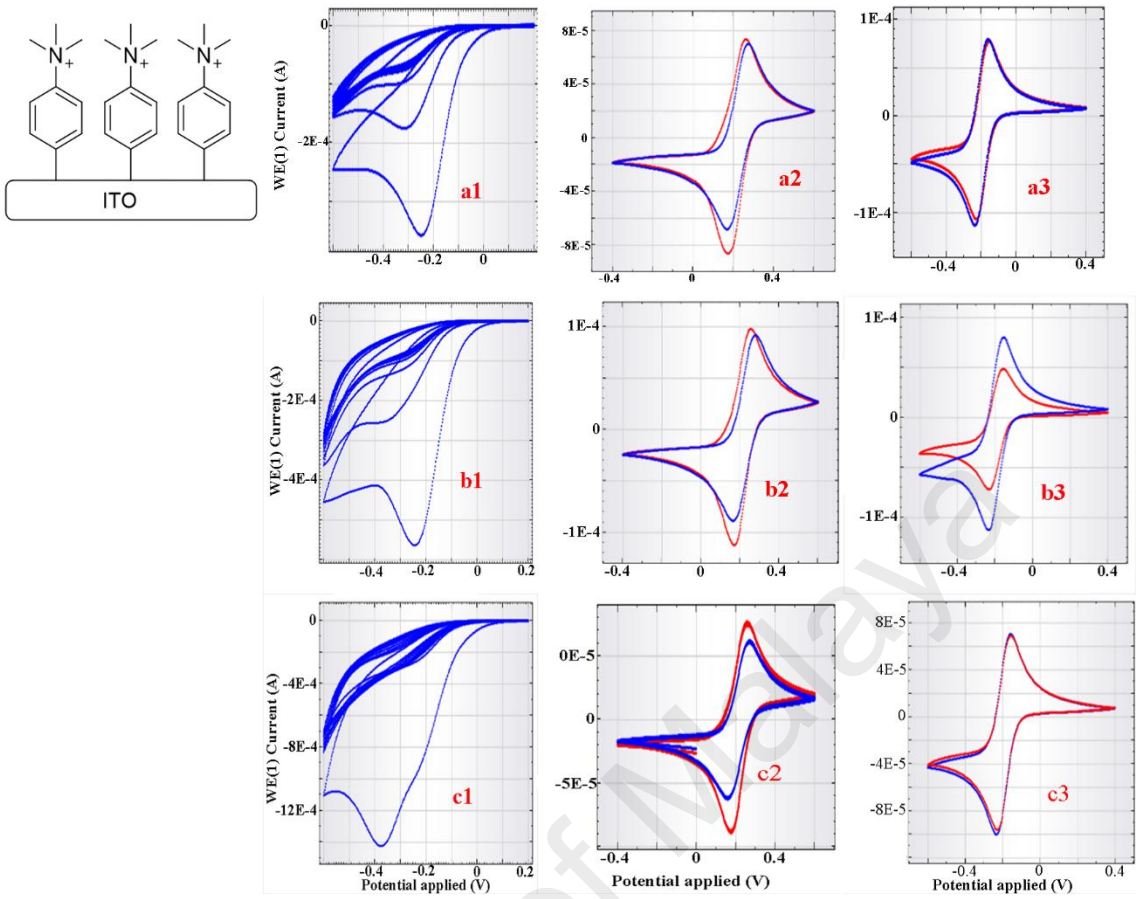

Figure 4-2: Cyclic voltammograms of reductive adsorption and surface passivation of 4-trimethylammoniophenyl (TMAP).
Cyclic voltammograms of (1) reductive adsorption; (2) surface passivation study tested in 1 mM Fe $(CN)_6]^{4-/3-}$ before (blue) and after (red) surface modification; (3) surface passivation study tested in 1 mM $[Ru(NH_3)_6]^{3+}$ before and after surface modification for (a) surface modified with 5 mM of 4-trimethylammoniophenyl (TMAP) (b) surface modified with 10 mM 4-Trimethylammoniophenyl (TMAP) (c) surface modified with 30 mM of 4-Trimethylammoniophenyl (TMAP) Note: the aryl diazonium cations were electrochemically reduced with two times the molar amount of $NaNO_2$, 0.5 M HCl, 10 cycles scans of CV at 100 mV s^{-1}).

4.1.3 Electrochemical measurements of 1, 4-phenylenediamine

The reductive adsorption peak of 1, 4-phenylenediamine (PPD) was observed at –0.36 V (Figure 4.3, b1). The reduction in peak currents confirms the deposition of PPD molecules on the ITO electrode surface. The electrodeposition of PPD resulted in densely packed surface coverage when 2 mM of PPD was used (Figure 4.3, a1-3). However, better surface blocking was obtained when 5 mM of PPD was used and high reduction current was observed after only two cycles of modification (Figure 4.3,b1-3).

Excellent passivation was observed toward the penetration of negatively or positively charged redox-active species when the surface was tested in $[Fe\ (CN)_6]^{4-/3-}$ or $[Ru(NH_3)_6]^{3+}$ respectively. An efficient PPD attachment on the glassy carbon surface has also been reported (Lyskawa & Belanger, 2006). This observation may be due to PPD, having the fastest diffusion rate and also the lowest molecular weight among the aryl diazonium cations used in this study (Polsky *et al.*, 2008).

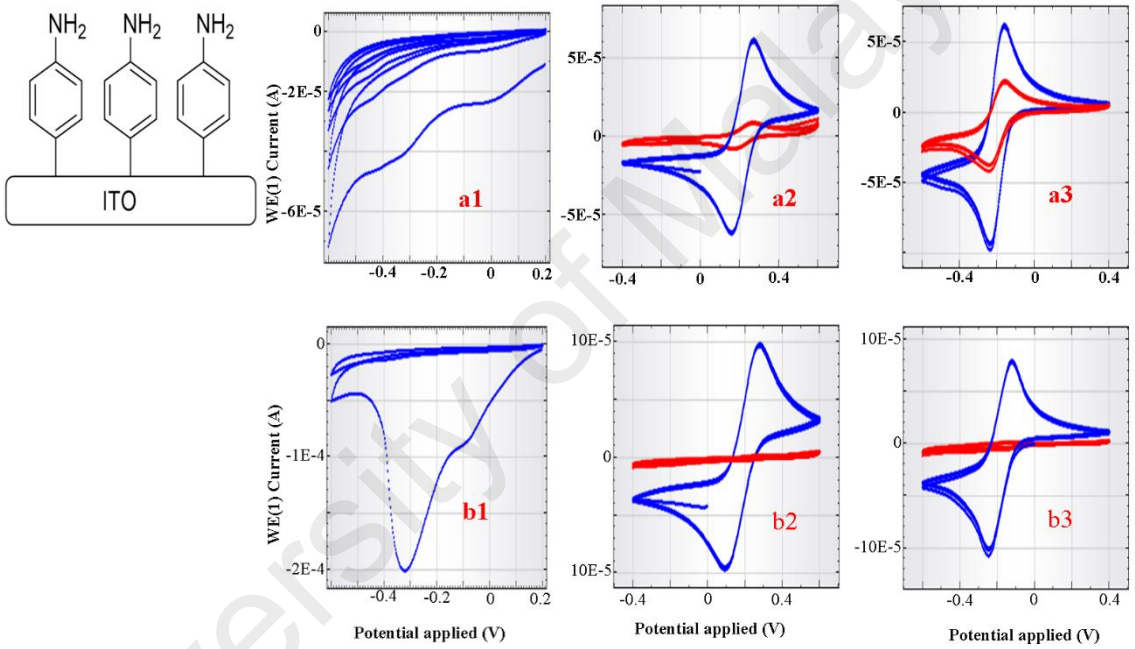

Figure 4-3: Cyclic voltammograms of reductive adsorption and surface passivation of 1,4-phenylenediamine (PPD)
Cyclic voltammograms of (1) reductive adsorption; (2) surface passivation study tested in 1 mM Fe $(CN)_6]^{4-/3-}$ before (blue) and after (red) surface modification; (3) surface passivation study tested in 1 mM $[Ru(NH_3)_6]^{3+}$ before and after surface modification for (a) surface modified with 2 mM of 1,4-phenylenediamine (PPD) (b) surface modified with 5 mM of 1,4-phenylenediamine (PPD) Note: the aryl diazonium cations were electrochemically reduced with two times the molar amount of $NaNO_2$, 0.5 M HCl, 5 cycles scans of CV at 100 mV s^{-1} with 2mM of PPD or 2 cycles scans of CV at 100 mV s^{-1} with 5mM of PPD

4.1.4 Electrochemical measurements of 4-aminobenzoic acid

A typical cyclic voltammogram of 4-aminobenzoic acid (PABA) diazonium cation solution showed a single irreversible cathodic peak at about -0.10 V (Figure 4.4, b1). The reduction in peak currents confirms the deposition of PABA molecules on the ITO electrode surface. The cyclic voltammograms for bare ITO in 1 mM $[Fe(CN)_6]^{4-/3-}$ exhibited a pair of well-defined redox peaks. Electrode surfaces showed good passivation toward the penetration of negatively charged redox-active species when ITO surfaces were modified with 5 mM (Figure 4.4, a1-3) and 10 mM (Figure 4.4, b1-3) and tested in $[Fe\ (CN)_6]^{4-/3-}$. However, less passivation was observed toward $[Fe\ (CN)_6]^{4-/3-}$ when the surface was modified with 30 mM (Figure 4.4, c1-3). The modified ITO surfaces indicated weak passivation properties toward the penetration of positively charged redox active species when the surfaces were tested in 1 mM $[Ru\ (NH_3)]_6^{3+}$. This weak passivation is probably the result of the negatively charged coating that was placed on ITO electrode surface, which repelled $[Fe(CN)_6]^{4-/3-}$, but it allowed the penetration of $[Ru(NH_3)_6]^{3+}$ from the solution to ITO electrode surface. The objective of studying electrochemical behaviour of deposited individual compounds has been achieved in this section by finding the electrochemical behaviour of deposited individual compounds: 4-sulfophenyl (SP), 4-trimethylammoniophenyl (TMAP), 1,4-phenylenediamine (PPD and 4-aminobenzoic acid (PABA).

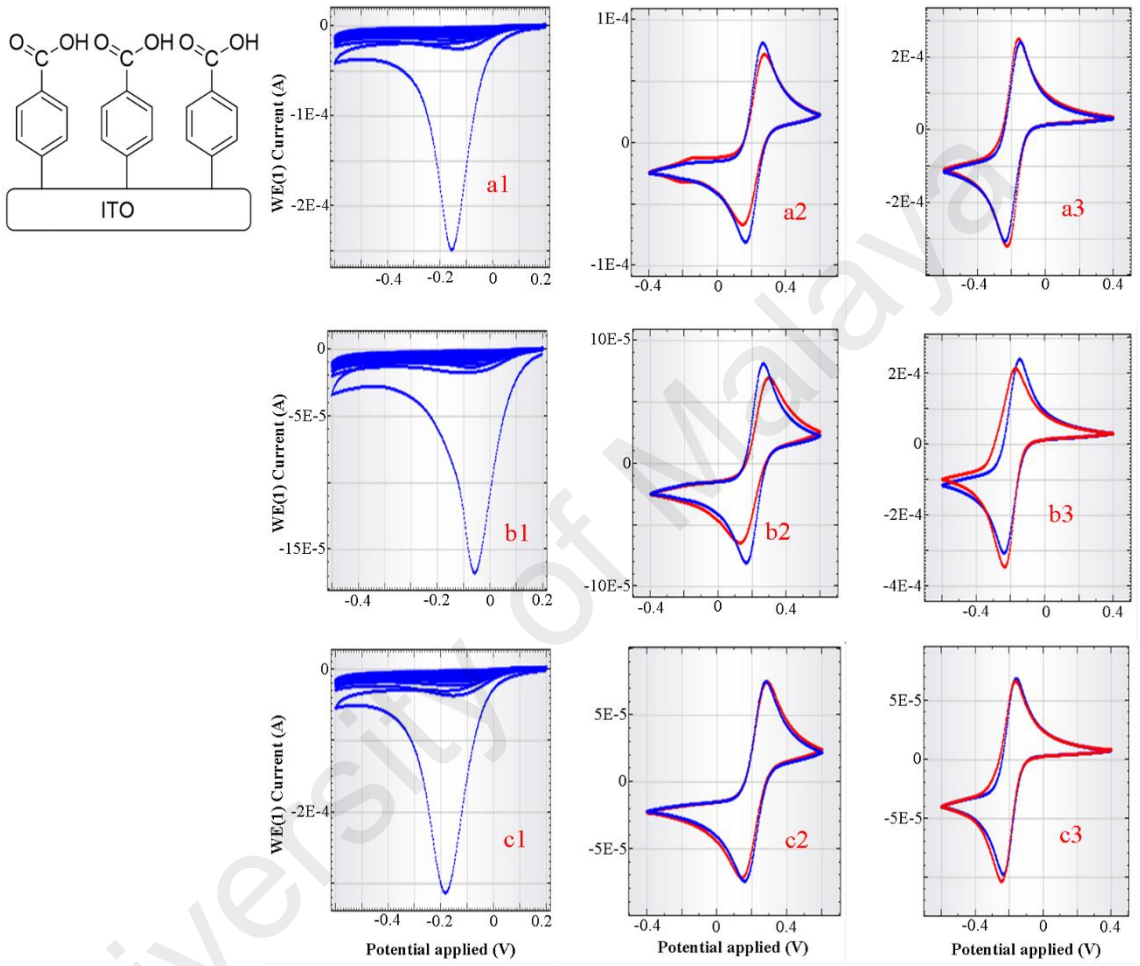

Figure 4-4: Cyclic voltammograms of reductive adsorption and surface passivation of 4-aminobenzoic acid (PABA)

Cyclic voltammograms of (1) reductive adsorption; (2) surface passivation study tested in 1 mM Fe $(CN)_6]^{4-/3-}$ before (blue) and after (red) surface modification; (3) surface passivation study tested in 1 mM $[Ru(NH_3)_6]^{3+}$ before and after surface modification for (a) surface modified with 5 mM of 4-aminobenzoic acid (PABA) (b) surface modified with 10 mM 4-aminobenzoic acid (PABA) (c) surface modified with 30 mM of 4-aminobenzoic acid (PABA). Note: the aryl diazonium cations were electrochemically reduced with two times the molar amount of $NaNO_2$, 0.5 M HCl, 10 cycles scans of CV at 100 mV s^{-1}).

4.2 Electrochemical measurements of aryl diazonium cations mixtures

4.2.1 Electrochemical measurements of SP:TMAP:PPD combination

The reductive-adsorption cyclic voltammograms of the mixture of 4-sulfophenyl, 4-trimethylammoniophenyl and 1, 4-phenylenediamine (SP: TMAP: PPD) exhibited reductive adsorption peaks at approximately -0.35 V and -0.1 V (Figure 4.5, c1). The peak potential for the mixture (SP: TMAP: PPD) was more positive than that required for the adsorption of an individual aryl diazonium cation: SP (-0.47 V), TMAP (-0.26 V) and PPD (-0.36 V). This change in the peak potential suggests that, in mixed layers, a decrease in the energy barriers for reducing diazonium cations may have occurred. Such decreases in the energy barrier probably occurred between (TMAP) and (PPD) reductive peaks to produce a single peak at -0.1 V. The first peak at -0.35 V may belong to (SP) diazonium with a small positive shift. Smaller reductive peak sizes with better passivation properties were detected for this mixture on ITO surface as compared to ITO surfaces modified with either (SP) or 4-trimethylammoniophenyl (TMAP) alone. The authors of the previous studies achieved similar results using glassy carbon surfaces (Gui *et al.*, 2013a; Vila & Belanger, 2012). The ITO interfaces were fabricated employing a combination of SP: TMAP: PPD at different molar ratios: 1:1:0.37 (mix 1) (Figure 4.5, a1-3), 1.5:0.5:0.37 (mix 2) (Figure 4.5, b1-3), 0.5:1.5:0.37 (mix 3) (Figure 4.5, c1-3). Different molarity ratios were used to find the ratio of molecules that produce a neutral and inert interface. The neutral and inert ITO interfaces are helpful and essential to resist the adsorption of non-specific protein interaction, which will be tested in second stage of this study. The combination of SP: TMAP: PPD at molar ratios 0.5:1.5:0.37 (mix 3) was the best combination with high resistance towards the penetration of both $[Fe\ (CN)_6]^{4-/3-}$ and $[Ru(NH_3)_6]^{3+}$ due to the overall neutral charge of mixtures on ITO surfaces.

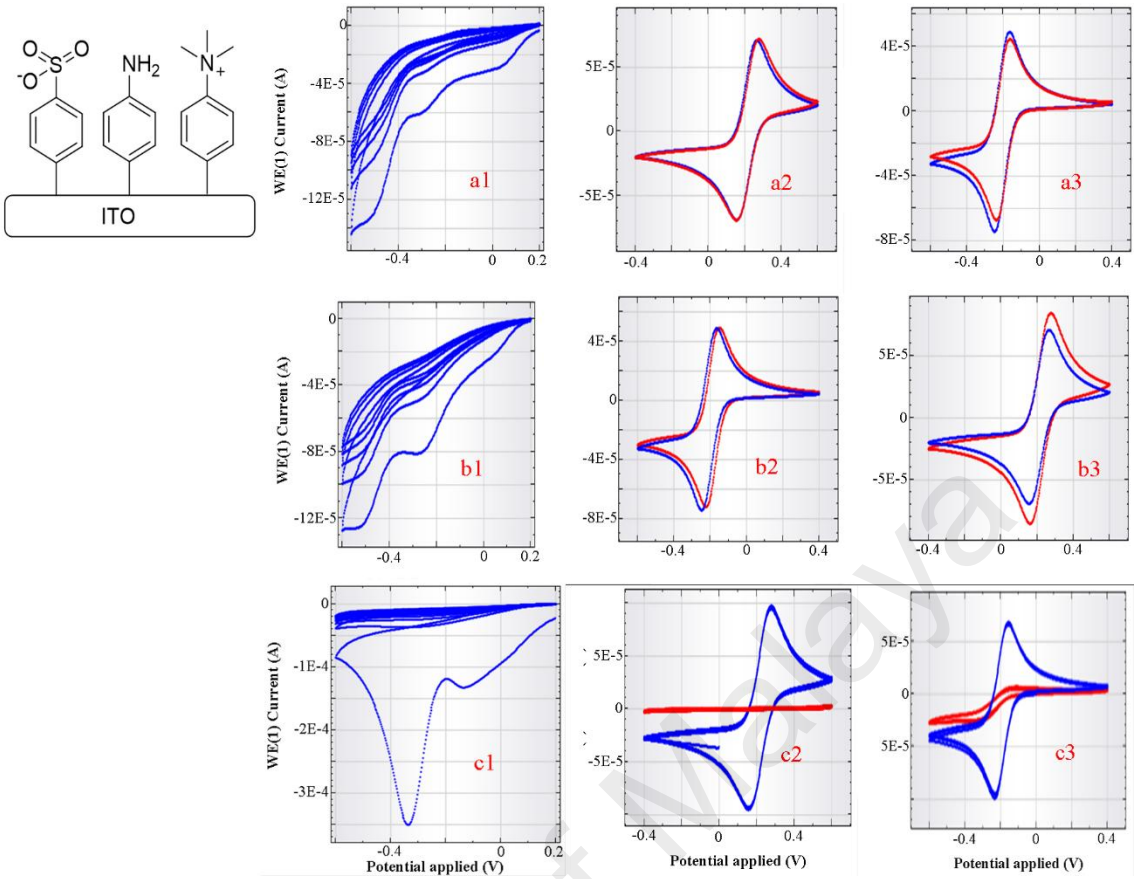

Figure 4-5: Cyclic voltammograms of reductive adsorption and surface passivation of mixed layers of SP: TMAP: PPD

Cyclic voltammograms of (1) reductive adsorption; (2) surface passivation study tested in 1 mM $[Fe(CN)_6]^{3-/4-}$ before (blue) and after (red) surface modification; (3) surface passivation study tested in 1 mM $[Ru(NH_3)_6]^{3+}$ before and after surface modification for (a) mixed layer of SP:TMAP:PPD at 1:1:0.37 (mix 1), (b) mixed layer of SP:TMAP:PPD at 1.5:0.5:0.37 (mix 2) , (c) mixed layer of SP:TMAP:PPD at 0.5:1.5:0.37 (mix 3); (Note: the aryl diazonium cations were electrochemically reduced with two times the molar amount of NaNO2 , 0.5 M HCl, 5 cycles scans of CV at 100 mV s^{-1}).

4.2.2 Electrochemical measurements of SP:TMAP:PABA combination.

The reductive-adsorption cyclic voltammograms of the mixture of SP: TMAP: PABA presented a main reductive adsorption peak approximately at -0.28 V (Figure 4.6, a1 and c1). This change in the peak potential suggests that, in mixed layers, a change in the energy level for reducing diazonium cations may have occurred. The passivation of the modified ITO electrode surface (from the second cycle of modifications) may indicate that the rate of radical deposition on the ITO surface was much higher in this mixture as compared with that on ITO surfaces modified with single species of radicals (Vila & Belanger, 2012).

The ITO electrodes were modified with a combination of SP:TMAP:PABA at five molar ratios: 0.8:1:0.2 (mix 1) (Figure 4.6, a1-3), 1:1:0.1 (mix 2) (Figure 4.6, b1-3) , 0.5:1:0.2 (mix 3) (Figure 4.6, c1-3) , 0.5:1:0.5 (mix 4) (Figure 4.6, d1-3) and 1:1:0.2 (mix 5) (Figure 4.6, e1-3) to obtain a neutral and inert interface. When the SP:TMAP:PABA mixtures were tested in $[Fe(CN)_6]^{4-/3-}$ and $[Ru(NH_3)_6]^{3+}$, a slight passivation of ITO electrode and reduced intensities of cathodic and anodic peaks were observed in the voltammograms of the $[Fe(CN)_6]^{4-/3-}$ test solutions. However, no such effects were observed in the voltammograms of $[Ru(NH_3)_6]^{3+}$ test solutions. These results are attributable to the coating of ITO with a thin SP: TMAP: PABA layer. Thin layer of SP: TMAP: PABA has a moderate resistance to inner-sphere electron-transferring redox probes. In inner-sphere electron-transfer system, the transfer of an electron requires the formation of a significant covalent bonding between the two species in a redox chemical reaction), such as $[Fe(CN)_6]^{4-/3-}$. In outer-sphere electron transfers, no such covalent bonding is required between the two species in a redox chemical reaction. Therefore, a minimal barrier effect on redox probes that perform outer-sphere electron transfers such as $[Ru\ (NH_3)_6]^{3+}$ was observed. Moreover, such observations may be due to the

domination of negatively charged PABA molecule, which repelled $[Fe(CN)_6]^{4-/3-}$, but allowed the penetration of $[Ru(NH_3)_6]^{3+}$ from the solution to ITO electrode surface. The dominance of PABA on ITO surface may belong to its lower negative reductive potential (-0.1 V) as compared to those of SP (-0.47 V) and TMAP (-0.26 V).

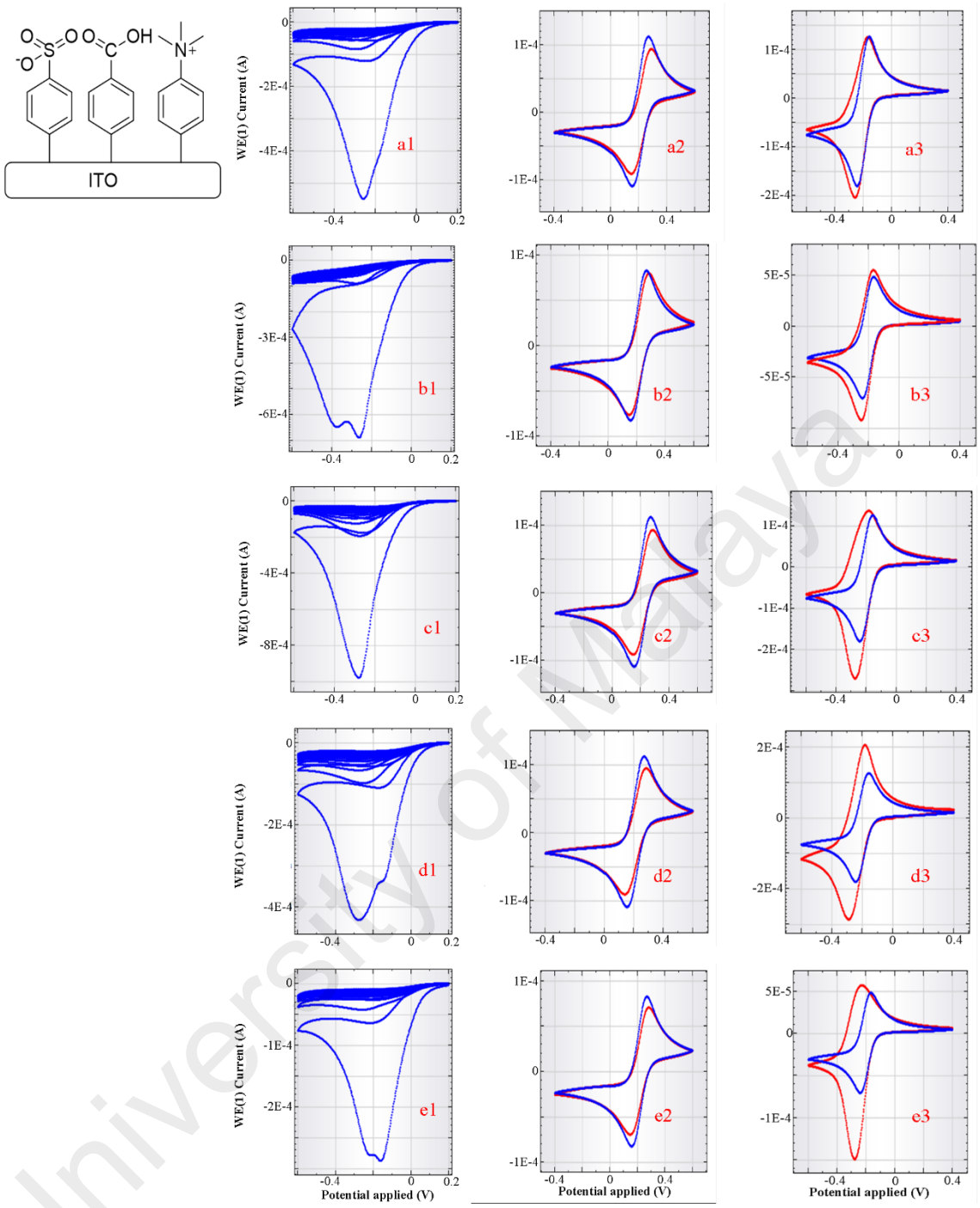

Figure 4-6: Cyclic voltammograms of reductive adsorption and surface passivation of mixed layers of SP: TMAP: PABA

Cyclic voltammograms of (1) reductive adsorption; (2) surface passivation study tested in 1 mM Fe $(CN)_6]^{4-/3-}$ before (blue) and after (red) surface modification; (3) surface passivation study tested in 1 mM $[Ru(NH_3)_6]^{3+}$ before and after surface modification for mixed layer of SP:TMAP:PABA at ratio 0.8:1:0.2 (mix 1), (b) 1:1:0.1 (mix 2), (c) 0.5:1:0.2 (mix 3) (d) 0.5:1:0.5 (mix 4) and (E) 1:1:0.2 (mix 5). (Note: the aryl diazonium cations were electrochemically reduced with two times the molar amount of $NaNO_2$, 0.5 M HCl, 5 cycles scans of CV at 100 mV s^{-1}).

The reductive-adsorption voltammograms of the mixture of PABA and PPD exhibited single reductive adsorption peaks at about -0.5 V (Figure 4.7, 1). The passivation of ITO electrode surface was obtained after 5 cycles of surface modification. The mixed layer of the PABA and PPD-modified ITO surface was further modified with the OEG aryl diazonium cation (Figure 4.7). The PABA- and PPD/OEG-modified ITO surface was tested in both $[Fe(CN)_6]^{4-/3-}$ and $[Ru(NH_3)_6]^{3+}$ redox-active solutions (1 mM, pH 7). A moderate reduction in the cathodic and anodic peaks, respectively, was observed. These decreases in cathodic and anodic peaks may be due to the passivation effect of OEG molecules, which is utilized in biomedical applications to provide anti fouling and biocompatible surface (Hu *et al.*, 2012) (Figure 4.7, 2-3).

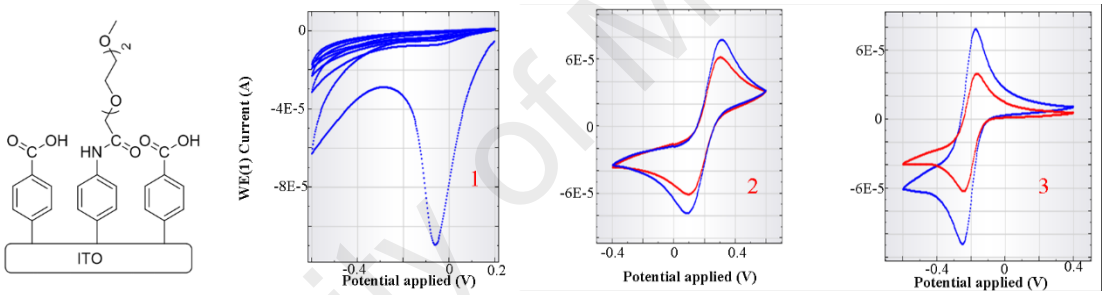

Figure 4-7: Cyclic voltammograms of reductive adsorption and surface passivation of mixed layer of PABA: PPD

Cyclic voltammograms of (1) reductive adsorption; (2) surface passivation study tested in 1 mM $[Fe(CN)_6]^{3-/4-}$ before (blue) and after (red) surface modification; (3) surface passivation study tested in 1 mM $[Ru(NH3)_6]^{3+}$ before and after surface modification for (a) mixed layer of PABA:PPD (Note: the aryl diazonium cations were electrochemically reduced with two times the molar amount of $NaNO_2$, 0.5 M HCl, 5 cycles scans of CV at 100 mV s^{-1}).

4.3 ITO surface characterization via XPS analysis

X-Ray photoelectron spectroscopy is a highly sensitive analytical method to assess the chemical composition of elements. The wide scan spectra for ITO surfaces modified with (SP: TMAP: PPD, mix 3) showed the existence of binding energies of 167, 285, 400 eV corresponding to the constituents sulfur (S 2p), carbon (1s) and nitrogen (1s), respectively (Figure 4.8). The presence of SP was also confirmed core level spectra analysis. A signal peak of sulfur (S2p) at 167.9 eV was detected and this confirms the deposition of 4-sulfophenyl molecule (Vila & Belanger, 2012; Vila *et al.*, 2007). In core level spectra analysis of C1s, the presence of a C-N linkage peak was confirmed. The C-N linkage peak represents the link between nitrogen and 4-methyl groups in 4-trimethylammoniophenyl TMAP. C-N linkage peak was detected at a binding energy of 285.0 eV (C2). Another peak (C1) centered at 284.4 eV in a narrow scan of the carbon region represents aromatic carbons in 4-sulfophenyl, 1,4-phenylenediamine and 4-trimethylammoniophenyl moieties (Lyskawa & Belanger, 2006; Vila & Belanger, 2012). In core level spectra analysis of N1s , 1,4-phenylenediamine PPD was characterized by N1 399.5 eV peak detected in the narrow scan of the N1s region, which is related to H_2N-C bond (Eissa *et al.*, 2012a; Liu *et al.*, 2009; Liu *et al.*, 2011b; Losito *et al.*, 2005).

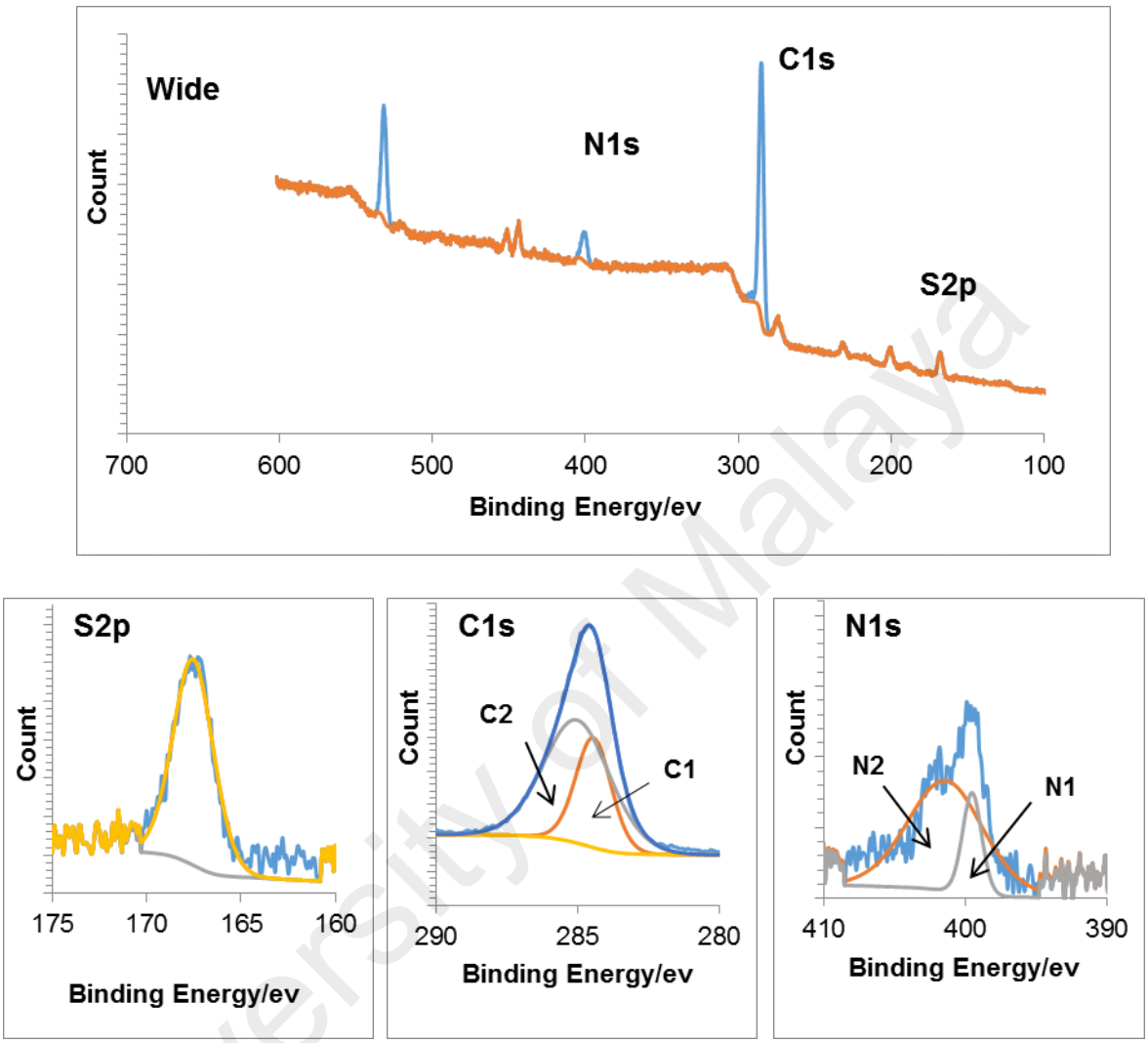

Figure 4-8: X-Ray photoelectron spectra (XPS) of SP: TMAP: PPD layer. ITO surfaces modified with molarity ratio of 0.5:1.5:0.37 (mix 3). The survey spectra with molecular structure of S2p, C1s and N1s core-level spectra.

The wide scan spectra for ITO surfaces modified with (SP: TMAP: PABA, mix 3) showed the existence of binding energies of 167, 285 and 400 eV corresponding to the constituents sulfur (S 2p), carbon (1s) and nitrogen (1s), respectively (Figure 4.9). Moreover, the narrow scan spectra of S2p showed a peak at 167.8 eV, which indicate SP grafting on ITO (Liu *et al.*, 2009; Vila & Belanger, 2012; Vila *et al.*, 2007). A narrow scan of the carbon C1s region revealed three peaks centered at 284.7 eV (C1), 286.1 eV (C2), and 288.5 eV (C3). The C1 and C2 peaks were attributed to aromatic carbon atoms and to N-$(CH_3)_3$ in the trimethylammonio group (TMAP), respectively. Regarding the C3 peak corresponded to COO^-, it can be observed that the presence of this peak confirms the successful grafting of (PABA) molecules onto ITO substrate (Chung *et al.*, 2012; Liu *et al.*, 2009; Yin *et al.*, 2009). The N1s core level spectra showed a single peak at 400 eV that was ascribed to the N-$(CH_3)_3$ in (TMAP) molecule. The XPS result also showed the domination of PABA molecule as expected in electrochemical measurements. The atomic ratio for C3 (represents 4-aminobenzoic acid molecule) was 2.9, while the atomic ratio for S2p (represents the 4-sulfophenyl molecule) and N1s (represents the 4-trimethylammoniophenyl molecule) were 0.4 and 1, respectively (Table 4.1).

Table 4.1: XPS Atomic Ratio comparison of S, C, N between SP: TMAP: PPD-ITO and SP: TMAP: PABA-ITO.

Core level peaks	S2p	C1s			N1s	
	S1	C1	C2	C3	N1	N2
SP: TMAP:PPD	3.43	2.1	25.7	-	0.64	2.75
SP: MAP:PABA	0.41	18.9	8.5	2.9	1.0	-

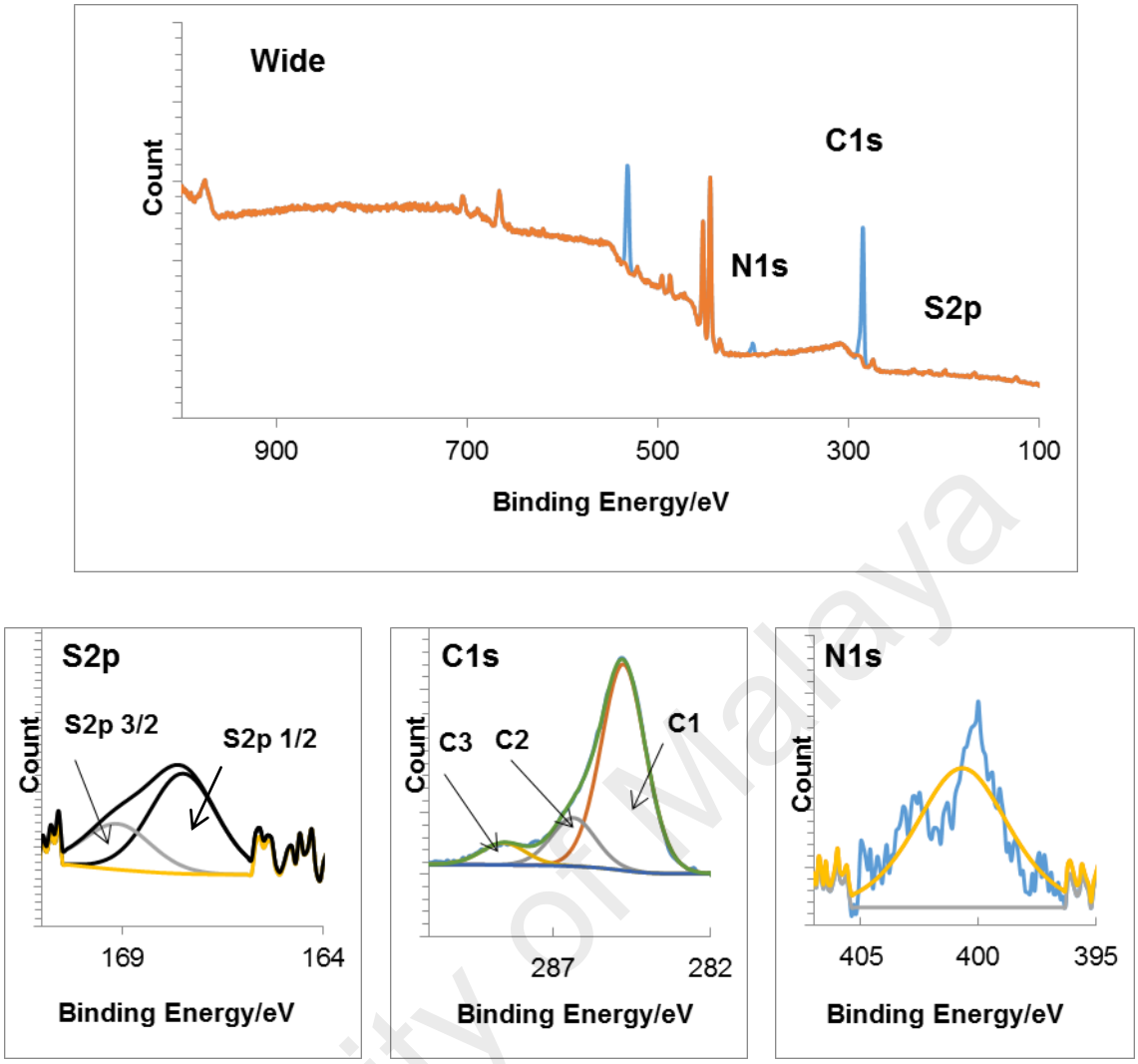

Figure 4-9: X-Ray photoelectron spectra (XPS) of SP: TMAP: BAPA layer. ITO surfaces modified with molarity ratio of (0.5:1:0.2) (mix 3). The survey spectra of S2p, C1s and N1s core-level spectra.

The wide scan spectra for bare ITO surfaces did not confirm the existence of binding energies of sulfur (S 2p), carbon (1s) or nitrogen (1s). Core level spectra for C1s and N1s showed the existence of two signal peaks. These signals may due to the non-inherent and adventitious substances. Other scholars have also reported such observations (Wang *et al.*, 2014; Zeppilli *et al.*, 2010). These studies suggested that ITO slide has a little quantity of carbon in the near-surface region, and its concentration is not highly affected by the pretreatments or cleaning procedure (Donley *et al.*, 2002). The atomic ratios of C1s and N1s have been remarkably increased in XPS spectra of ITO modified with SP: TMAP: PPD and SP: TMAP: PABA as compared to the bare ITO surface. The atomic ratio of C1s was 52 in spectra of bare ITO, while it was 78.4 and 61.2 in XPS spectra of SP: TMAP: PPD and SP: TMAP: PABA, respectively. The atomic ratio of N1s was 1.1 in spectra of bare ITO, while it was 5.4 and 1.6 in XPS spectra of SP: TMAP: PPD and SP: TMAP: PABA, respectively (Table 4.2). These results confirmed that TMAP, PPD and PABA molecules were deposited on ITO interfaces.

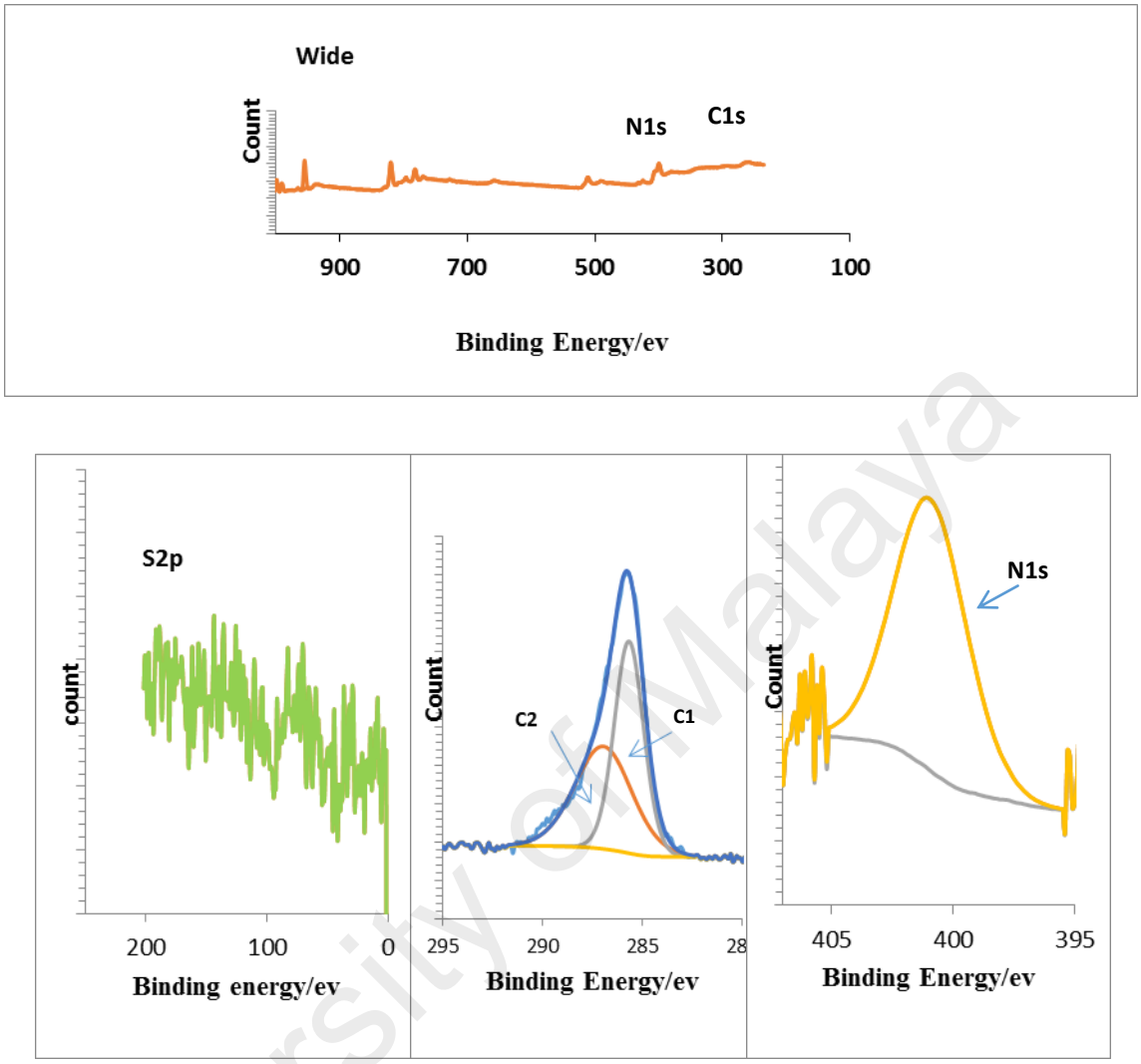

Figure 4-10: X-Ray photoelectron spectrum of bare indium tin oxide.
The survey spectra with molecular structure of S2p, C1s and N1s core- level spectra.

Table 4.2: XPS Atomic Ratio comparison of S, C, N between SP: TMAP: PPD-ITO and SP: TMAP: PABA-ITO

Surface Type	S2p	C1s	N1s
ITO/ SP:TMAP:PPD	4.77	78.4	5.4
ITO/ SP:TMAP:PABA	0.4	61.2	1.6
Bare ITO	-	52	1.1

4.4 ITO surface characterization via FE-SEM analysis

The FE-SEM image of the bare ITO electrode showed the absence of AuNPs (Figure 4.11, a), when ITO was modified with SP: TMAP: PPD (Figure 4.11, b). A uniform and homogeneous distribution of AuNPs was observed. The Energy-dispersive X-ray (EDX) results confirmed the deposition of AuNPs onto ITO electrode surfaces at an atomic ratio of 2.11 (Figure 4.12). The linkage of amines in the mixture of SP: TMAP: PPD to AuNPs was more likely to occur by dehydrogenation from NH- AuNPs, because of its stronger covalent bond (Liu *et al.*, 2011; Liu *et al.*, 2011b). Such observations confirmed the homogeneous grafting of the linker molecule (PPD) onto the ITO surface. The image of SP: TMAP: PABA-modified ITO electrode showed a thin, smooth and featureless morphology (Figure 4.11, c). An obvious difference is noticed in images for both bare and ITO modified with SP: TMAP: PABA which were captured at 1500× magnification (Figure 4.11, d). The second objective of this study is to fabricate a biosensing interfaces on ITO electrode via electrodeposition of linker moieties (COOH or NH_2) and charged, antifouling moieties (($-SO^{3-}$ and $^{+}(Me)_3$). The electrochemical measurements, the X-Ray photoelectron spectroscopy and the FE-SEM results confirmed the success in achieving this milestone in this research.

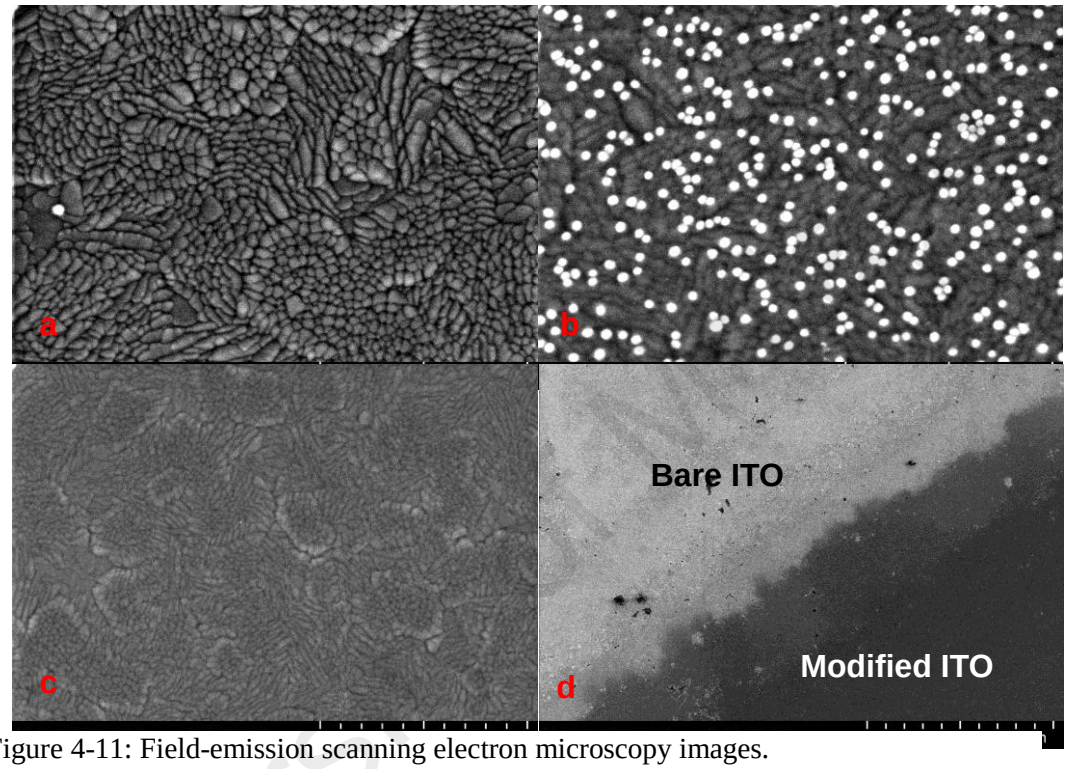

Figure 4-11: Field-emission scanning electron microscopy images.
FE-SEM image of (a) ITO/GNP. (b) ITO/SP:TMAP:PPD/GNP with molarity ratio (0.5:1.5:0.37). (c) ITO/SP:TMAP:PABA with molarity ratio (0.5:1:0.2) under magnification 50 K. (d) ITO/SP:TMAP:PABA and bare ITO surface under magnification 1.5 K.

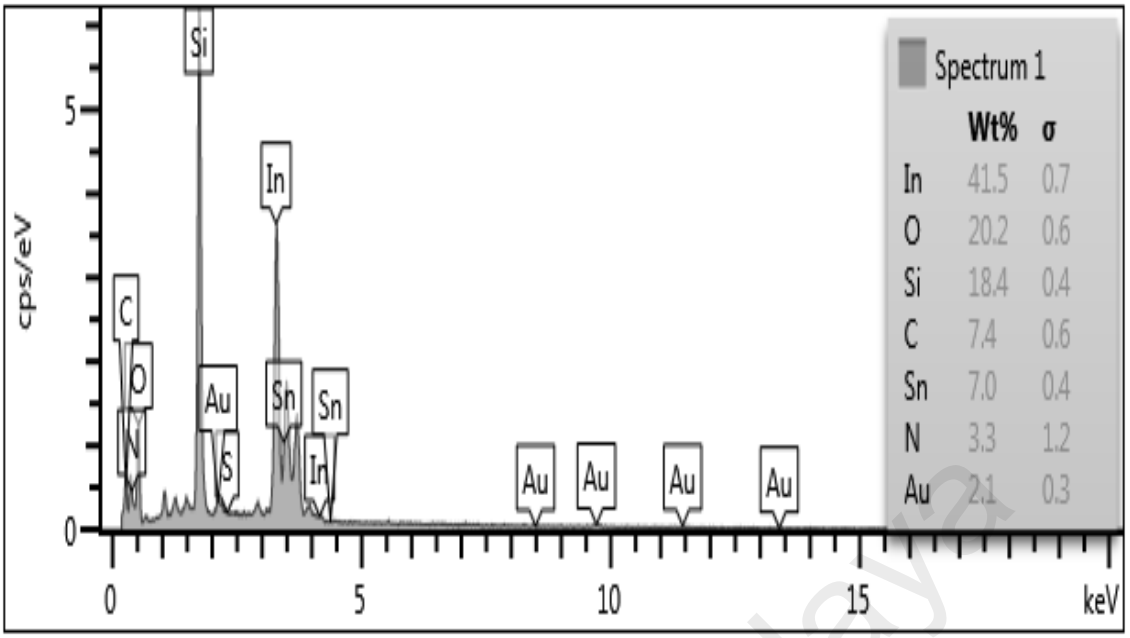

Figure 4-12: Energy-dispersive X-ray (EDX) spectrum of ITO/SP: TMAP: PPD/GNP obtained with the FESEM system.

4.5 Antifouling study by confocal laser scanning microscopy (CLSM)

4.5.1 Conjugation of Cyt c with (RBITC) dye

The bond of Cyt c with rhodamine B isothiocyanate (RBITC) occurs based on a reactive isothiocyanate group of RBITC. The conjugation of Cyt c with rhodamine B isothiocyanate was confirmed using fluorescence spectroscopy. The fluorescence spectra of RBITC shows the emission peak at 583 nm and the fluorescence spectra of the conjugated Cyt c with RBITC shows the emission peak at 587 nm. This small shift in fluorescence emission may be due to the slight pH shift in PBS, when it was used to dilute Cyt c –RBITC (Ostuni *et al.*, 1999). A little increase in the fluorescence intensity was observed in the fluorescence spectra of Cyt c –RBITC solution. This increment in fluorescent intensity can be justified as related to five-fold molar excess of Cyt c relative to RBITC used in conjugation step that subsequently increased the concentration of the Rhodamine dyes fluoresce conjugated to Cyt c protein.

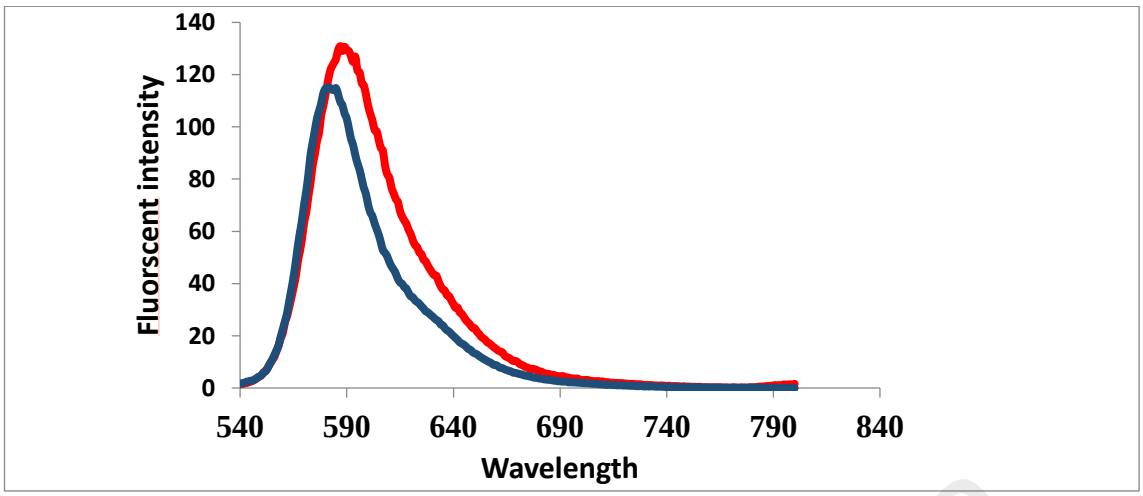

Figure 4-13: Fluorescent spectrophotometer of Rhodamine B Isothiocyanate and conjugated Cytochrome c with Rhodamine B Isothiocyanate.
Fluorescent spectrophotometer of Rhodamine B Isothiocyanate (Blue) and conjugated Cytochrome c with Rhodamine B Isothiocyanate (Red). The fluorescent dye rhodamine B and RBITC-Cyt c prepared in PBS pH 7.4.

4.5.2 Antifouling study for the mixture of SP: TMAP: PPD by CLSM

ITO surfaces functionalized with widely used antifouling molecules, OEG (ITO modified with PPD: PABA/OEG), were compared to ITO surfaces functionalized with (SP: TMAP: PPD) at different molarity ratios of 1:1:0.37 (mix 1), 1.5:0.5:0.37 (mix 2) and 0.5:1.5:0.37 (mix 3). Noticeably lower fluorescence intensity was observed for SP: TMAP: PPD mixtures; the lowest fluorescence intensity was observed for a layer of mix 3 as shown in images taken under 63x magnification (Figure 4.14, a and b). Significant finding in this study can be mentioned as the ITO surface modified with SP: TMAP: PPD was capable of resisting and repelling both BSA-FITC and Cyt c- RBITC, as indicated by the low fluorescence intensities. (Note that percentages of fluorescent adsorptions for different ITO surfaces were calculated based on the mean gray value, where all values were normalized to the ITO electrode modified with PPD: PABA/OEG) (Table 4.3).

Table 4.3: The percentage of BSA-FITC and RBITC-Cyt c adsorption at different surfaces.
The percentage represented by the normalized fluorescence intensities relative to ITO electrode modified with PPD: PABA/OEG.

Surface Type	The percentage of the fluorescent intensity for adsorbed BSA-FITC	The percentage of the fluorescent intensity for adsorbed RBITC-Cyt c
Bare ITO	35.68%	87.89%
ITO/PPD	109.54%	16.45%
ITO/SP:TMAP:PPD with molarity ratio of 1:1:0.37 (Mix 1)	75.94%	16.10%
ITO/SP:TMAP:PPD with molarity ratio of 1.5:0.5:0.37 (Mix 2)	95.62%	15.86%
ITO/SP:TMAP:PPD with molarity ratio of 0.5:1.5:0.37 (Mix 3)	63.33%	6.99%
ITO/PABA	175.64%	42.68%
ITO/SP:TMAP:PABA with molarity ratio of 0.8:1:0.2 (Mix 1)	132.14%	64.82%
ITO/SP:TMAP:PABA with molarity ratio of 1:1:0.1 (Mix 2)	104.58%	68.45%
ITO/SP:TMAP:PABA with molarity ratio of 0.5:1:0.2 (Mix 3)	86.72%	50.52%
ITO/PPD:PABA/OEG	100.0%	100.0%

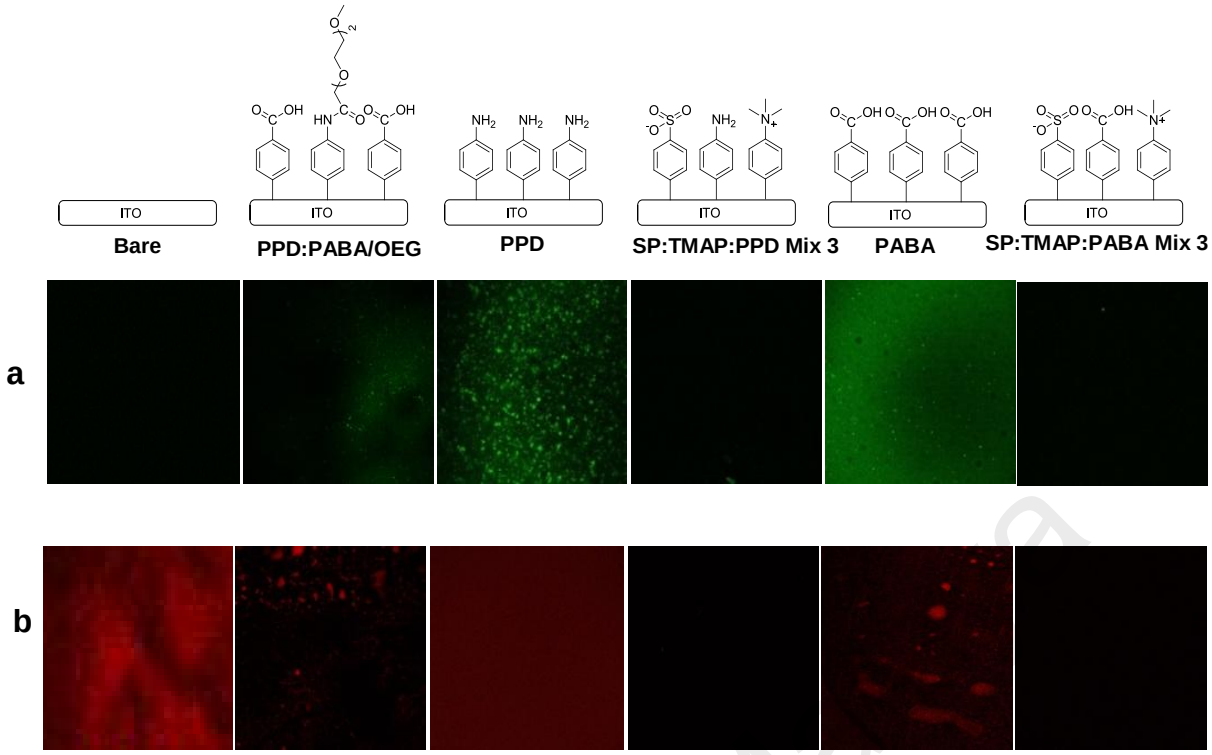

Figure 4-14: Confocal laser scanning microscopy (CLSM) image under 63x magnification from (a) FITC-BSA and (b) RBITC-Cyt c adsorbed on different surfaces.

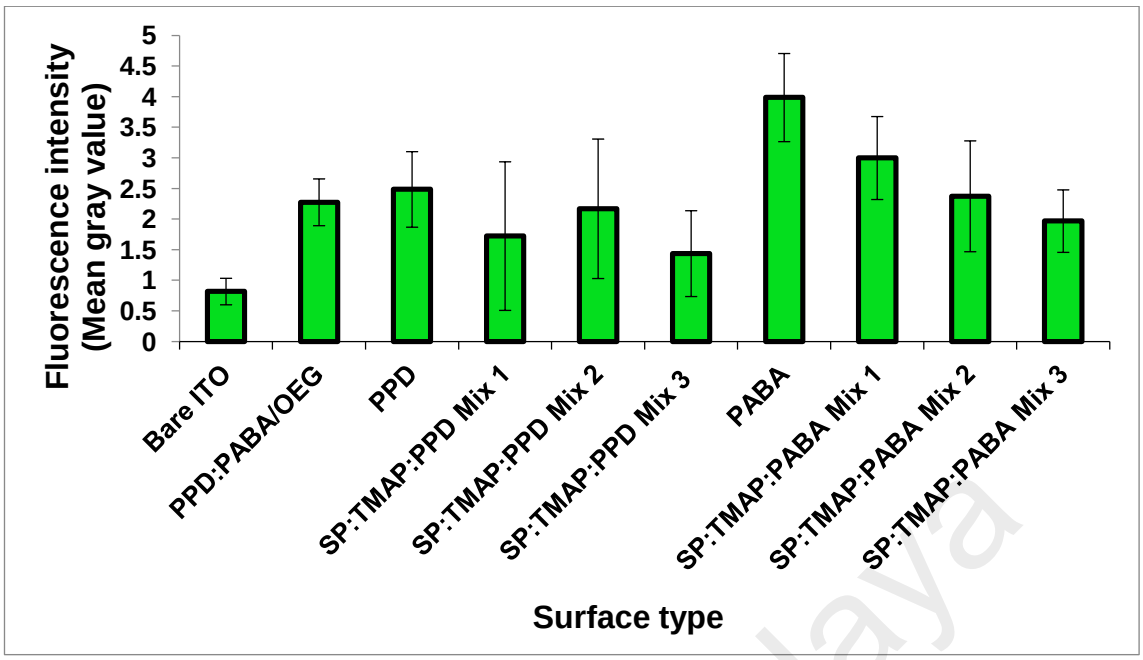

Figure 4-15: Comparison of intensity of FITC-BSA adsorbed on different surfaces

The fluorescence intensity percentage for adsorbed BSA-FITC on SP: TMAP: PPD-modified ITO surfaces for mixtures 1, 2 and 3 were lower than that for ITO functionalized with PPD: PABA/OEG. However, mix 3 exhibited the greatest resistance to BSA-FITC adsorption at 63% (a mean gray value of 1.4, s = 0.7 and n = 3) as compared with the 100% absorption of BSA-FITC in the control experiment (a mean gray value of 2.2, s = 0.3 and n = 3), which involved an ITO surface functionalized with PPD: PABA /OEG (Figure 4.15 and Table 4.3). The ITO modified with SP: TMAP: PPD mixtures 1, 2 or 3 also exhibited excellent resistance to nonspecific protein adsorption. Mixture 3 exhibited the best resistance, because the fluorescence intensity percentage for the amount of adsorbed Cyt c- RBITC on mix 3 was only 6.9% (a mean gray value of 0.15, s = 0.05 and n = 3) as compared with the 100% absorption of Cyt c-RBITC of the control experiment (a mean gray value 2.1, s = 0.4 and n = 3). Control slides were functionalized with PPD: PABA/OEG molecules (Figure 4.16. and Table 4.3).

Remarkably, the bare ITO exhibited the best capability to repel BSA-FITC (Figure 4.15, Table 4.3), with a fluorescence intensity percentage of 35.6% and a mean gray value of only 0.81 (s = 0.2, n = 3). In contrast, the bare ITO exhibited a high fluorescence intensity of 1.9 (s = 0.3, n = 3) after adsorbing Cyt c- RBITC (Figure 4.16). This observation is explained by the chemical composition of ITO surfaces, which consist of negatively charged complexes of stoichiometric oxide, hydroxides, oxyhydroxides, and physisorbed indium hydroxides. Hence, these negative charges may repel BSA-FITC but increase the adsorption of positively charge proteins such as Cyt c- RBITC (Chockalingam *et al.*, 2011).

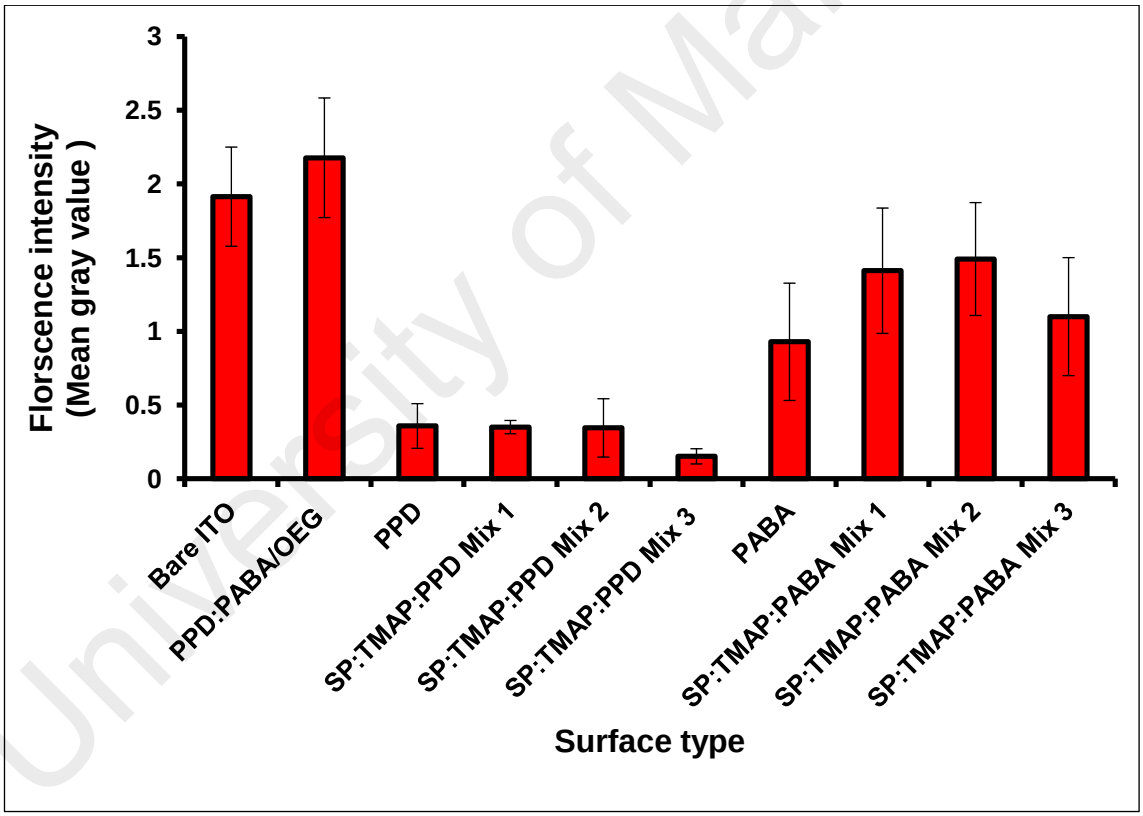

Figure 4-16: Comparison of intensity of RBITC-Cyt c adsorbed on different surfaces.

In conclusion, a surface modified with zwitterionic or similar molecules presented better antifouling properties in repelling BSA-FITC and Cyt c- RBITC as compared with ITO/PPD: PABA/OEG. This better antifouling performance may be due to good packing and charge balancing of zwitterionic groups (Gui *et al.*, 2013a) on the ITO modified with SP: TMAP: PPD mixtures. The ITO surface modified with SP: TMAP: PPD (mix 3) exhibited the best resistance to nonspecific adsorptions of BSA-FITC and Cyt c- RBITC as compared with mix 1 and mix 2. The differences in the antifouling capability of SP: TMAP: PPD mixtures may be attributed to the electrostatic interaction between the three molecules used to fabricate the inert surfaces. At this ratio, the electrostatic interaction between the positively charged tail group (TMAP: PPD) and the negatively charged tail group (SP) presented producing the best electrically neutral electronic structure.

4.5.3 Antifouling study for SP: TMAP: PABA mixture by CLSM

ITO surfaces were modified with SP: TMAP: PABA at different molar ratios of 0.8:1:0.2 (mix 1), 1:1:0.1 (mix 2) and 0.5:1:0.2 (mix 3). Mix 3 showed the best antifouling performance among the three combinations in resisting both BSA-FITC (86.7% fluorescent intensity, a mean gray value of 1.96; s = 0.5, n = 3) (Figure 4.15, Table 4.3). Mix 3 of SP: TMAP: PABA also exhibited a better resistance to Cyt c- RBITC (50.5% fluorescent intensity, a mean gray value of 1.1; s = 0.4, n = 3) (Figure 4.16, Table 4.3). As compared with the ITO surface functionalized with PPD: PABA/OEG (100% BSA-FITC fluorescent intensity, a mean gray value of 2.2; s = 0.3, n = 3); (100% Cyt c- RBITC fluorescent intensity and a mean gray value of 2.1; s = 0.4, n = 3) (Figure 4.15, Figure 4.16 and Table 4.3).

The ITO electrode modified with PPD: PABA/OEG adsorbed a significant amount of Cyt c- RBITC showing the highest fluorescence intensity among the investigated surface types (Figure 4.15 and Table 4.3). The adsorption of Cyt c- RBITC on ITO electrode modified with PPD: PABA/OEG may be due to the ability of Cyt-c to change its conformation upon adsorption onto a wide range of interfaces such as SAMs produced from alkanethiols terminating in trimethylammonium, sulfonate, methyl, amine, and carboxylic acid groups and from an aromatic thiol (Chen *et al.*, 2002; Hobara *et al.*, 2002). Moreover, the failure of OEG moieties to repel the nonspecific adsorption of undesired proteins may due to auto-oxidation of OEG moieties (Gui *et al.*, 2013 b; Holmlin, Chen, *et al.*, 2001), which makes the PPD: PABA /OEG layer unable to resist BSA-FITC and Cyt c- RBITC. Therefore, finding an antifouling coating which are more effective than OEG is significantly important.

ITO modified with SP:TMAP:PPD mixtures showed a better resistance to the nonspecific adsorption of BSA-FITC and Cyt c- RBITC as compared with SP:TMAP:PABA. This better performance can be explained by the domination of PABA molecules in SP: TMAP: PABA mixtures. The adsorption of aryl diazonium cation mixtures was dominated by the aryl diazonium cation, which was easier to reduce (e.g., having a less negative potential) (Louault *et al.*, 2008). Such behaviours later reduced the adsorptions of the other two molecules (e.g., SP and TMAP, which were necessary for a neutral charge interface. In the SP: TMAP: PPD mixture, no such domination was observed for the PPD molecule. The XPS analysis indicated that the atomic ratios for (SP) and (TMAP) were higher in SP: TMAP: PPD than in SP: TMAP: PABA mixtures (Table 4.1).

In contrast to PABA, PPD could be utilized as a linker molecule which can be combined with zwitterionic molecules (e.g., SP and TMAP) to resist the nonspecific adsorption of

BSA-FITC and Cyt c- RBITC. PPD was more easily deposited onto the electrode surface, and the complete passivation of the ITO surface required only two cycles (Figure 4.3, b). With PABA molecule, the passivation was significantly less efficient, in resisting the $[Fe(CN)_6]^{4-/3-}$ and $[Ru(NH_3)_6]^{3+}$ redox probes (Figure 4.4). PPD alone can resist the nonspecific adsorption of BSA-FITC and Cyt c- RBITC (Figure.4.15, Figure 4.16 and Table 4.3). Such behaviours enhanced the antifouling efficiency of zwitterionic molecules *(e.g.*, SP and TMAP). Moreover, the reductive adsorption potential for PPD was -0.36 V, which was closer to reductive adsorptions of SP (-0.473 V) and TMAP (-0.26 V), in comparison to the potential for PABA (-0.1 V). As a result, aryl diazonium cations with closer reductive adsorption potentials prohibited the domination of one aryl diazonium cation over the other, which assisted the fabrication of a neutrally charged antifouling coating. In this part of the present study, the objective of investigation of the antifouling capability of the two combinations, combination 1: 4-sulfophenyl, 4-trimethylammoniophenyl and 1,4-phenylenediamine (SP:TMAP:PPD) and combination 2: 4-sulfophenyl, 4-trimethylammoniophenyl and 4-aminobenzoic acid (SP:TMAP:PABA) at different ratios against BSA-FITC and Cyt c- RBITC has been fulfilled.

4.6 An electrochemical immunosensor for the detection of the NS1 antigen

4.6.1 The monitoring of the immunosensor fabrication by EIS

Electrochemical impedance spectroscopy (EIS) technique was used to observe the stepwise fabrication of the immunosensor by using 1 mM $Fe(CN)_6^{3-}/Fe(CN)_6^{4-}$ redox probe (Figure 4.17, a). A Randles' equivalent circuit was used to fit the impedance results containing the following 4 elements: the resistance of the electrolyte solution (RS), phase constant element (Q), Warburg impedance (W), and charge transfer resistance (RCT). The RS and W elements belong to the properties of the electrolyte

solution and the diffusion features of the redox probe, respectively. The diffusion of the redox probe is represented on a Nyquist plot by the straight line at low frequencies. The RCT and Q elements are related to the dielectric and insulating characteristics at the electrode/electrolyte interface and therefore, the values of these two elements are affected by the changes of the electrode surface. They are represented by the semicircle of the Nyquist plot. The semicircle diameter is typically proportional to the resistance of the deposited layers on the electrode surface. Forming a well-organized layer on the surface of the electrode usually obstructs the diffusion of the redox probe, the increase in the diameter of the semicircle suggests a high electron transfer resistance.

The changes in the diameter of the semicircle on the Nyquist plot and the charge transfer resistance (R_{ct}) were examined during the steps in the fabrication of the NS1 immunosensor (Figure 4.17, a). The immunosensor fabrication steps were illustrated in schematic diagram as can be seen in Figure 3.1. After the modification of ITO with 4-sulfophenyl, 4-trimethylammoniophenyl and 1,4-phenylenediamine molecules to produce surface ITO/SP: TMAP:PPD, an increase in the R_{ct} was observed (Figure 4.17, a, ii), because this organic layer prohibited the redox molecule from accessing the electrode. However, when AuNPs were attached, there was a significant decrease in the R_{ct} (Figure 4.17, a, iii), and this observation is consistent with other researches, which have shown that AuNPs can decrease the resistance of the charge transfer when they have been attached onto the blocking layers (Fayazfar *et al.*, 2014) (Ensafi *et al.*, 2011). The deposition of 1,4-phenylenediamine caused an increase in R_{ct} (Figure 4.17, a, iv) and further increases in the R_{ct} were also detected when the monoclonal antibodies were covalently bound to 1,4-phenylenediamine by using EDC/NHS (Figure 4.17, a, v). An increase in R_{ct}, was also observed as the NS1 antigen is specifically bound to the monoclonal antibody layer. The values of equivalent circuit parameters of the stepwise

fabrication of the NS1 immunosensor were also calculated by Nova software (Table 4.4).

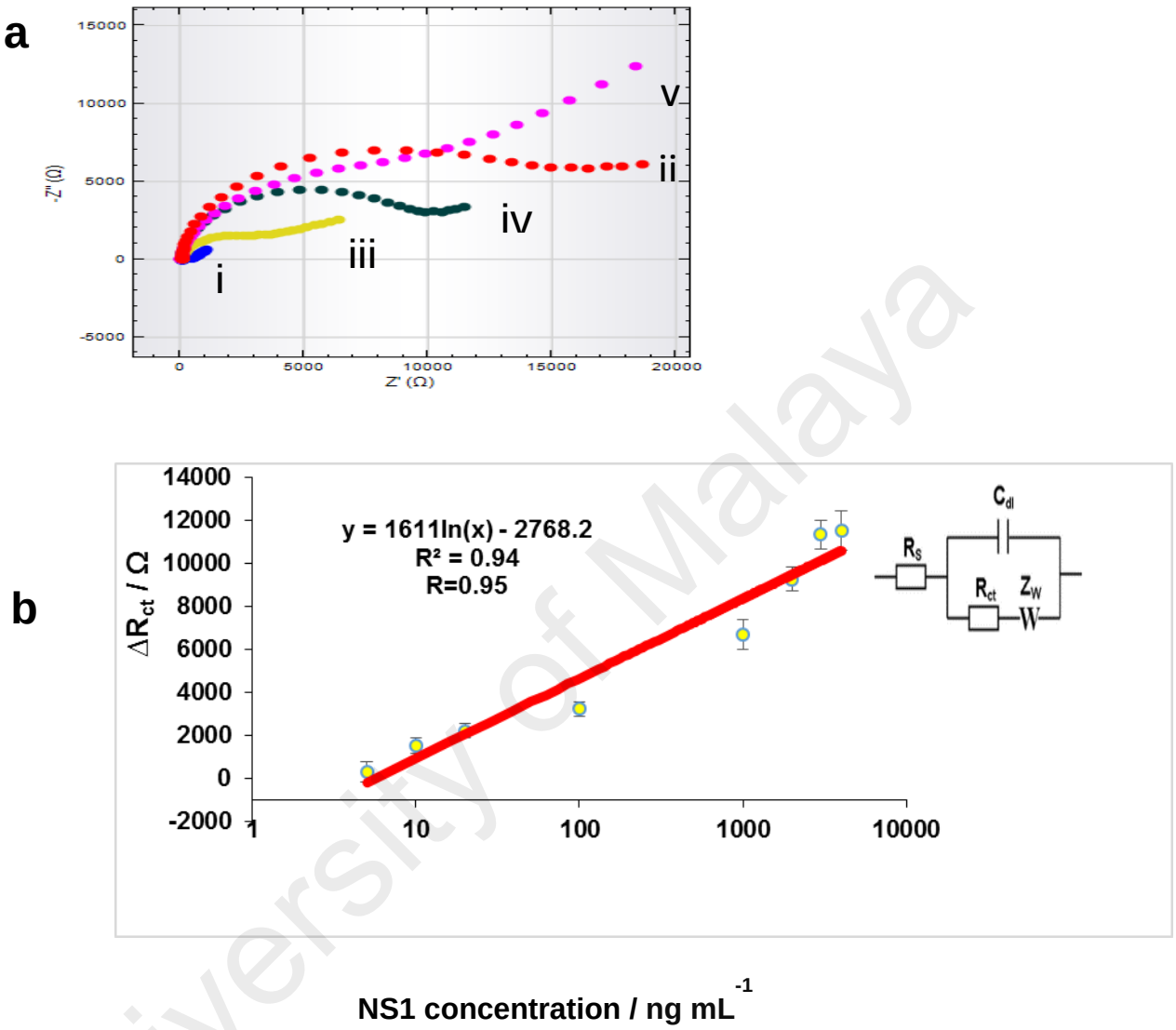

Figure 4-17: Nyquist plots of immunosensor fabrication and calibration plot for impedance measurement

(a) Nyquist plots recorded in phosphate buffer solution containing 0.05 M KCl and 1 mM $Fe(CN)_6^{3-}/Fe(CN)_6^{4-}$ for impedance measurement for stepwise surface modification of

- **(i) bare ITO electrode**
- **(ii) ITO/SP:TMAP:PPD**
- **(iii) ITO/SP:TMAP:PPD/GNPs**
- **(iv) ITO/SP:TMAP:PPD/GNPs/PPD**
- **(v) ITO/SP:TMAP:PPD/GNPs/PPD/NS1 monoclonal IgG antibody (50 µg mL^{-1}).**

(b) The calibration plot corresponding to the increase of electron transfer resistance of the immunosensor with concentration of NS1 antigen (5, 10, 20, 100, 1000, 2000, 3000 and 4000 ng mL^{-1}). Note: (a) inset is the Randles equivalent circuit for the impedance spectroscopy measurement.

Table 4.4: Values of equivalent circuit parameters of the fitting curve. The values for the bottom-up stepwise fabrication of the NS1 electrochemical impedance immunosensor interface by Nova software

Electrodes*	R_s **(Ω)**	R_{ct} **(Ω)**	**CPE**	**N**	χ^2
Bare ITO	39.0 ± 5.4	279.3 ± 64.1	65701 E-06 ± 1.01E-06	0.9± 0.03	0.007 ± 0.007
ITO/SP:TMAP:PPD	34.0 ± 1.0	10072.2 ± 3075	6.4E-06 ± 4.1E-07	0.9 ± 0.009	0.01 ± 0.006
ITO/ SP:TMAP:PPD /GNPs	39.6 ± 9.5	2012.1 ± 1174	77E-06 ± 1.3E-06	0.9± 0.02	0.03± 0.02
ITO/ SP:TMAP:PPD /GNPs/PPD	30.3 ± 2.5	6537.4 ± 2555	7.5E-06± 1.8E-06	0.9± 0.01	0.01± 0.008
ITO/SP:TMAP:PPD/GNPs/PPD/Monoclonal anti-NS1 IgG antibody	27.7 ± 1.7	7510.2 ± 1716	6E-6 ± 7.6E-07	0.9± 0.01	0.004± 0.002

*Values correspond to the average of three separate measurements with ± standard deviation.

4.6.2 The monitoring of the immunosensor fabrication by DPV

Electrochemical characterization of the fabricated NS1 immunosensor was also performed using differential pulse voltammetry (Figure.4.18, a). $Fe(CN)_6^{3-}/Fe(CN)_6^{4-}$ solution (1 mM) was used as a redox probe when the ITO electrode was first modified with a mixture of two antifouling molecules (4-sulfophenyl, 4-trimethylammoniophenyl) and a linker molecule (1,4-phenylenediamine) to produce ITO/SP:TMAP:PPD surface. The DPV peak currents decreased due to the insulating nature of these molecules (Figure.4.18, a, ii). However, when AuNPs were attached via forming a covalent C-Au bond (after the distal amine group of 1,4-phenylenediamine was converted to a diazonium group by keeping the surface (ITO/SP: TMAP: PPD) in $NaNO_2$ and 0.5 M HCl for 15 minutes to fabricate ITO/SP: TMAP: PPD/GNP surface, an increase in peak currents was observed in the DPV measurement (Figure.4.18, a, iii). These increases were expected, because the AuNPs generate conducting channels through the passivated surface, helping to minimize the background capacitance and to create well-defined sensing sites (Ensafi *et al.*, 2011; Fayazfar *et al.*, 2014). The AuNPs that were functionalized with 1,4-phenylenediamine (this layer (ITO/SP: TMAP: PPD/GNPs/PPD) was used to immobilize the monoclonal anti-NS1 IgG antibody afterward) showed a decrease in peak current (Figure.4.18, a, iv). Further, the decreases in peak current were also observed after immobilization of the monoclonal anti-NS1 IgG antibody (Figure.4.18, a, v). This observation may be due to large protein molecules on the electrode surface that prohibited the mass transfer of the redox probe (Yang *et al.*, 2013), and this reduction in the peak current was an indicator that the monoclonal anti-NS1 IgG antibodies were successfully bound to the electrode surface. To assure that the reduction in the peak current was not due to non-specific protein adsorption, 50 mM NaCl and 10 mM PBS (pH 7.4) were used to rinse the

immunosensing interface after the attachment of the monoclonal anti-NS1 IgG antibody (Dias *et al.*, 2013). A further decrease in peak current was observed when the NS1 antigen was bound to the monoclonal antibodies layer.

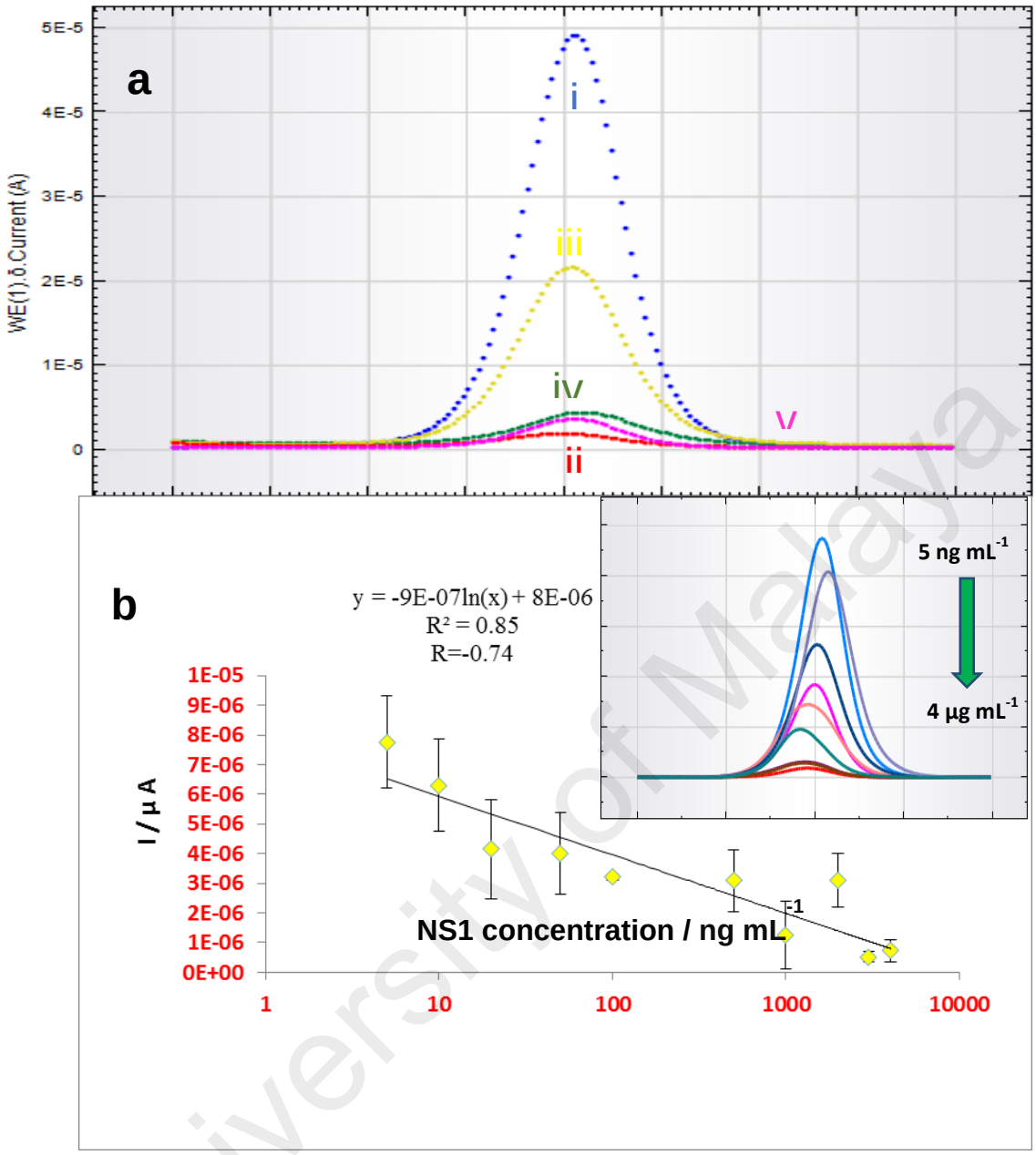

Figure 4-18: Immunosensor fabrication and calibration plots for differential pulse voltammetry.

(a) Differential pulse voltammetry plots recorded in phosphate buffer solution containing 0.05 M KCl and 1 mM $Fe(CN)_6^{3-}$/$Fe(CN)_6^{4-}$ for stepwise surface modification of

(i) bare ITO electrode
(ii) ITO/SP:TMAP:PPD
(iii) ITO/SP:TMAP:PPD/GNP
(iv) ITO/SP:TMAP:PPD/GNPs/PPD
(v) ITO/SP:TMAP:PPD/GNPs/PPD/NS1 monoclonal IgG antibody (50 µg mL^{-1}).

(b) The calibration plot corresponding to the attenuation of current peak of the immunosensor with increasing concentration of NS1 antigen (5, 10, 20, 100, 1000, 2000, 3000 and 4000 ng mL^{-1}). Note: (b) inset the differential pulse voltammetry plots corresponding to the attenuation of current peak of the immunosensor with increasing concentration of NS1 antigen (5-4000 ng mL^{-1}).

4.6.3 A quantitative analysis of the NS1 biomarker in human sera

The immunosensor for NS1 antigen functionalized with the monoclonal anti-NSI IgG antibody was used to obtain the calibration curve through detecting the NS1 antigen at different concentrations, which have been prepared in 10% human sera diluted with PBS (pH 7.4). The calibration curve obtained from a Nyquist plot of the impedance spectra showed a good logarithmic relationship between R_{ct} and various concentrations of the NS1 antigen spiked into the diluted human sera. The coefficient of determination (R^2) was 0.94 and the correlation coefficient (R) was 0.95 for the dynamic range from 5 to 4000 ng mL^{-1} (Figure 4.17, b). Moreover, the capability of the fabricated immunosensor to detect the NS1 antigen in serum samples with a detection limit of 5 ng mL^{-1} is satisfactory for clinical applications, because the levels of NS1 antigen in human sera ranged from 0.04 to 2 μg mL^{-1} in primary infection sera and from 0.01 to 2 μg mL^{-1} in secondary infection sera (Alcon *et al.*, 2002). The detection limit or lower detection limit (LOD) of 5 ng mL^{-1} was obtained based on absolute Rct value in EIS measurements and absolute signal of peak current in DPV measurements.

Furthermore, differential pulse voltammetry techniques were also utilized to find the relationship between the concentration of the NS1 antigen and the peak current of DPV. The reduction in peak current was attributed to the increase in the concentration of NS1 antigen. The values for the peak current in the DPV measurements were employed to obtain the calibration curve using $Fe(CN)_6^{3-}/Fe(CN)_6^{4-}$ redox solution. The DPV peak currents decreased with an increase in the NS1 concentration due to the insulating features of proteins (Figure 4.18, b). The fabricated immunosensor showed a linear response between 5 and 4000 ng mL^{-1}, with a R^2 coefficient of determination of 0.85 and correlation coefficient of -0.73. Three replicates were tested for each concentration of NS1 antigen.

The attenuation of the current as obtained was proportional to the increment of the concentration of NS1 antigen except 2000 ng mL^{-1} and 4000 ng mL^{-1}.The capability of the NS1 immunosensor to approach such a low detection limit may be resulted from the use of antifouling molecules in fabricated immunosensor. In our previous work (Darwish *et al.*, 2014), it was shown that these antifouling molecules with their charged terminal groups can resist the non-specific adsorption of different proteins molecules naturally found in biological samples. The usage of a monoclonal antibody might also provide highly specific recognition, because this type of antibody has monovalent affinity and can bind to the same epitope of its own antigen. Other reported immunosensors using gold nanoparticles modified with polyvinyl butyral (PVB) (Oliveira *et al.*, 2009b), concanavalin A (Oliveira *et al.*, 2009a), polyaniline hybrid (Andrade *et al.*, 2011) or Fe_3O_4 nanoparticles (Oliveira *et al.*, 2011) utilized as a model for the detection of dengue virus. In these biosensors, lectins (proteins or glycoproteins from different sources) were deposited on the biosensor interface in order to detect the glycoproteins, which were produced in patients sera infected by the dengue virus as an immune response. It is necessary to mention that lectins are carbohydrate-binding proteins; therefore, they are able to bind to serum glycoproteins (Andrade *et al.*, 2011; Oliveira *et al.*, 2011). The majority of serum proteins are glycosylated if there is any disease infection, and glycoproteins will be changed to abnormal glycoproteins under the conditions such as liver disease, cancer or dengue fever. These changes could provide the basis for clinical tests (Turner, 1992).

However, the existence of these glycoproteins might be due to a dengue virus infection or other diseases. This suggests that the biosensors, which are based on serum glycoproteins, are not greatly specific to dengue virus infection. Serum glycoproteins could be found in both the infected and non-infected serum samples (Andrade *et al.*, 2011). As the fabricated immunosensor showed the ability to detect the NS1 biomarker

in human sera using EIS and DPV techniques, finding the calibration plot corresponding to the change of NS1 antigen concentration as one of the objectives of this study has been achieved.

4.6.4 The analytical performance of the NS1 immunosensor:

4.6.4.1 The reproducibility study of NS1 immunosensor

The reproducibility of the immunosensor was tested by examining five different electrodes incubated with 100 ng mL^{-1} NS1 antigen. Excellent reproducibility was achieved with relative standard deviation (RSD = 2.1%) (Figure 4.19) showing that the electrochemical measurements were more stable than immunosensors prepared for NS1 detection in other studies (Dias *et al.*, 2013) and (Cavalcanti *et al.*, 2012a) showing a reproducibility of RSD = 3.4% and RSD = 4.8%, respectively. Reproducibility is one of the important characteristics that can limit the commercialization of any biosensor. Excellent reproducibility of the developed NS1 immunosensor can be attributed to the biosensor design and fabrication procedure (Fam *et al.*, 2011). Utilizing a monoclonal antibody for the specific detection of the NS1 antigen could improve the reproducibility of the immunosensor (Wang *et al.*, 2014). Moreover, using antifouling molecules can also control/resist the non-specific protein adsorption to the immunosensing interface. Consequently, the obtained current peak measurements were stable and only proportional to the concentration of NS1 antigen. Furthermore, the reproducibility and the robustness of the developed immunosensor may indicate that the monoclonal anti-NS1antibodies were homogeneously distributed on the electrode matrix (Serra *et al.*, 2002).

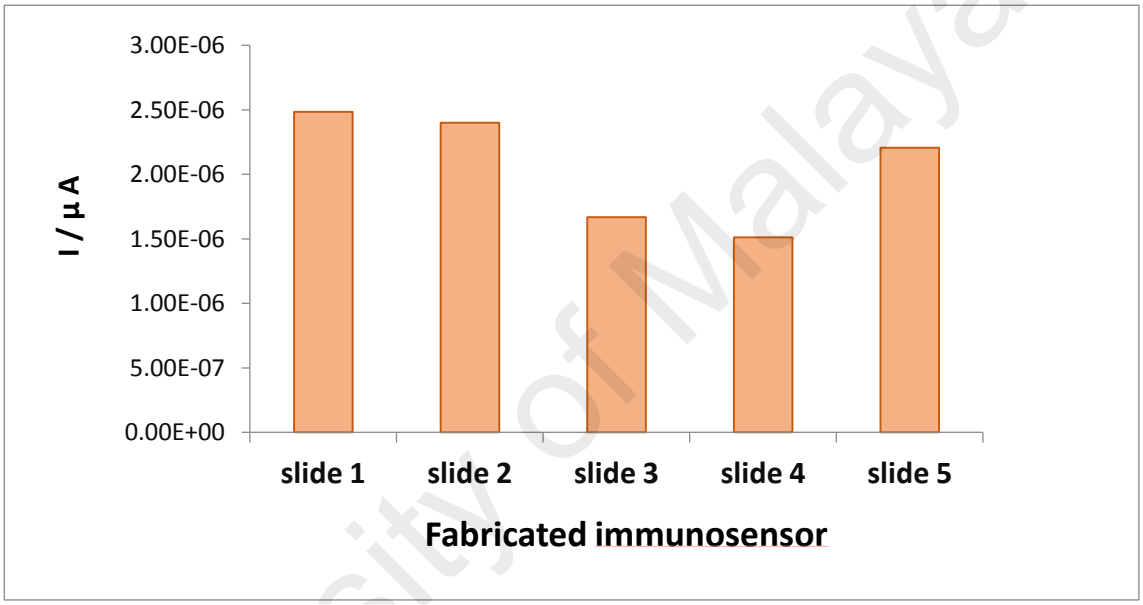

Figure 4-19: The reproducibility study for the fabricated NS1 immunosensor

The measurement for five different electrodes incubated in NS1 antigen solution 100 ng mL^{-1} the relative standard deviation obtained was 2.1%.

4.6.4.2 The selectivity and cross-reactivity studies

To investigate the selectivity of the developed NS1 immunosensor to the NS1 antigen, human IgG and human serum albumin (HSA) were examined to test whether the NS1 immunosensor yields any positive response signals to these molecules in the absence of the NS1 antigen. Human IgG and HSA were tested in the selectivity study, because they are the major blood proteins in human sera and they are the main components, which compete with the NS1 antigen. The NS1 immunosensor did not give a significant response to HSA and human IgG (Figure 4.20, a). In contrast, the NS1 immunosensor exhibited a much greater response to the NS1 antigen. This result indicates that the NS1 immunosensor has a high specificity for the detection of the NS1 antigen only.

In some clinical diagnostic procedures that have been used to detect dengue virus infection, such as the Hemagglutination-inhibition (HAI) assay and the MAC-ELISA-IgM assay, false-positive readings have been reported. These results have been mainly attributed to the cross-reactivity with co-circulating antibodies from other flaviviruses such as Japanese encephalitis or those which can be circulated in the serum of patients infected with leptospirosis or chikungunya (A-Nuegoonpipat *et al.*, 2008; Guzman & Kouri, 2004). Cross-reactivity between dengue and some malaria-positive patients is a noted issue in some parts of the world such as West Africa. Though, the association between these two diseases is not well-defined. False-positive samples have been reported and therefore, the cross-reactivity is considered as an issue to commercially-available serological kits and rapid diagnostic tests used for dengue virus clinical diagnosis (Stoler *et al.*, 2014 ; Karia *et al.*, 2008). For that reason, in this research, a cross-reactivity study has also been done in order to investigate if the sera taken from patients infected with the malaria parasites cause a positive response for NS1 antigen detection. The NS1 immunosensor did not show a significant response to malaria-infected sera (Figure. 4.20, b). On the other hand, the NS1 immunosensor gave a much

greater response to NS1 antigen. Selectivity is the most significant feature of any biosensor. The developed immunosensor in this study showed very good selectivity as compared to other reported biosensors which presented no evaluation for the sensor selectivity (Dias *et al.*, 2013; Silva *et al.*, 2014; Silva *et al.*, 2015). In the study carried by (Cavalcanti *et al.*, 2012a) selectivity study was carried out against bovine serum albumin, l-cysteine and IgG (unknown if it is human IgG, mouse IgG or other type of immunoglobulin). Using such biomolecules in these studies may not represent the actual interferences normally available in human sera. An impedimetric label-free immunosensor based on an anti-NS1 modified gold electrode was also reported recently and this immunosensor shows to be also selective to NS1 antigen when the immunosensor tested by using fetuin as nonspecific protein (Juliana *et al.*, 2015). The high selectivity of the developed immunosensor in this study could attribute to the high affinity between a biorecognition (monoclonal Ab) and the target analyte (NS1 antigen) as the binding between antibody and antigen is the most promising approach for detecting trace quantities of a specific biomarker in complex matrices and samples. The study carried out by Juliana and co-workers may also support our claim about the importance of using monoclonal Ab in order to increase the selectivity of immunosensor (Juliana *et al.*, 2015). Furthermore, using antifouling moieties (zwitterionic molecules) in developed immunosensor improved the selectivity, because it helped to overcome the problem of protein fouling, which is the non-specific molecular binding to biosensor interface, especially while identifying biomarkers in biological samples such as human serum.

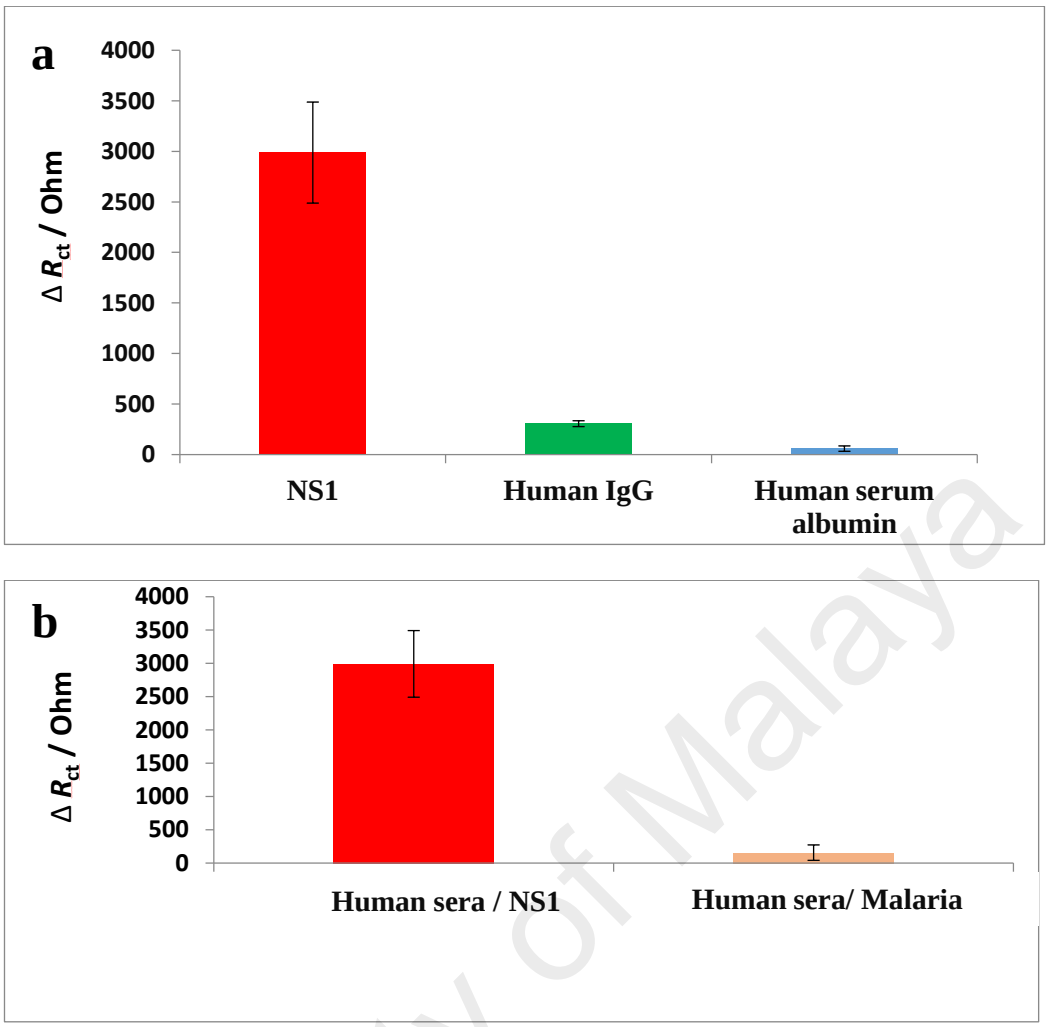

Figure 4-20: The selectivity and cross reactivity studies for the fabricated NS1 immunosensor
(a) The changes of impedance observed in the selectivity study where the immunosensing interface were tested with 50 ng mL^{-1} of target NS1 antigen, human IgG, and human serum albumin, respectively (b) The changes of impedance observed in the cross-reactivity study where the immunosensing interface were incubated in 10% human sera spiked with NS1 (1 µg mL^{-1}) and 10% human sera infected with malaria parasites, respectively The error bar indicates the standard deviation of three replicates.

4.6.4.3 The stability study of NS1 immunosensor

The stability of the fabricated NS1 immunosensor was evaluated by performing the experiments at the interval of a week. The developed immunosensing interface retains 95.2% of its activity after being stored for 21 days at 4°C, demonstrating that the monoclonal anti-NS1 IgG antibody used to modify the immunosensing interface holds good storage stability (Figure. 4.21). Nevertheless, after 30 days, the immunosensor maintained 71.4% its activity as compared to the initial peak current (day 1). It should be noted that the DPV peak currents increase with a decrease in the NS1 detected antigen due to the fact that the insulating features of proteins inhibit the current from passing through the electrode interface. This change in peak current was expected, as typical shelf life for antibodies is 1 month and chemical change such as oxidation and proteolytic degradation can occur if these antibodies are stored for more than 30 days at 4°C (Johnson, 2012; Szenczi *et al.*, 2006). The less attenuation in peak current after 30 days is due to the the proteolytic degradation of the surface bound antibody for the affinity binding with NS1 antigen. The significant decrease in peak current after 60 days was attributed to the degradation of the modified immunosensing interface after long term storage (60 days stored at 4 °C) The large error bar in DPV measurements for day 7, 14 and 21 may due to the difference in level of denaturation of Ab layer for slides incubated at 4 °C (Johnson, 2012). It is important to mention that although there is a slight change in monoclonal Ab layer but the immunosensor retained 95.2% of its activity during 21 Days of incubation. The small error bar in DPV measurements after 30 and 60 days of incubation is due to the stability of GNP and SP: TMAP: PPD as compared to Ab layer which may oxidize and got a proteolytic degradation (Johnson, 2012).

The stability of a stock antibody can be prolonged if they are stored at -20°C for one year or -80°C for more than one year (Johnson, 2012). The good operational and storage features of the developed NS1 immunosensor can be attributed to the fabrication procedure. Using EDC and NHS could tightly bind the antibody to the amine group of 1,4-phenylenediamine attached on the AuNPs surface through an amide bond, which could significantly improve the stability of the prepared electrode (Sharma *et al.*, 2010).

Furthermore, the electrochemical deposition of the AuNPs was an effective technique to obtain a film of AuNPs on the electrode. The AuNPs particles were homogeneously deposited and could tightly bind to the electrode, giving a powerful and stable immunosensing interface (Liu *et al.*, 2011b; D. Wang *et al.*, 2014). The fabrication design is a significant step and another advantage for developed biosensor by maintaining the immunosensor stability, which is essential for practical and clinical applications. The objective of studying the reproducibility, selectivity, cross reactivity and stability of the NS1 immunosensor has been fulfilled in this section of research.

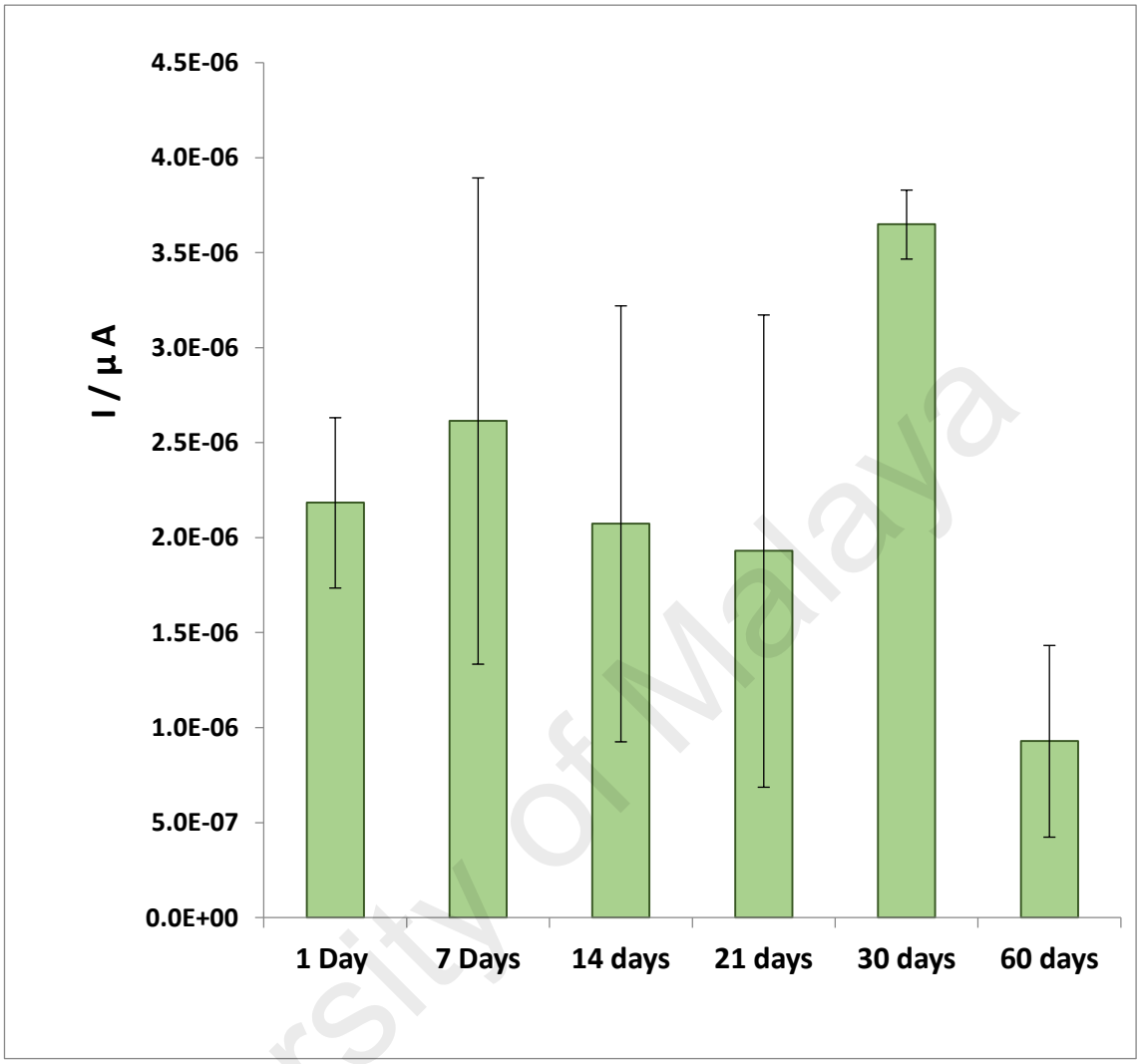

Figure 4-21: The stability study for the fabricated NS1 immunosensor
The stability study where the peak height of Differential pulse voltammetry measurement were recorded and compared for electrodes tested with fixed NS1 concentration at 100 ng mL^{-1} for 60 days stored at 4ºC. The error bar indicates the standard deviation of three replicates.

4.6.4.4 The testing of NS1 immunosensor in clinical samples.

The developed NS1 immunosensor exhibited promising analytical performance for clinical diagnosis because it can be used directly to detect the NS1 protein in a single step in sera samples of patients infected with DENV. There was a remarkable decrease in the R_{ct} value for positive sera samples, and this decrease was proportional to the dilution factor (Figure. 4.22). However, no significant change in R_{ct} value was detected for negative sera samples at different dilutions. The change in R_{ct} value might be ascribed to the change in NS1 antigen concentration in the tested samples. The proposed immunosensor demonstrated selectivity for DENV NS1 protein detection with satisfactory differentiation from the negative sera (Figure. 4.22).

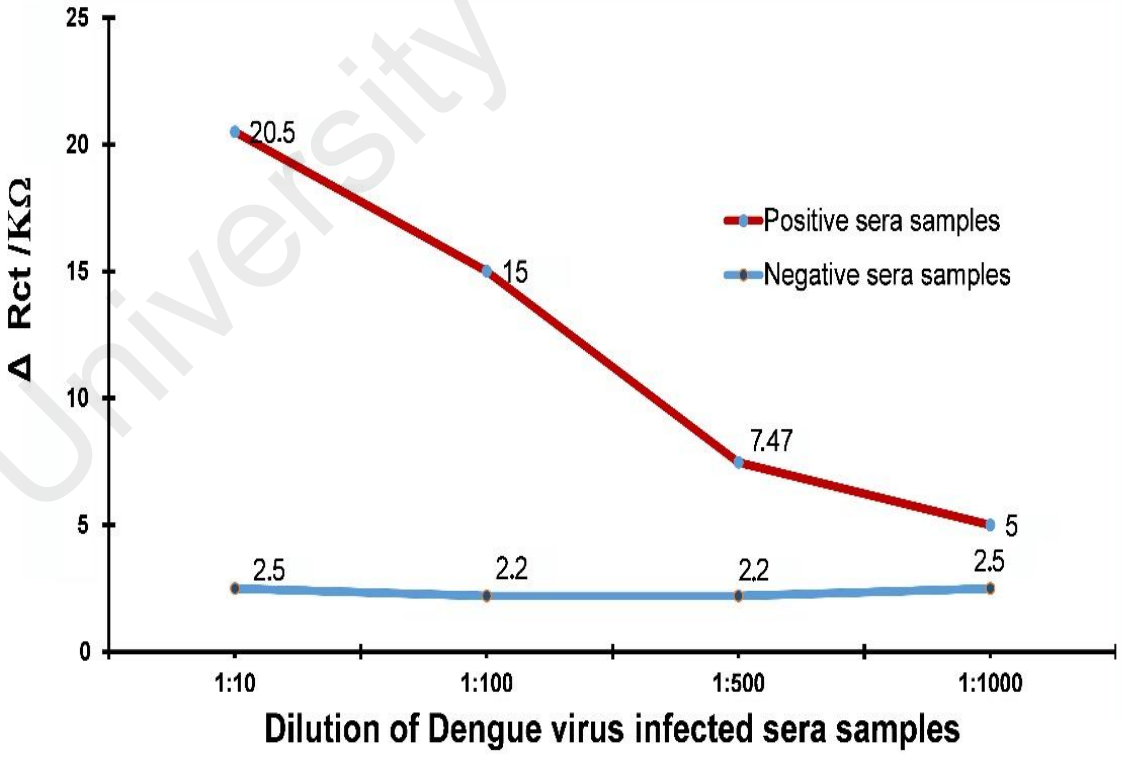

Figure 4-22: Response to the NS1 antigen in positive and negative human sera at different dilution factors (1:10, 1:100, 1:500, and 1:1000) from a patient infected with the Dengue virus

CHAPTER 5: CONCLUSIONS AND FUTURE PERSPECTIVES

The differences in electrochemical behaviours among all types of modified surfaces (either with the individual compound or combined layer of aryl diazonium cations) were examined and evaluated. As compared to molecules 4-sulfophenyl (SP) , 4-trimethylammoniophenyl (TMAP) and 4-aminobenzoic acid (PABA), compound 1,4-phenylenediamine (PPD) showed excellent passivation against the access of negatively and positively charged redox-active species $[Fe(CN)_6]^{4-/3-}$ and $[Ru(NH_3)_6]^{3+}$, respectively.

The combination which contains 4-sulfophenyl, 4-trimethylammoniophenyl and 1, 4-phenylenediamine (SP: TMAP: PPD), at ratio 0.5:1.5:0.37 was the best in resisting the penetration of both $[Fe(CN)_6]^{4-/3-}$ and $[Ru(NH_3)_6]^{3+}$ redox probes. SP: TMAP: PPD mixture, at ratio 0.5:1.5:0.37 (mix 3) provided better neutrally charged ITO surfaces as compared to combination at ratio 1:1:0.37 (mix 1) and 1.5:0.5:0.37 (mix 2). The resistivity of SP: TMAP: PPD combination at ratio 0.5:1.5:0.37 (mix 3) to redox probes indicates the ability of this combination to resist the adsorption of positively and negatively undesired substances. In the combination containing 4-sulfophenyl, 4-trimethylammoniophenyl and 4-aminobenzoic acid (SP: TMAP: PABA), a slight passivation of the ITO interface at different ratios was observed when they were tested in the $[Fe(CN)_6]^{4-/3-}$ test solutions. However, no such passivation was observed in the voltammograms when these modified interfaces were examined in $[Ru(NH_3)_6]^{3+}$ test solutions.

A biosensing interface containing antifouling and linker molecules based on *in-situ*-generated aryl diazonium cations was fabricated on indium tin oxide electrode. An antifouling study carried out by using confocal laser scanning microscopy showed that the ITO surfaces coated with mixed layers of 4-sulfophenyl, 4-trimethylammoniophenyl

and 1,4-phenylenediamine (SP:TMAP:PPD) 0.5:1.5:0.37 (mix 3) or 4-sulfophenyl, 4-trimethylammoniophenyl, and 4-aminobenzoic acid (SP:TMAP:PABA) 0.5:1:0.2 (mix 3) exhibited better antifouling capabilities against both BSA-FITC and Cyt c- RBITC as compared to the ITO surfaces coated with PPD:PABA/OEG. However, the PPD:PABA /OEG-coated ITO surfaces showed lower amounts of BSA-FITC adsorbed as compared to SP:TMAP:PABA coated ITO surfaces. The mixture of SP:TMAP:PPD indicated better resistance to nonspecific adsorptions of BSA-FITC and Cyt c- RBITC as compared to SP:TMAP:PABA. The analyses of XPS survey spectra further confirmed the deposition of (SP: TMAP: PPD) and (SP: TMAP: PABA) onto ITO surfaces. FE-SEM and EDX analyses showed dense and homogenous distributions of AuNPs, which indicated a good distribution of linker and antifouling molecules on the ITO sensing interfaces.

A label-free electrochemical immunosensor for the specific detection of the NS1 antigen was successfully developed. A sensing surface consisting of antifouling molecules and monoclonal anti-NS1 IgG antibody was fabricated based on the in situ-generated aryl diazonium cations. DPV and EIS techniques were used to monitor the bottom-up stepwise fabrication of the NS1 immunosensor. The dynamic ranges for the NS1 antigen detection were from 5-4000 ng mL^{-1}, indicating good analytical performance, with coefficients of determination (R^2) = 0.94, and correlation coefficient (R) 0.95 using the EIS technique. For the DPV study, the linear range obtained was 5-4000 ng mL^{-1} with R^2 = 0.85 and R = -0.73. The developed NS1 immunosensor exhibited excellent reproducibility, with a relative standard deviation of 2.1% for the response of five independently prepared immunosensors to 100 ng mL^{-1} NS1 antigen. The NS1 immunosensor showed good stability (up to 21 days storage at 4°C), high selectivity to only the NS1 antigen (no response to human IgG and HSA) and no cross-reactivity with malaria-infected sera. Moreover, he developed immunosensor was able

to detect the NS1 antigen in actual serum specimens from patients infected with Dengue virus. All of the experimental data acquired in this study demonstrate the potential use of the aryl-diazonium-cation-derived zwitterionic antifouling molecules and monoclonal anti-NS1 IgG antibody for the generation of a specific ITO immunosensing interface for the detection of the NS1 antigen. Furthermore, this study highlights the potential of the NS1 immunosensor as a potential clinical diagnostic test because the immunosensor has shown abilities to specifically detect the NS1 antigen in the complex serum specimens.

As for future perspectives, it is suggested to use simultaneous detection of two analytes, both represented different stages in dengue infection: viremia phase by using RNA or one of dengue antigens as the first analyte and fever phase by using IgG or IgM as the second analyte. Simultaneous diagnosis is highly valuable, because it allows for better management and fast clinical follow up, especially because dengue fever can be found with a broad range of symptoms, from asymptomatic to harsh disease. Detection of IgG or IgM is useful in diagnosis of dengue infection when the NS1 or the RNA of dengue virus is no more available in sera of infected patient.

Moreover, it is suggested to test the fabricated immunosensor in serum samples from patients infected with other flaviviruses such as Japanese encephalitis and yellow fever. These cross reactivity studies can be carried out after getting the approval from the Research Ethics Committees in University Malaya Medical Centre which is important in biomedical research to sustain the safety of society.

REFERENCES

A-Nuegoonpipat, A., Panthuyosri, N., Anantapreecha, S., Chanama, S., Sa-Ngasang, A., Sawanpanyalert, P. , and Kurane, I. (2008). Cross-reactive IgM responses in patients with dengue or Japanese encephalitis. *Journal of Clinical Virology, 42*: 75-77.

Akkahat, P., Kiatkamjornwong, S., Yusa, S. i., Hoven, V. P. , and Iwasaki, Y. (2012). Development of a Novel Antifouling Platform for Biosensing Probe Immobilization from Methacryloyloxyethyl Phosphorylcholine-Containing Copolymer Brushes. *Langmuir, 28*: 5872-5881.

Alcon, S., Talarmin, A., Debruyne, M., Falconar, A., Deubel, V. , and Flamand, M. (2002). Enzyme-linked immunosorbent assay specific to dengue virus type 1 nonstructural protein NS1 reveals circulation of the antigen in the blood during the acute phase of disease in patients experiencing primary or secondary infections. *Journal of Clinical Microbiology, 40*: 376-381.

Allongue, P., Delamar, M., Desbat, B., Fagebaume, O., Hitmi, R., Pinson, J. , and Savéant, J.-M. (1997). Covalent Modification of Carbon Surfaces by Aryl Radicals Generated from the Electrochemical Reduction of Diazonium Salts. *Journal of the American Chemical Society, 119*: 201-207.

Amorim, J. H., Porchia, B. F. M. M., Balan, A., Cavalcante, R. C. M., da Costa, S. M., de Barcelos Alves, A. M. , and de Souza Ferreira, L. C. (2010). Refolded dengue virus type 2 NS1 protein expressed in Escherichia coli preserves structural and immunological properties of the native protein. *Journal of Virological Methods, 167*: 186-192.

Andrade, C. A. S., Oliveira, M. D. L., de Melo, C. P., Coelho, L. C. B. B., Correia, M. T. S., Nogueira, M. L., Singh, P. R. , and Zeng, X. (2011). Diagnosis of dengue infection using a modified gold electrode with hybrid organica-inorganic nanocomposite and Bauhinia monandra lectin. *Journal of Colloid and Interface Science, 362*: 517-523.

Anez, M., Putonti, C., Fox, G. E., Fofanov, Y. , and Willson, R. C. (2008). Exhaustive computational identification of pathogen sequences far-distant from background genomes: Identification and experimental verification of human-blind dengue PCR primers. *Journal of Biotechnology, 133*: 267-276.

Ashley, E. A. (2011). Dengue fever. *Trends in Anaesthesia and Critical Care, 1*: 39-41.

Atias, D., Liebes, Y., Chalifa-Caspi, V., Bremand, L., Lobel, L., Marks, R. S. , and Dussart, P. (2009). Chemiluminescent optical fiber immunosensor for the detection of IgM antibody to dengue virus in humans. *Sensors and Actuators, B: Chemical, 140*: 206-215.

Baeuner, A. J., Humiston, M. C., Montagna, R. A. , and Durst, R. A. (2001). Detection of viable oocysts of Cryptosporidium parvum following nucleic acid sequence based amplification. *Analytical Chemistry, 73*: 1176-1180.

Baeumner, A. J., Schlesinger, N. A., Slutzki, N. S., Romano, J., Lee, E. M. , and Montagna, R. A. (2002). Biosensor for dengue virus detection: Sensitive, rapid, and serotype specific. *Analytical Chemistry, 74*: 1442-1448.

Bakshi, A. S. (2007). Dengue Fever, DHF and DSS. *Apollo Medicine, 4*: 111-117.

Barkham, T. M., Chung, Y. K., Tang, K. F. , and Ooi, E. E. (2006). The performance of RT-PCR compared with a rapid serological assay for acute dengue fever in a diagnostic laboratory. *Transactions of the Royal Society of Tropical Medicine and Hygiene, 100*: 142-148.

Bessaud, M., Pastorino, B. A. M., Peyrefitte, C. N., Rolland, D., Grandadam, M. , and Tolou, H. J. (2006). Functional characterization of the NS2B/NS3 protease complex from seven viruses belonging to different groups inside the genus Flavivirus. *Virus Research, 120*: 79-90.

Bhakat, S., Karubiu, W., Jayaprakash, V. , and Soliman, M. E. S. (2014). A perspective on targeting non-structural proteins to combat neglected tropical diseases: Dengue, West Nile and Chikungunya viruses. *European Journal of Medicinal Chemistry, 87*: 677-702.

Brahim, S., Narinesingh, D. , and Guiseppi-Elie, A. (2002). Bio-smart hydrogels: co-joined molecular recognition and signal transduction in biosensor fabrication and drug delivery. *Biosensors and Bioelectronics, 17*: 973-981.

Cavalcanti, I. T., Guedes, M. I. F., Sotomayor, M. D. P. T., Yamanaka, H. , and Dutra, R. F. (2012a). A label-free immunosensor based on recordable compact disk chip for early diagnostic of the dengue virus infection. *Biochemical Engineering Journal, 67*: 225-230.

Cavalcanti, I. T., Silva, B. V. M., Peres, N. G., Moura, P., Sotomayor, M. D. P. T., Guedes, M. I. F. , and Dutra, R. F. (2012 b). A disposable chitosan-modified carbon fiber electrode for dengue virus envelope protein detection. *Talanta, 91*: 41-46.

CDC. (2010). Laboratory Guidance and Diagnostic Testing. Retrieved 28/6/2012, 2012, from http://www.cdc.gov/dengue/clinicalLab/laboratory.html

Chae, K. H., Jang, Y. M., Kim, Y. H., Sohn, O.-J. , and Rhee, J. I. (2007). Anti-fouling epoxy coatings for optical biosensor application based on phosphorylcholine. *Sensors and Actuators B: Chemical, 124*: 153-160.

Chang, G. J. J., Trent, D. W., Vorndam, A. V., Vergne, E., Kinney, R. M. , and Mitchell, C. J. (1994). An integrated target sequence and signal amplification assay, reverse transcriptase-PCR-enzyme-linked immunosorbent assay, to detect and characterize flaviviruses. *Journal of Clinical Microbiology, 32*: 477-483.

Chen, R.-F., Yang, K. D., Wang, L., Liu, J.-W., Chiu, C.-C. , and Cheng, J.-T. (2007). Different clinical and laboratory manifestations between dengue haemorrhagic fever and dengue fever with bleeding tendency. *Transactions of the Royal Society of Tropical Medicine and Hygiene, 101*: 1106-1113.

Chen, S. H., Chuang, Y. C., Lu, Y. C., Lin, H. C., Yang, Y. L. , and Lin, C. S. (2009). A method of layer-by-layer gold nanoparticle hybridization in a quartz crystal microbalance DNA sensing system used to detect dengue virus. *Nanotechnology, 20*.

Chen, W. H., Hsu, I. H., Sun, Y. C., Wang, Y. K. , and Wu, T. K. (2013). Immunocapture Couples with Matrix-Assisted Laser Desorption/Ionization Time-of-Flight Mass Spectrometry for Rapid Detection of Type 1 Dengue Virus. *Journal of Chromatography A, 1288*: 21-27.

Chen, X., Ferrigno, R., Yang, J. , and Whitesides, G. M. (2002). Redox Properties of Cytochrome c Adsorbed on Self-Assembled Monolayers: A Probe for Protein Conformation and Orientation. *Langmuir, 18*: 7009-7015.

Cheng, M. S., Ho, J. S., Tan, C. H., Wong, J. P. S., Ng, L. C. , and Toh, C.-S. (2012). Development of an electrochemical membrane-based nanobiosensor for ultrasensitive detection of dengue virus. *Analytica Chimica Acta, 725*: 74-80.

Chockalingam, M., Darwish, N., Le Saux, G. , and Gooding, J. J. (2011). Importance of the Indium Tin Oxide Substrate on the Quality of Self-Assembled Monolayers Formed from Organophosphonic Acids. *Langmuir, 27*: 2545-2552.

Choi, C. K., English, A. E., Jun, S.-I., Kihm, K. D. , and Rack, P. D. (2007). An endothelial cell compatible biosensor fabricated using optically thin indium tin oxide silicon nitride electrodes. *Biosensors and Bioelectronics, 22*: 2585-2590.

Chung, D.-J., Oh, S.-H., Komathi, S., Gopalan, A. I., Lee, K.-P. , and Choi, S.-H. (2012). One-step modification of various electrode surfaces using diazonium salt compounds and the application of this technology to electrochemical DNA (E-DNA) sensors. *Electrochimica Acta, 76*: 394-403.

Combellas, C., Kanoufi, F., Pinson, J. , and Podvorica, F. I. (2008). Sterically Hindered Diazonium Salts for the Grafting of a Monolayer on Metals. *Journal of the American Chemical Society, 130*: 8576-8577.

Dale Carroll, I., Toovey, S. , and Gompel, A. V. (2007). Dengue fever and pregnancy-A review and comment. *Travel Medicine and Infectious Disease, 5*: 183-188.

Darwish, N. T., Alias, Y. B. , and Khor, S. M. (2014). Indium Tin Oxide with Zwitterionic Interfacial Design for Biosensing Applications in Complex Matrices. *Applied surface Science, 325*: 91–99.

Das, D., Mongkolaungkoon, S. , and Suresh, M. R. (2009). Super induction of dengue virus NS1 protein in E. coli. *Protein Expression and Purification, 66*: 66-72.

Dash, P. K., Parida, M., Santhosh, S. R., Saxena, P., Srivastava, A., Neeraja, M., Lakshmi, V. , and Rao, P. V. L. (2008). Development and evaluation of a 1-step duplex reverse transcription polymerase chain reaction for differential

diagnosis of chikungunya and dengue infection. *Diagnostic Microbiology and Infectious Disease, 62*: 52-57.

De Paula, S. O., de Melo Lima, C., Torres, M. P., Pereira, M. r. R. G. , and Lopes da Fonseca, B. A. n. (2004). One-Step RT-PCR protocols improve the rate of dengue diagnosis compared to Two-Step RT-PCR approaches. *Journal of Clinical Virology, 30*: 297-301.

Decker, K. D. (2012). Dengue Fever: Re-Emergence of an Old Virus. *The Journal for Nurse Practitioners, 8*: 389-393.

Deubel, V., Laille, M., Hugnot, J. P., Chungue, E., Guesdon, J. L., Drouet, M. T., Bassot, S. , and Chevrier, D. (1990). Identification of dengue sequences by genomic amplification: Rapid diagnosis of dengue virus serotypes in peripheral blood. *Journal of Virological Methods, 30*: 41-54.

Dias, A. C. M. S., Gomes-Filho, S. L. R., Silva, M. M. S. , and Dutra, R. F. (2013). A sensor tip based on carbon nanotube-ink printed electrode for the dengue virus NS1 protein. *Biosensors and Bioelectronics, 44*: 216-221.

Donley, C., Dunphy, D., Paine, D., Carter, C., Nebesny, K., Lee, P., Alloway, D. , and Armstrong, N. R. (2002). Characterization of Indium−Tin Oxide Interfaces Using X-ray Photoelectron Spectroscopy and Redox Processes of a Chemisorbed Probe Molecule: Effect of Surface Pretreatment Conditions. *Langmuir, 18*: 450-457.

Eissa, S., Tlili, C., L'Hocine, L. , and Zourob, M. (2012a). Electrochemical immunosensor for the milk allergen β-lactoglobulin based on electrografting of organic film on graphene modified screen-printed carbon electrodes. *Biosensors and Bioelectronics, 38*: 308-313.

Eissa, S., Tlili, C., L'Hocine, L. , and Zourob, M. (2012b). Electrochemical immunosensor for the milk allergen β-lactoglobulin based on electrografting of organic film on graphene modified screen-printed carbon electrodes. *Biosensors and Bioelectronics, 38*: 308-313.

El ouadi, Y., Bouyanzer, A., Majidi, L., Paolini, J., Desjobert, J. M., Costa, J., Chetouani, A. , and Hammouti, B. (2014). Salvia officinalis essential oil and the extract as green corrosion inhibitor of mild steel in hydrochloric acid *Journal of Chemical and Pharmaceutical Research, 6*: 1401-1416.

Ensafi, A. A., Taei, M., Rahmani, H. R. , and Khayamian, T. (2011). Sensitive DNA impedance biosensor for detection of cancer, chronic lymphocytic leukemia, based on gold nanoparticles/gold modified electrode. *Electrochimica Acta, 56*: 8176-8183.

Fam, D. W. H., Palaniappan, A., Tok, A. I. Y., Liedberg, B. , and Moochhala, S. M. (2011). A review on technological aspects influencing commercialization of carbon nanotube sensors. *Sensors and Actuators B: Chemical, 157*: 1-7.

Fayazfar, H., Afshar, A., Dolati, M. , and Dolati, A. (2014). DNA impedance biosensor for detection of cancer, TP53 gene mutation, based on gold nanoparticles/aligned carbon nanotubes modified electrode. *Analytica Chimica Acta, 836*: 34-44.

Fletcher, S. J., Phillips, L. W., Milligan, A. S. , and Rodda, S. J. (2010). Toward specific detection of Dengue virus serotypes using a novel modular biosensor. *Biosensors and Bioelectronics, 26*: 1696-1700.

Gabriel, M., Strand, D. , and Vahl, C.-F. (2012). Cell Adhesive and Antifouling Polyvinyl Chloride Surfaces Via Wet Chemical Modification. *Artificial Organs, 36*: 839-844.

Gittens, J. E., Smith, T. J., Suleiman, R. , and Akid, R. (2013). Current and emerging environmentally-friendly systems for fouling control in the marine environment. *Biotechnology Advances, 31*: 1738-1753.

Gole, A., Dash, C., Ramakrishnan, V., Sainkar, S. R., Mandale, A. B., Rao, M. , and Sastry, M. (2001). Pepsin-gold colloid conjugates: Preparation, characterization, and enzymatic activity. *Langmuir, 17*: 1674-1679.

Gui, A. L., Yau, H. M., Thomas, D. S., Chockalingam, M., Harper, J. B. , and Gooding, J. J. (2013a). Using Supramolecular Binding Motifs To Provide Precise Control over the Ratio and Distribution of Species in Multiple Component Films Grafted on Surfaces: Demonstration Using Electrochemical Assembly from Aryl Diazonium Salts. *Langmuir, 29*: 4772-4781.

Gui, A. L., Luais, E., Peterson, J. R. , and Gooding, J. J. (2013 b). Zwitterionic Phenyl Layers: Finally, Stable, Anti-Biofouling Coatings that Do Not Passivate Electrodes. *ACS Applied Materials & Interfaces, 5*: 4827-4835.

Guzman, M., Meschino, G. J., Dai Pra, A. L., Trivi, M., Passoni, L. I. , and Rabal, H. (2010). *Dynamic laser speckle: Decision models with computational intelligence techniques.* Paper presented at the Proceedings of SPIE - The International Society for Optical Engineering.

Guzman, M. G. , and Kouri, G. (2003). Dengue and dengue hemorrhagic fever in the Americas: lessons and challenges. *Journal of Clinical Virology, 27*: 1-13.

Guzman, M. G. , and Kouri, G. (2004). Dengue diagnosis, advances and challenges. *International Journal of Infectious Diseases, 8*: 69-80.

Harris, E., Roberts, T. G., Smith, L., Selle, J., Kramer, L. D., Valle, S., Sandoval, E. , and Balmaseda, A. (1998). Typing of dengue viruses in clinical specimens and mosquitoes by single- tube multiplex reverse transcriptase PCR. *Journal of Clinical Microbiology, 36*: 2634-2639.

Hayward, J. , and Chapman, D. (1984). Biomembrane surfaces as models for polymer design: the potential for haemocompatibility. *Biomaterials, 5*: 135–142.

Henchal, E. A., McCown, J. M. , and Seguin, M. C. (1983). Rapid identification of dengue virus isolates by using monoclonal antibodies in an indirect

immunofluorescent assay. *American Journal of Tropical Medicine and Hygiene, 32*: 164-169.

Hobara, D., Imabayashi, S.-i. , and Kakiuchi, T. (2002). Preferential Adsorption of Horse Heart Cytochrome c on Nanometer-Scale Domains of a Phase-Separated Binary Self-Assembled Monolayer of 3-Mercaptopropionic Acid and 1-Hexadecanethiol on Au(111). *Nano Letters, 2*: 1021-1025.

Holmlin, R. E., Xiaoxi, C., Robert, G. C., Shuichi, T. , and George, M. W. (2001). Zwitterionic SAMs that Resist Nonspecific Adsorption of Protein from Aqueous Buffer. *Langmuir, 17*: 2841-2850.

Houde, A., Leblanc, D., Poitras, E., Ward, P., Brassard, J., Simard, C. , and Trottier, Y.-L. (2006). Comparative evaluation of RT-PCR, nucleic acid sequence-based amplification (NASBA) and real-time RT-PCR for detection of noroviruses in faecal material. *Journal of Virological Methods, 135*: 163-172.

Houng, H.-S. H., Chung-Ming Chen, R., Vaughn, D. W. , and Kanesa-thasan, N. (2001). Development of a fluorogenic RT-PCR system for quantitative identification of dengue virus serotypes 1-4 using conserved and serotype-specific 3 noncoding sequences. *Journal of Virological Methods, 95*: 19-32.

Hu, W.-P., Huang, L.-Y., Kuo, T.-C., Hu, W.-W., Chang, Y., Chen, C.-S., Chen, H.-C. , and Chen, W.-Y. (2012). Optimization of DNA-directed immobilization on mixed oligo(ethylene glycol) monolayers for immunodetection. *Analytical Biochemistry, 423*: 26-35.

Huang, C.-H., Kuo, L.-L., Yang, K. D., Lin, P.-S., Lu, P.-L., Lin, C.-C., Chang, K., Chen, T.-C., Lin, W.-R., Lin, C.-Y., Chen, Y.-H. , and Wu, H.-S. (2013). Laboratory diagnostics of dengue fever: An emphasis on the role of commercial dengue virus nonstructural protein 1 antigen rapid test. *Journal of Microbiology, Immunology and Infection, 46*: 358-365.

Hue, K. D. T., Tuan, T. V., Thi, H. T. N., Bich, C. T. N., Anh, H. H. L., Wills, B. A. , and Simmons, C. P. (2011). Validation of an internally controlled one-step real-time multiplex RT-PCR assay for the detection and quantitation of dengue virus RNA in plasma. *Journal of Virological Methods, 177*: 168-173.

Iqbal, S. S., Mayo, M. W., Bruno, J. G., Bronk, B. V., Batt, C. A. , and Chambers, J. P. (2000). A review of molecular recognition technologies for detection of biological threat agents. *Biosensors and Bioelectronics, 15*: 549-578.

Johnson, M. (2012). Antibody Shelf Life/How to Store Antibodies.

Juliana, C. , Fernando,C. C., Adriano, S., Flavio, C. B. F., Paulo, R. B. (2015). An impedimetric biosensor to test neat serum for dengue diagnosis. *Sensors and Actuators B: Chemical,* 213: 150-154.

Karia, J., Shah, H., Patel, P., Bhalodia, J., Bhavsar, H., Shrimali, G. , and Patel, C. (2011). Evaluation of commertial newer rapid test for detection of early acute dengue infection. *National journal of medical science*, 1: 31-33.

Kevin, L. P. , and Whitesides, G., M. (1993). Adsorption of Proteins onto Surfaces Containing End-Attached Oligo(ethylene oxide): A Model System Using Self-Assembled Monolayers. *American Chemical Society, 115*: 10714-10721.

Kryscio, D. R. , and Peppas, N. A. (2012). Critical review and perspective of macromolecularly imprinted polymers. *Acta Biomaterialia, 8*: 461-473.

Kumarasamy, V., Wahab, A. H. A., Chua, S. K., Hassan, Z., Chem, Y. K., Mohamad, M. , and Chua, K. B. (2007). Evaluation of a commercial dengue NS1 antigen-capture ELISA for laboratory diagnosis of acute dengue virus infection. *Journal of Virological Methods, 140*: 75-79.

Kumaria, R. , and Chakravarti, A. (2005). Molecular detection and serotypic characterization of dengue viruses by single-tube multiplex reverse transcriptase- polymerase chain reaction. *Diagnostic Microbiology and Infectious Disease, 52*: 311-316.

Kumbhat, S., Sharma, K., Gehlot, R., Solanki, A. , and Joshi, V. (2010). Surface plasmon resonance based immunosensor for serological diagnosis of dengue virus infection. *Journal of Pharmaceutical and Biomedical Analysis, 52*: 255-259.

Kwakye, S., Goral, V. N. , and Baeumner, A. J. (2006). Electrochemical microfluidic biosensor for nucleic acid detection with integrated minipotentiostat. *Biosensors and Bioelectronics, 21*: 2217-2223.

Lanciotti, R. S., Calisher, C. H., Gubler, D. J., Chang, G. J. , and Vorndam, A. V. (1992). Rapid detection and typing of dengue viruses from clinical samples by using reverse transcriptase-polymerase chain reaction. *Journal of Clinical Microbiology, 30*: 545-551.

Lapphra, K., Sangcharaswichai, A., Chokephaibulkit, K., Tiengrim, S., Piriyakarnsakul, W., Chakorn, T., Yoksan, S., Wattanamongkolsil, L. , and Thamlikitkul, V. (2008). Evaluation of an NS1 antigen detection for diagnosis of acute dengue infection in patients with acute febrile illness. *Diagnostic Microbiology and Infectious Disease, 60*: 387-391.

Laue, T., Emmerich, P. , and Schmitz, H. (1999). Detection of dengue virus RNA in patients after primary or secondary dengue infection by using the TaqMan automated amplification system. *Journal of Clinical Microbiology, 37*: 2543-2547.

Lee, Y. F., Lien, K. Y., Lei, H. Y. , and Lee, G. B. (2009). An integrated microfluidic system for rapid diagnosis of dengue virus infection. *Biosensors and Bioelectronics, 25*: 745-752.

Lemes, E. M. B., Miagostovicsh, M. P., Alves, A. M. B., Costa, S. M., Fillipis, A. M. B., Armoa, G. R. G. , and Araujo, M. A. V. (2005). Circulating human antibodies against dengue NS1 protein: potential of recombinant D2V-NS1 proteins in diagnostic tests. *Journal of Clinical Virology, 32*: 305-312.

Lemmer, K., Donoso Mantke, O., Bae, H.-G., Groen, J., Drosten, C. , and Niedrig, M. (2004). External quality control assessment in PCR diagnostics of dengue virus infections. *Journal of Clinical Virology, 30*: 291-296.

Li, M., Su, Z.-G. , and Janson, J.-C. (2004). In vitro protein refolding by chromatographic procedures. *Protein Expression and Purification, 33*: 1-10.

Li, Y., Giesbers, M., Gerth, M. , and Zuilhof, H. (2012). Generic Top-Functionalization of Patterned Antifouling Zwitterionic Polymers on Indium Tin Oxide. *Langmuir, 28*: 12509-12517.

Libraty, D. H., Young, P. R., Pickering, D., Endy, T. P., Kalayanarooj, S., Green, S., Vaughn, D. W., Nisalak, A., Ennis, F. A. , and Rothman, A. L. (2002). High circulating levels of the dengue virus nonstructural protein NS1 early in dengue illness correlate with the development of dengue hemorrhagic fever. *Journal of Infectious Diseases, 186*: 1165-1168.

Liew, K. J. L. , and Chow, V. T. K. (2006). Microarray and real-time RT-PCR analyses of a novel set of differentially expressed human genes in ECV304 endothelial-like cells infected with dengue virus type 2. *Journal of Virological Methods, 131*: 47-57.

Lim, S. P., Wang, Q.-Y., Noble, C. G., Chen, Y.-L., Dong, H., Zou, B., Yokokawa, F., Nilar, S., Smith, P., Beer, D., Lescar, J. , and Shi, P.-Y. (2013). Ten years of dengue drug discovery: Progress and prospects. *Antiviral Research, 100*: 500-519.

Lin, J., Qu, W. , and Zhang, S. (2007a). Disposable biosensor based on enzyme immobilized on Au-chitosan-modified indium tin oxide electrode with flow injection amperometric analysis. *Analytical Biochemistry, 360*: 288-293.

Lin, J., Zhang, L. , and Zhang, S. (2007b). Amperometric biosensor based on coentrapment of enzyme and mediator by gold nanoparticles on indium tin oxide electrode. *Analytical Biochemistry, 370*: 180-185.

Liu, G., Chockalingham, M., Khor, S. M., Gui, A. L. , and Gooding, J. J. (2009). A Comparative Study of the Modification of Gold and Glassy Carbon Surfaces with Mixed Layers of In Situ Generated Aryl Diazonium Compounds. *Electroanalysis, 22*: 918-926.

Liu, G., Iyengar, S. G. , and Gooding, J. J. (2012). An Electrochemical Impedance Immunosensor Based on Gold Nanoparticle-Modified Electrodes for the Detection of HbA1c in Human Blood. *Electroanalysis, 24*: 1509-1516.

Liu, G., Liu, J., Davis, T. P. , and Gooding, J. J. (2011a). Electrochemical impedance immunosensor based on gold nanoparticles and aryl diazonium salt functionalized gold electrodes for the detection of antibody. *Biosensors and Bioelectronics, 26*: 3660-3665.

Liu, G., Luais, E. , and Gooding, J. J. (2011b). The Fabrication of Stable Gold Nanoparticle-Modified Interfaces for Electrochemistry. *Langmuir, 27*: 4176-4183.

Liu, P. , and Su, Z. (2006). Surface-initiated atom transfer radical polymerization (SI-ATRP) of styrene from chitosan particles. *Materials Letters, 60*: 1137-1139.

Liu, W.-T., Lin, W.-T., Tsai, C.-C., Chuang, C.-C., Liao, C.-L., Lin, H.-C., Hung, Y.-W., Huang, S.-S., Liang, C.-C., Hsu, H.-L., Wang, H.-J. , and Liu, Y.-T. (2006). Enhanced immune response by amphotericin B following NS1 protein prime-oral recombinant Salmonella vaccine boost vaccination protects mice from dengue virus challenge. *Vaccine, 24*: 5852-5861.

Lopez Rodriguez, M. L., Benimeli, C., Madrid, R. E. , and Giacomelli, C. E. (2015). A simple Streptomyces spore-based impedimetric biosensor to detect lindane pesticide. *Sensors and Actuators B: Chemical, 207, Part A*: 447-454.

Losito, I., Malitesta, C., De Bari, I. , and Calvano, C.-D. (2005). X-ray photoelectron spectroscopy characterization of poly(2,3-diaminophenazine) films electrosynthesised on platinum. *Thin Solid Films, 473*: 104-113.

Louault, C., D'Amours, M. , and Bélanger, D. (2008). The Electrochemical Grafting of a Mixture of Substituted Phenyl Groups at a Glassy Carbon Electrode Surface. *ChemPhysChem, 9*: 1164-1170.

Lyskawa, J. , and Belanger, D. (2006). Direct Modification of a Gold Electrode with Aminophenyl Groups by Electrochemical Reduction of in Situ Generated Aminophenyl Monodiazonium Cations. *Chemistry of Materials, 18*: 4755-4763.

M. Chockalingam, N. Darwish, G. Le Saux , and J.J. Gooding. (2011). The importance of the Indium Tin Oxide substrate on the quality of self assembled monolayers formed from organophosphonic acids. *Langmuir, 27*: 2545-2552.

Mairhofer, J., Roppert, K. , and Ertl, P. (2009). Microfluidic Systems for Pathogen Sensing: A Review. *sensors, 9*: 4804-4823.

Martins De Souza, E., Nascimento, G. A., Santana, N. A., Bruneska, D. , and Lima Filho, J. L. (2009). Development of electrochemical biosensor for virus dengue diagnostic using graphite electrode. *New Biotechnology, 25, Supplement*: S378.

McBride, W. J. H. (2009). Evaluation of dengue NS1 test kits for the diagnosis of dengue fever. *Diagnostic Microbiology and Infectious Disease, 64*: 31-36.

Meiyu, F., Huosheng, C., Cuihua, C., Xiaodong, T., Lianhua, J., Yifei, P., Weijun, C. , and Huiyu, G. (1997). Detection of flaviviruses by reverse transcriptase-polymerase chain reaction with the universal primer set. *Microbiology and Immunology, 41*: 209-213.

Melendez, J., Carr, R., Bartholomew, D., Taneja, H., Yee, S., Jung, C. , and Furlong, C. (1997). Development of a surface plasmon resonance sensor for commercial applications. *Sensors and Actuators B: Chemical, 39*: 375-379.

Mizuno, Y., Kotaki, A., Harada, F., Tajima, S., Kurane, I. , and Takasaki, T. (2007). Confirmation of dengue virus infection by detection of dengue virus type 1

genome in urine and saliva but not in plasma. *Transactions of the Royal Society of Tropical Medicine and Hygiene, 101*: 738-739.

Morita, K., Tanaka, M. , and Igarashi, A. (1991). Rapid identification of dengue virus serotypes by using polymerase chain reaction. *Journal of Clinical Microbiology, 29*: 2107-2110.

Mozaffari, S. A., Rahmanian, R., Abedi, M. , and Amoli, H. S. (2014). Urea impedimetric biosensor based on reactive RF magnetron sputtered zinc oxide nanoporous transducer. *Electrochimica Acta, 146*: 538-547.

Muller, D. A., Frentiu, F. D., Rojas, A., Moreira, L. A., O-Neill, S. L. , and Young, P. R. (2010). A portable approach for the surveillance of dengue virus-infected mosquitoes. *Journal of Virological Methods, 183*: 90-93.

Najioullah, F., Combet, E., Paturel, L., Martial, J., Koulmann, L., Thomas, L., Hatchuel, Y., Cabie, A. , and Cesaire, R. (2011). Prospective evaluation of nonstructural 1 enzyme-linked immunosorbent assay and rapid immunochromatographic tests to detect dengue virus in patients with acute febrile illness. *Diagnostic Microbiology and Infectious Disease, 69*: 172-178.

Nascimento, H. P. O., Oliveira, M. D. L., de Melo, C. P., Silva, G. J. L., Cordeiro, M. T. , and Andrade, C. A. S. (2011). An impedimetric biosensor for detection of dengue serotype at picomolar concentration based on gold nanoparticles-polyaniline hybrid composites. *Colloids and Surfaces B: Biointerfaces, 86*: 414-419.

Nguyen, B. T. T., Peh, A. E. K., Chee, C. Y. L., Fink, K., Chow, V. T. K., Ng, M. M. L. , and Toh, C.-S. (2012). Electrochemical impedance spectroscopy characterization of nanoporous alumina dengue virus biosensor. *Bioelectrochemistry*.

Oliveira, M. D. L., Correia, M. T. S. , and Diniz, F. B. (2009a). Concanavalin A and polyvinyl butyral use as a potential dengue electrochemical biosensor. *Biosensors and Bioelectronics, 25*: 728-732.

Oliveira, M. D. L., Correia, M. T. S. , and Diniz, F. B. (2009b). A novel approach to classify serum glycoproteins from patients infected by dengue using electrochemical impedance spectroscopy analysis. *Synthetic Metals, 159*: 2162-2164.

Oliveira, M. D. L., Nogueira, M. L., Correia, M. T. S., Coelho, L. C. B. B. , and Andrade, C. A. S. (2011). Detection of dengue virus serotypes on the surface of gold electrode based on Cratylia mollis lectin affinity. *Sensors and Actuators B: Chemical, 155*: 789-795.

Ostuni, E., Yan, L. , and Whitesides, G. M. (1999). The interaction of proteins and cells with self-assembled monolayers of alkanethiolates on gold and silver. *Colloids and Surfaces B: Biointerfaces, 15*: 3-30.

Polsky, R., Harper, J. C., Wheeler, D. R., Dirk, S. M., Arango, D. C. , and Brozik, S. M. (2008). Electrically addressable diazonium-functionalized antibodies for

multianalyte electrochemical sensor applications. *Biosensors and Bioelectronics, 23*: 757-764.

Prado, I., Rosario, D., Bernardo, L., arez, M., Rodriguez, R., Vazquez, S. , and Guzman, M. G. (2005). PCR detection of dengue virus using dried whole blood spotted on filter paper. *Journal of Virological Methods, 125*: 75-81.

Puttikhunt, C., Kasinrerk, W., Srisa-ad, S., Duangchinda, T., Silakate, W., Moonsom, S., Sittisombut, N. , and Malasit, P. (2003). Production of anti-dengue NS1 monoclonal antibodies by DNA immunization. *Journal of Virological Methods, 109*: 55-61.

Raengsakulrach, B., Nisalak, A., Maneekarn, N., Yenchitsomanus, P.-t., Limsomwong, C., Jairungsri, A., Thirawuth, V., Green, S., Kalayanarooj, S., Suntayakorn, S., Sittisombut, N., Malasit, P. , and Vaughn, D. W. (2002). Comparison of four reverse transcription-polymerase chain reaction procedures for the detection of dengue virus in clinical specimens. *Journal of Virological Methods, 105*: 219-232.

Raggi, C. C., P. Pinzani, A. Paradiso, M. Pazzagli , and C. Orlando. (2003). External qualitiy assurance program for PCR amplification of genomic DNA: An Italian experience. *Clinical Chemistry, 49*: 72–91.

Ramirez, A. H., Moros, Z., Comach, G., Zambrano, J., Bravo, L., Pinto, B., Vielma, S., Cardier, J. , and Liprandi, F. (2009). Evaluation of dengue NS1 antigen detection tests with acute sera from patients infected with dengue virus in Venezuela. *Diagnostic Microbiology and Infectious Disease, 65*: 247-253.

Rivet, C., Lee, H., Hirsch, A., Hamilton, S. , and Lu, H. (2011). Microfluidics for medical diagnostics and biosensors. *Chemical Engineering Science, 66*: 1490-1507.

Rivetz, B., Siman-Tov, D., Ambal, E., Jaramillo, A.-C., Ben-Zvi, A., Tartakovsky, B. , and Fish, F. (2009). New dengue antibody assay with unique differential detection of IgG and IgM antibodies. *Clinical Biochemistry, 42*: 180-184.

Rosen, L., Khin, M. M. , and U, T. (1989). Recovery of virus from the liver of children with fatal dengue: Reflections on the pathogenesis of the disease and its possible analogy with that of yellow fever. *Research in Virology, 140*: 351-360.

Rozen-Gagnon, K., Moreland, N. J., Ruedl, C. , and Vasudevan, S. G. (2012). Expression and immunoaffinity purification of recombinant dengue virus 2 NS1 protein as a cleavable SUMOstar fusion. *Protein Expression and Purification, 82*: 20-25.

Salomon, S., Leichle, T., Dezest, D., Seichepine, F., Guillon, S., Thibault, C., Vieu, C. , and Nicu, L. (2012). Arrays of nanoelectromechanical biosensors functionalized by microcontact printing. *Nanotechnology, 23*: 495501.

Schilling, S., Ludolfs, D., Van An, L. , and Schmitz, H. (2004). Laboratory diagnosis of primary and secondary dengue infection. *Journal of Clinical Virology, 31*: 179-184.

Seah, C. L. K., Chow, V. T. K. , and Chan, Y. C. (1995). Semi-nested PCR using NS3 primers for the detection and typing of dengue viruses in clinical serum specimens. *Clinical and Diagnostic Virology, 4*: 113-120.

Serra, B., Jimenez, S., Mena, M. L., Reviejo, A. J. , and Pingarron, J. M. (2002). Composite electrochemical biosensors: a comparison of three different electrode matrices for the construction of amperometric tyrosinase biosensors. *Biosensors and Bioelectronics, 17*: 217-226.

Shah, S. S., Howland, M. C., Chen, L.-J., Silangcruz, J., Verkhoturov, S. V., Schweikert, E. A., Parikh, A. N. , and Revzin, A. (2009). Micropatterning of Proteins and Mammalian Cells on Indium Tin Oxide. *ACS Applied Materials & Interfaces, 1*: 2592-2601.

Sharma, A., Matharu, Z., Sumana, G., Solanki, P. R., Kim, C. G. , and Malhotra, B. D. (2010). Antibody immobilized cysteamine functionalized-gold nanoparticles for aflatoxin detection. *Thin Solid Films, 519*: 1213-1218.

Shenoy, B., Menon, A. , and Biradar, S. (2014). Diagnostic utility of dengue NS1 antigen. *Pediatric Infectious Disease, 6*: 110-113.

Shi, Q., Su, Y., Chen, W., Peng, J., Nie, L., Zhang, L. , and Jiang, Z. (2011). Grafting short-chain amino acids onto membrane surfaces to resist protein fouling. *Journal of Membrane Science, 366*: 398-404.

Shiddiky, M. J. A., Kithva, P. H., Kozak, D. , and Trau, M. (2012a). An electrochemical immunosensor to minimize the nonspecific adsorption and to improve sensitivity of protein assays in human serum. *Biosensors and Bioelectronics, 38*: 132-137.

Shiddiky, M. J. A., Kithva, P. H., Sakandar, R. , and Trau, M. (2012b). Femtomolar detection of a cancer biomarker protein in serum with ultralow background current by anodic stripping voltammetry. *Chemical Communication, 48*: 6411–6413.

Shinde, S. B., Fernandes, C. B. , and Patravale, V. B. (2011). Recent trends in in-vitro nanodiagnostics for detection of pathogens. *Journal of Controlled Release, 159*: 164-180.

Silva, M. M. S., Dias, A. C. M. S., Cordeiro, M. T., Marques Jr, E., Goulart, M. O. F. , and Dutra, R. F. (2014). A thiophene-modified screen printed electrode for detection of dengue virus NS1 protein. *Talanta, 128*: 505-510.

Silva, M. M. S., Dias, A. C. M. S., Silva, B. V. M., Gomes-Filho, S. L. R., Kubota, L. T., Goulart, M. O. F. , and Dutra, R. F. (2015). Electrochemical detection of dengue virus NS1 protein with a poly(allylamine)/carbon nanotube layered immunoelectrode. *Journal of Chemical Technology & Biotechnology, 90*: 194-200.

Singh, M. P., Majumdar, M., Singh, G., Goyal, K., Preet, K., Sarwal, A., Mishra, B. , and Ratho, R. K. (2010). NS1 antigen as an early diagnostic marker in dengue: report from India. *Diagnostic Microbiology and Infectious Disease, 68*: 50-54.

Somnuke, P., Hauhart, R. E., Atkinson, J. P., Diamond, M. S. , and Avirutnan, P. (2011). N-linked glycosylation of dengue virus NS1 protein modulates secretion, cell-surface expression, hexamer stability, and interactions with human complement. *Virology, 413*: 253-264.

Stoler, J., al Dashti, R., Anto, F., Fobil, J. N. , and Awandare, G. A. (2014). Deconstructing "malaria": West Africa as the next front for dengue fever surveillance and control. *Acta Tropica, 134*: 58-65.

Su, C.-C., Wu, T.-Z., Chen, L.-K., Yang, H.-H. , and Tai, D.-F. (2003). Development of immunochips for the detection of dengue viral antigens. *Analytica Chimica Acta, 479*: 117-123.

Sudiro, T. M., Ishiko, H., Rothman, A. L., Kershaw, D. E., Green, S., Vaughn, D. W., Nisalak, A., Kalayanarooj, S. , and Ennis, F. A. (1998). Microplate-reverse hybridization method to determine dengue virus serotype. *Journal of Virological Methods, 73*: 229-235.

Suwandono, A., Kosasih, H., Nurhayati, Kusriastuti, R., Harun, S., Maaroef, C., Wuryadi, S., Herianto, B., Yuwono, D., Porter, K. R., Beckett, C. G. , and Blair, P. J. (2006). Four dengue virus serotypes found circulating during an outbreak of dengue fever and dengue haemorrhagic fever in Jakarta, Indonesia, during 2004. *Transactions of the Royal Society of Tropical Medicine and Hygiene, 100*: 855-862.

Szenczi, A., Kardos, J., Medgyesi, G. A. , and Zavodszky, P. (2006). The effect of solvent environment on the conformation and stability of human polyclonal IgG in solution. *Biologicals, 34*: 5-14.

Tahir, M., Gupta, E., Salmani, S., Padma, M. V., Singh, M. B., Dar, L., Broor, S. , and Sharma, S. K. (2006). Dengue fever with papilledema: A case of dengue-3 virus infection in central nervous system. *Journal of Clinical Virology, 37*: 65-67.

Tai, D. F., Lin, C. Y., Wu, T. Z., Huang, J. H. , and Shu, P. Y. (2006). Artificial receptors in serologic tests for the early diagnosis of dengue virus infection. *Clinical Chemistry, 52*: 1486-1491.

Teles, F. R. R., Dos Prazeres, D. M. F. , and De Lima-Filho, J. L. (2007). Electrochemical detection of a dengue-related oligonucleotide sequence using ferrocenium as a hybridization indicator. *Sensors, 7*: 2510-2518.

Teles, F. S. (2011). Biosensors and rapid diagnostic tests on the frontier between analytical and clinical chemistry for biomolecular diagnosis of dengue disease: A review. *Analytica Chimica Acta, 687*: 28-42.

Turner, G. A. (1992). N-glycosylation of serum proteins in disease and its investigation using lectins. *Clinica Chimica Acta, 208*: 149-171.

Vazquez, S., Valdes, O., Pupo, M., Delgado, I., Alvarez, M., Pelegrino, J. L. , and Guzman, M. G. (2003). MAC-ELISA and ELISA inhibition methods for detection of antibodies after yellow fever vaccination. *Journal of Virological Methods, 110*: 179-184.

Vila , N. , and Belanger, D. (2012). Mixtures of functionalized aromatic groups generated from diazonium chemistry as templates towards bimetallic species supported on carbon electrode surfaces. *Electrochimica Acta, 85*: 538-547.

Vila , N., Brussel, M. V., DAmours, M., Marwan, J., Buess-Herman, C. , and Belanger, D. (2007). Metallic and bimetallic Cu/Pt species supported on carbon surfaces by means of substituted phenyl groups. *Journal of Electroanalytical Chemistry, 609*: 85-93.

Volonte, F., Marinelli, F., Gastaldo, L., Sacchi, S., Pilone, M. S., Pollegioni, L. , and Molla, G. (2008). Optimization of glutaryl-7-aminocephalosporanic acid acylase expression in E. coli. *Protein Expression and Purification, 61*: 131-137.

Wang, D., Dou, W., Zhao, G. , and Chen, Y. (2014). Immunosensor based on electrodeposition of gold-nanoparticles and ionic liquid composite for detection of Salmonella pullorum. *Journal of Microbiological Methods, 106*: 110-118.

Wang, H., Li, H., Wang, J., Wu, J., Li, D., Liu, M. , and Su, P. (2014). Nitrogen-doped TiO2 nanoparticles better TiO2 nanotube array photo-anodes for dye sensitized solar cells. *Electrochimica Acta, 137*: 744-750.

Wang, J., Luck, L. A. , and Suni, I. I. (2007). Immobilization of the glucose-galactose receptor protein onto a Au electrode through a genetically engineered cysteine residue. *Electrochemical and Solid-State Letters, 10*: 33-36.

Wang, N., Burugapalli, K., Song, W., Halls, J., Moussy, F., Ray, A. , and Zheng, Y. (2013). Electrospun fibro-porous polyurethane coatings for implantable glucose biosensors. *Biomaterials, 34*: 888-901.

Watthanaworawit, W., Turner, P., Turner, C. L., Tanganuchitcharnchai, A., Jarman, R. G., Blacksell, S. D. , and Nosten, F. o. H. (2011). A prospective evaluation of diagnostic methodologies for the acute diagnosis of dengue virus infection on the Thailand-Myanmar border. *Transactions of the Royal Society of Tropical Medicine and Hygiene, 105*: 32-37.

Wright, W. F. , and Pritt, B. S. (2012). Update: The diagnosis and management of dengue virus infection in North America. *Diagnostic Microbiology and Infectious Disease*.

Wu, S. J. L., Eun Mi, L., Putvatana, R., Shurtliff, R. N., Porter, K. R., Suharyono, W., Watts, D. M., King, C. C., Murphy, G. S., Hayes, C. G. , and Romano, J. W. (2001). Detection of dengue viral RNA using a nucleic acid sequence-based amplification assay. *Journal of Clinical Microbiology, 39*: 2794-2798.

Wu, T.-Z., Su, C.-C., Chen, L.-K., Yang, H.-H., Tai, D.-F. , and Peng, K.-C. (2005). Piezoelectric immunochip for the detection of dengue fever in viremia phase. *Biosensors and Bioelectronics, 21*: 689-695.

Xu, H., Di, B., Pan, Y. X., Qiu, L. W., Wang, Y. D., Hao, W., He, L. J., Yuen, K. Y. , and Che, X. Y. (2006). Serotype 1-specific monoclonal antibody-based antigen capture immunoassay for detection of circulating nonstructural protein NS1: Implications for early diagnosis and serotyping of dengue virus infections. *Journal of Clinical Microbiology, 44*: 2872-2878.

Yamada, K.-I., Takasaki, T., Nawa, M. , and Kurane, I. (2002). Virus isolation as one of the diagnostic methods for dengue virus infection. *Journal of Clinical Virology, 24*: 203-209.

Yang, H., Li, Z., Wei, X., Huang, R., Qi, H., Gao, Q., Li, C. , and Zhang, C. (2013). Detection and discrimination of alpha-fetoprotein with a label-free electrochemical impedance spectroscopy biosensor array based on lectin functionalized carbon nanotubes. *Talanta, 111*: 62-68.

Yeh, P.-Y. J., Kizhakkedathu, J. N., Madden, J. D. , and Chiao, M. (2007). Electric field and vibration-assisted nanomolecule desorption and anti-biofouling for biosensor applications. *Colloids and Surfaces B: Biointerfaces, 59*: 67-73.

Yenchitsomanus, P. T., Sricharoen, P., Jaruthasana, I., Pattanakitsakul, S. N., Nitayaphan, S., Mongkolsapaya, J. , and Malasit, P. (1996). Rapid detection and identification of dengue viruses by polymerase chain reaction (PCR). *Southeast Asian Journal of Tropical Medicine and Public Health, 27*: 228-236.

Yin, M., Yuan, Y., Liu, C. , and Wang, J. (2009). Development of mussel adhesive polypeptide mimics coating for in-situ inducing re-endothelialization of intravascular stent devices. *Biomaterials, 30*: 2764-2773.

Young, P. R., Hilditch, P. A., Bletchly, C. , and Halloran, W. (2000). An antigen capture enzyme-linked immunosorbent assay reveals high levels of the dengue virus protein NS1 in the sera of infected patients. *Journal of Clinical Microbiology, 38*: 1053-1057.

Yu, Q., Zhang, Y., Wang, H., Brash, J. , and Chen, H. (2011). Anti-fouling bioactive surfaces. *Acta Biomaterialia, 7*: 1550-1557.

Zaytseva, N. V., Montagna, R. A. , and Baeumner, A. J. (2005). Microfluidic biosensor for the serotype-specific detection of dengue virus RNA. *Analytical Chemistry, 77*: 7520-7527.

Zeppilli, S., Arnault, J. C., Gesset, C., Bergonzo, P. , and Polini, R. (2010). Thermal stability and surface modifications of detonation diamond nanoparticles studied with X-ray photoelectron spectroscopy. *Diamond and Related Materials, 19*: 846-853.

Zhang, G.-J., Zhang, L., Huang, M. J., Luo, Z. H. H., Tay, G. K. I., Lim, E.-J. A., Kang, T. G. , and Chen, Y. (2010). Silicon nanowire biosensor for highly sensitive and rapid detection of Dengue virus. *Sensors and Actuators B: Chemical, 146*: 138-144.

Zhang, H., Li, W., Wang, J., Peng, H., Che, X., Chen, X. , and Zhou, Y. (2014). NS1-based tests with diagnostic utility for confirming dengue infection: a meta-analysis. *International Journal of Infectious Diseases, 26*: 57-66.

Zhang, S., Wright, G. , and Yang, Y. (2000). Materials and techniques for electrochemical biosensor design and construction. *Biosensors and Bioelectronics, 15*: 273-282.

SUPPLEMENTARY

LIST OF PUBLICATION AND PAPERS PRESENTED

1. Nadia T Darwish, Yatimah Alias, Sook Mei Khor. 2014. Indium Tin Oxide with Zwitterionic Interfacial Design for Biosensing Applications in Complex Matrices. Applied Surface Science. 2015, 325: 91–99. (ISI-Cited Publication).

2. Nadia T Darwish, Yatimah Alias, Sook Mei Khor. 2015. An introduction to dengue-disease diagnostics. Trends in Analytical Chemistry. 2015, 67: 45-55. (ISI-Cited Publication)
3. Nadiya Taha Darwish, Aoday Hashim Al-rawi, Yatimah binti Alias, Sook Mei Khor. 2015. The development of an electrochemical immunosensor for the direct detection of the NS1 antigen biomarker in the early stage of dengue virus infection. Journal of electrochemical society. 2015, 163: B19-B25 (ISI-Cited Publication).
4. Nadia T Darwish, Yatimah Alias, Sook Mei Khor, Asia sense conference 'Melaka, Malaysia. August 27-29, 2013. An electrochemical sensing interface for immunological application, Poster Presentation.
5. Nadia T Darwish, Yatimah Alias, Sook Mei Khor, ICLSE conference, Kuala Lumpur, Malaysia, December 13-14, 2014. Immunosensing Interface Based On Diazonium Cations Modified Indium Tin Oxide. Oral presentation.